eman ta zabal zazu

Universidad del País Vasco
Euskal Herriko Unibertsitatea

Departamento de Ingeniería Química

Ingenieritza Kimikoa Saila

Department of Chemical Engineering

ALTERNATIVE CATALYTIC PROCESSES FOR THE VALORIZATION OF PLASTIC WASTES TO FUELS

MEMORIA

para optar al grado de Doctor Internacional

en Ingeniería Química presentada por

Joseba Andoni Salbidegoitia Samperio

Leioa, Julio 2016

Quisiera comenzar agradeciendo especialmente a mis directores Dra. María Pilar González Marcos y Dr. Juan Ramón González Velasco por la confianza que han depositado en mí para realizar esta tesis doctoral y por el compromiso mostrado durante estos años de investigación.

Al Ministerio de Educación y Ciencia, por la financiación a través del Proyecto de Investigación (CTQ2010-17277) y al Gobierno Vasco por la ayuda económica para mi formación y para la estancia en Japón (BFI-2010-150).

A los doctores José Antonio González Marcos, José Ignacio Gutiérrez Ortiz, Miguel Ángel Gutiérrez Ortiz, José Luis Ayastuy Arizti, Asier Aranzabal Maiztegi, Rubén López Fonseca, Jon Iñaki Álvarez Uriarte, Unai Iriarte Velasco, José María Castresana Pelayo, Beatriz de Rivas Martín, Zouhair Boukha, Beñat Pereda Ayo y a Willy de UMI.

A todos los investigadores y técnicos del Servicio General de Análisis (SGIKER) de la UPV/EHU por su colaboración en la caracterización de tan variadas muestras, especialmente a Luis Bartolomé y Aitor Larrañaga.

Kamo sensei, thank you so much for giving me the opportunity to work with you and for your continuous support during my days in Japan, not only at job but also for the daily life. I really appreciate your help and the assistance of all of the members of your group, especially Shimizu san and Itou san. I would extend my thanks to Professor Thallada Bhaskar for the useful working time and all the good advice that has been given to me.

También quiero agradecer a todos los compañeros y amigos que me han ayudado durante estos años de investigación y han hecho la faena más llevadera: Adrián, Adriana, Ainara, Aitor, Alberto, Álvaro, Angélica, Arkaitz, Carmen, Cristina, Edwin, Fan, Itxaso, Jon Ander, Jonatan, Karina, Laura, Maider, Hola Maitane, Manu, Miren, Miryam, Noe, Olatz, Pantxi, Ricardo, Roberto, Unai, Unai Elizundia, Vanessa, Xabi, Xandra.

A mi familia por vuestra ayuda incondicional que siempre me brindáis; este trabajo no hubiera sido posible sin vosotros. A mis amigos, que sois un apoyo fundamental y siempre estáis ahí. A ti Elena, que me has enseñado que con esfuerzo y a pesar de las adversidades, todo tiene su recompensa. ¡EQUIPAZO!

A mi familia, mis amigos y a Elena

Index

Índice

Chapter 1

INTRODUCTION AND OBJECTIVES

Capítulo 1

INTRODUCCIÓN Y OBJETIVOS

RESUMEN.

La gran versatilidad de los productos plásticos ha producido un crecimiento exponencial en la demanda de este tipo de materiales en los últimos años. Muchos de los porductos fabricados con estos materiales, además, presentan tiempos de vida muy cortos. Por ello, los residuos plásticos generados al final de la vida útil del producto presentan también una tendencia de crecimiento exponencial. Este crecimiento, junto con la elevada estabilidad de los plásticos, genera un importante problema de gestión.

Este capítulo introductorio discute el estado del arte en la producción de componentes plásticos, centrándose en los residuos que generan así como en las diferentes soluciones para gestionarlos, buscando siempre la solución más comprometida con el medio ambiente y la sociedad. Entre estas opciones, el trabajo realizado en esta tesis se enfoca hacia la valorización de residuos plásticos complejos mediante procesos catalíticos, en particular los residuos obtenidos de componentes electrónicos y de automóviles, para obtener productos de alto valor añadido, como combustibles líquidos e hidrógeno.

1. INTRODUCTION AND OBJECTIVES

1.1. PLASTIC CONSUMPTION SCENERY

Nowadays we cannot imagine a world without plastics. Most of the daily products we use are made of plastic. With continuous growth for more than 50 years, global plastic production in 2013 rose to 299 million tons, which means a 3.9 % increase compared to 2012. Plastic production uses 4–8 % of global crude oil production, i.e. 4 % as feedstock and 4 % during conversion [1]. Figure 1.1 shows the main world plastic manufacturers.

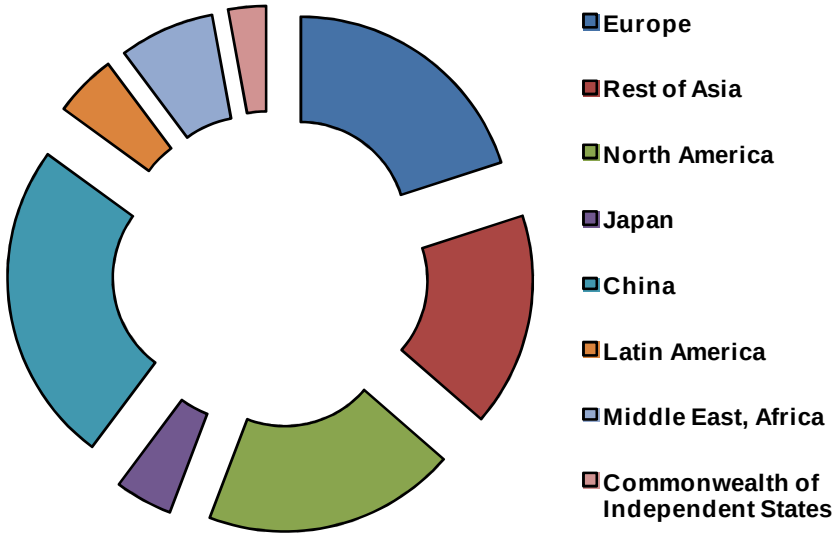

Figure 1.1 World production of plastic materials [2].

China can be appreciated to produce the highest amount of plastics, with 25 %, and Europe occupies the second position, amounting to 20 % of the global production, which means around 60 million tons.

Plastic markets is divided into packaging, building and construction, automotive, electrical and electronic equipments, agriculture and others and the scenery in Europe is drawn in Figure 1.2.

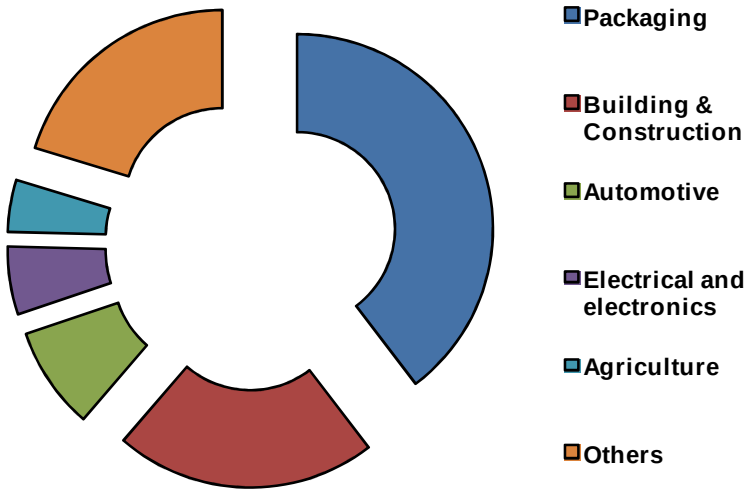

Figure 1.2. Plastic applications in Europe [2].

Packaging is the largest application sector for the plastics industry and represents 39.6 % of the total plastics demand. Building and construction is the second largest application sector with 20.3 % of the total European demand. Automotive and Electrical and electronic applications represent 14 % of the total plastic demand [2].

Most demanded polymers (Table 1.1) for final plastic products are polyethylene terephthalate (PET), high density polyethylene (HDPE), polyvinyl chloride (PVC), low density polyethylene (LDPE), polypropylene (PP), polystyrene (PS) and, in the last years, the demand of polymers such as high impact acrylonitrile-butadiene-styrene (ABS) and styrene-acrylonitrile (SAN), polyamides (PA), polyurethane (PUR), polybutadiene (PB) and high impact polystyrene (HIPS) has increased.

These plastics represent 85 wt.% of the total demand; however, five families of plastics —PE, PP, PS, PVC and PET—, account for around 73 wt.% of total

Europe plastic demand [2]. Molecule structures of the most common polymers are presented in Figure 1.3.

Table 1.1. Properties and utilities of most common plastics [3].

Polymer	Properties and utilities
PET – Code 1	Clear, and tough, heat resistant. Plastic bottles for soft drinks, polyester.
HDPE – Code 2	Stiff, strong, and tough, moisture and chemicals resistant. Plastic bottles, plastic bags, etc.
PVC – Code 3	Versatile, strong, and tough, chemical resistant. Medical material pipes, window frames, and flooring.
LDPE – Code 4	Resistant to acids, bases, and vegetable oils. Bags, container lids, toys, and bottles.
PP – Code 5	Strong, tough, versatile, and heat, chemicals and oil resistant. Food and medicine containers, bottles, closures and caps.
PS – Code 6	Versatile, rigid or foamed. Cups, plates, packaging, electronic cases, etc.
Other– Code 7	Made with a resin other than the six listed above, or made up of multiple resins.

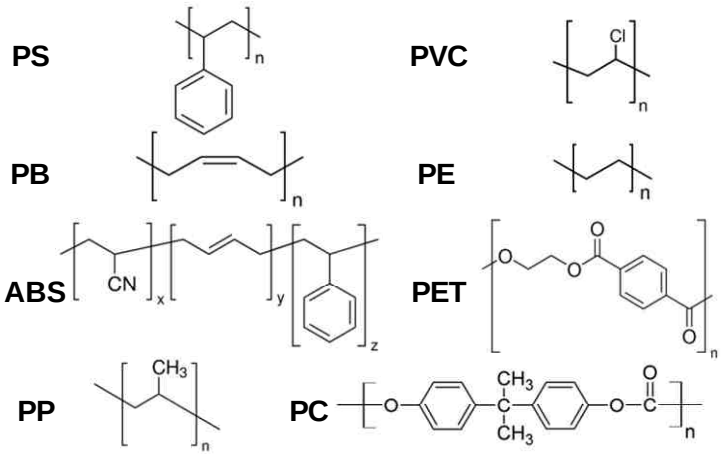

Figure 1.3. Molecule structures of most common polymers.

1.2. PLASTIC WASTES

The increasing trend in plastic innovation and consumption all over the world has led to increase plastic wastes and the difficulties for their management. Generally, two main groups of plastic wastes (PW) can be distinguished: industrial plastic wastes (IPW) and municipal plastic wastes (MPW).

These groups have different qualities and properties, and are subject to different management strategies. IPW are homogeneous and easily located and managed. On the other hand, MPW are post-consume residues generated after the use of plastic products and are usually found in municipal solid wastes (MSW), construction wastes and residues from electrical and electronic equipment [4].

The percentage of plastics in MSW has increased significantly. In 2006, waste plastics amounted to around 11.7 % of the weight of all MSW. In Europe, plastic wastes represent 15–25 wt.% of municipal waste. In China (2000) and Japan (2001), plastics in MSW constitute 13 wt.% and 7 wt.%, respectively. Similar values are found for India in 2003, where 9 wt.% of total MSW is related to plastic wastes. There are different sources of MPW such as domestic items (food containers, packaging foam, drink bottles, etc.) and most of these collected materials from MPW are a mixture of PE, PP, PS, PVC, PET, etc. [4].

However, there are more important sources for PW, such as industry or agriculture, which may contain much higher proportion of plastics. IPW (so-called primary waste) come mainly from construction and demolition companies (PVC pipes and materials), electrical and electronics industries (PVC cable sheaths, screens, etc.) and the automotive industries (car dashboards, seats, battery containers and more plastic materials) [4].

Plastic products may contain a wide concentration of different elements in the polymeric chain or as additives to improve the properties of the product. When these plastic products are discarded in landfills or incinerated, some elements such as halogen compounds and heavy metals can be hazardous components for environment and human health.

For PVC wastes, the chlorine of the polymer chain can be oxidized in the environment and produce toxic compounds. On the other hand, wastes from electrical and electronic equipment (WEEE or e-waste) and automotive shedder

residue (ASR) contain a big amount of metals apart from the halogenated flame retardants contained in plastics.

1.2.1. POLYVINYL CHLORIDE

PVC is one of the most commonly used thermoplastic material, its demand exceeding 35 million tons per year. PVC has a low commercial cost and inherent properties that make it a suitable plastic for the production of different products such as packaging materials, textiles, medical devices, pipes, windows, cable insulation, floors and roofs. Thus, as PVC is a highly demanded plastic, there is an increment on its production as well as a growth of PVC wastes [5].

Management of PVC wastes is not easy and has some disadvantages due to the characteristics of the material. PVC contains around 60 wt.% of chlorine and, when landfilled, it can be easily degraded by oxidation producing toxic halogenated compounds for the environment.

1.2.2. WASTE ELECTRICAL AND ELECTRONIC EQUIPMENT

Due to the high and constant demand of more efficient technology, electronic industry is constantly producing and selling newer devices, such as cell phones and computers, which have two years of lifespan more or less; thus, the old ones are obsolete and discarded [6].

Global production of WEEE amounts to around 40 million tons per year, and presents the fastest increment in MSW, with a rate of about three times the average [7]. Mobile phones represent one of the most valuable electronic wastes [8, 9] due to the presence of more than 30 elements, including precious metals (e.g., gold, cobalt, palladium and rhodium) [10]. About 100 million mobile phones and 17 million computers are estimated to be wasted annually around the world [11]. As estimation, around 8 million tons of computers, 1,300,000 TV sets and half a million of mobile phones will be produced as electronic wastes in 2016 [12]. In USA alone, over 30 million computers and 100 million cell phones are discarded every year. Only these phones will contribute with more than 10,000 tons of WEEE annually [13].

In China, for example, at least 4 million computers, 70 million cell phones, 5 million TV sets, 4 million refrigerators and 6 million washing machines have been abandoned annually since 2003 [12]. By year 2010, 610 million cell phones were disposed of WEEE in Japan [14]. In Europe, the amount of WEEE generated is 12 million tons per year, only 18 % of which is treated [15]. From this WEEE generated, a minimum recovery target must be achieved according to European regulations [16].

In general terms, WEEE is composed of metal (40 %), plastic, thermoplastic and thermoset polymers (30 %), and refractory oxides (30 %) [17]. Typical metal scrap consists of copper (20 %), iron (8 %), tin (4 %), nickel (2 %), lead (2 %), zinc (1 %), silver (0.2 %), gold (0.1 %), palladium (0.005 %) and beryllium, cadmium, mercury, etc. [18, 19].

Regarding the plastic fraction of WEEE, there is a wide variety of polymers (more than 15), but the most common constituents are HIPS (42 %), ABS (38 %) and PP (10 %) [20]. HIPS is the predominant plastic in TV housings, while ABS is the most common plastic found in computers, monitors and printers.

Small amounts of other plastics, such as PC, PVC, PA and a blend of ABS and PC, can also be found in WEEE. Phenol and epoxy resins are important thermosetting materials widely used for printed circuit boards (PCB) due to excellent thermal, mechanical and electrical properties [21, 22].

Moreover, plastics from WEEE may contain hazardous substances, such as heavy metals [23], brominated flame retardants (BFRs) [24-27] such as tetrabromobisphenol A and triphenyl phosphate [28, 29] and phosphorus flame retardants [30]. Some routes have been studied to reduce the brominated concentrations in WEEE [31, 32]. Thus, WEEE is considered as hazardous waste which must be treated in special facilities.

1.2.3. AUTOMOTIVE SHREDDER RESIDUES

End life vehicles (ELV) are one of the most difficult residues to manage due to wide composition of different materials. ELV are first disassembled to separate some parts, such as tires and batteries. Then, extrusion process is widely used to obtain

the automotive shredder residue. ASR is classified, in Europe, as hazardous waste due to its complex composition.

ASR is an heterogeneous mixture of materials composed by 19–50 wt.% of plastics and rubbers (PET, PUR, PP, PS, ABS, PC and PB), 8 wt.% of metals (steel, aluminum, copper and brass), wood (2–5 wt.%), textiles and fiber materials (10–42 wt.%), glass, fibers, rubbers and automobile oils (5 wt.%) and more hazardous substances (10 wt.%) such as polyhalogenated biphenyls, cadmium and lead [33-35].

Since 1979, the amount of plastic reinforced composites used in automotive industry has nearly tripled to reach around 10 wt.% in average of a modern vehicle. These new reinforced materials are composed by different substances such as polymers, flame retardants, inorganic fillers and glass fibers which improve the properties of the product. The use of these materials in automotive industry contributes to reduce vehicle weight, thus increasing fuel efficiency and decreasing CO_2 emissions from its use. However, the use of plastics also makes the management and recycle of ELV difficult [36, 37].

1.3. PLASTIC MANAGEMENT AND RECYCLING SCENERY

In 2012, 25.2 million tons of post-consumer plastic waste ended up in the waste upstream in Europe. 62 % was recovered through recycling and energy recovery processes, while 38 % still went to landfill (almost 10 million tons a year). In Spain, around 60 % of plastics are destined to landfill and there is no date of future landfill ban [2]. Increasing cost and decreasing space for landfills are forcing considerations of alternative options for PW treatment, recycling and recovery methods that can be economically and environmentally viable [1].

In 2008, the European Commission established new aims and objectives for EU waste policy [38] (2008/98/CE). The European Union's approach is based on the "waste hierarchy", which sets a priority order to waste management (Figure 1.4): prevention, reuse, recycling, energy recovery and, as the least preferred option, disposal (which includes landfilling and incineration without energy recovery) [38]. Figure 1.5 shows the destination of the different plastic wastes in Europe in 2010 [39].

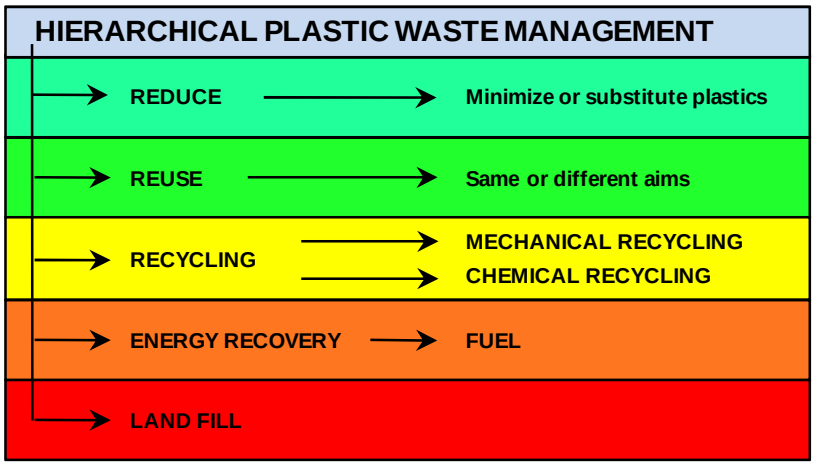

Figure 1.4. Hierarchical plastic waste management [38].

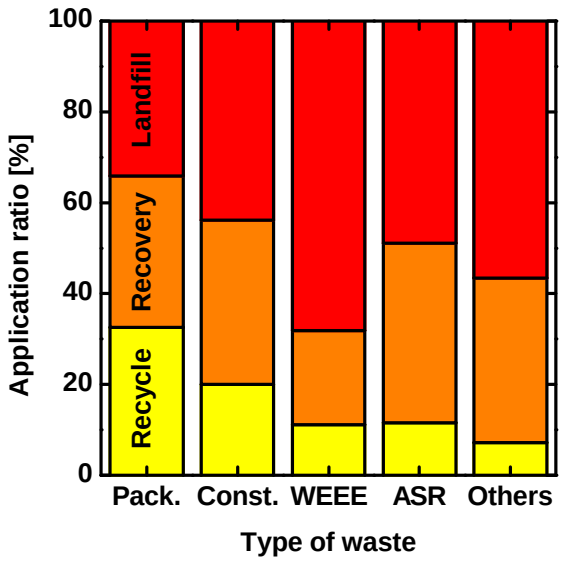

Figure 1.5. Type and application ratio of plastic wastes.

We can see packaging (Pack.) and construction (Const.) plastic residues have the highest recycling rate among the different types of wastes. However, for WEEE and ASR, landfill is nowadays the most used option and more efforts are needed in recycling and energy recovery methods.

1.3.1. REUSE

When a plastic product has reached its lifespan, reusing is the first option that should be considered. This method can be carried out to obtain a product with the same meaning, such as returnable packaging materials, or totally different products such as fillers for pavements. The main important advantages of re-using plastics are conservation of fossil fuels, reduction of energy and MSW and reduction of carbon dioxide (CO_2), nitrogen oxides (NO_X) and sulfur dioxide (SO_2) emissions [1].

1.3.2. RECYCLING

Recycling is the way to valorize residues that implies the transformation of the plastic residues into new products or valuable materials, reducing energy and pollution. PW recycling processes can be divided in three main categories: mechanical recycling (secondary), chemical recycling (tertiary) and energy recovery (quaternary).

Mechanical recycling involves physical treatment, whereas chemical recycling produces valuable hydrocarbons for the industry. There is another option called energy recovery, which involves the combustion of the material to produce energy [1]. Although this process is usually called quaternary recycling, in this thesis energy recovery has been considered a different process out from recycling options.

IPW are produced in large quantities and they are sufficiently clean to have an effective recycling of the materials by repelletization and remolding. On the other hand, MPW are heterogeneous wastes, and thermal cracking into hydrocarbons may provide a suitable means of recycling these wastes.

1.3.2.1. Mechanical recycling

Mechanical recycling is the process of recovering PW to be reused in manufacturing plastic products via mechanical and thermal ways. Mechanical recycling of PW can only be performed on single thermoplastic polymers, e.g. PE, PP, PS, etc., and the waste stream should be as clean as possible. One of the main issues in mechanical recycling is that PW is a heterogeneous stream composed by polymers, metals, additives, fillers; etc.

Therefore, sorting and washing pretreatments before mechanical recycling are needed to obtain valuable materials with high purity. Another inherent problem of mechanical recycling is that sometimes the temperature of the thermal process can affect the polymeric materials producing a certain degradation and, consequently, the lost of properties in the final plastic product [1].

1.3.2.2. Chemical recycling

Another way to reduce the impact of plastic wastes is tertiary recycling, also known as chemical or feedstock recycling. This method involves the transformation of polymer wastes into the original monomer or valuable hydrocarbons by chemical reactions. Through this method, quality of the new products is enhanced and they can be used in petrochemistry or as fuels. Moreover, heterogeneous and contaminated polymers may be easily removed in a treatment stage before or after the feedstock recycling process.

- **Solvolysis**

Solvolysis is a type of chemical recycling where nucleophilic reactions take place between weak bonds of polymer chains and the solvent to produce the monomer molecule. Most studied solvolysis reactions for polymer wastes are methanolysis and glycolysis of PET [40, 41].

- **Thermal cracking or pyrolysis**

Pyrolysis is the most common process for chemical recycling of plastic wastes. This process consists of the thermal cracking of polymer chains in inert atmosphere to produce gas, liquid and solid hydrocarbons. Product distribution depends on plastic waste composition, reaction time, pressure and temperature.

In thermal degradation, plastic is first decomposed to hydrocarbons related to its characteristic chemical structure (monomer and oligomers). The second step is the secondary thermal reaction of the oligomers to produce final hydrocarbons with lower molecular weight. The presence of heteroatoms in the polymer structure and in the additives to the plastic allows the formation of undesired compounds in the liquid fraction.

Regarding to operational conditions, higher reaction temperatures favor cracking reaction to gas products, aromatic hydrocarbons and char, while high pressures promote condensation reactions to yield heavy hydrocarbons. Increasing reaction time favors cracking secondary reactions to produce gases and char in detriment of the liquid fraction. Table 1.2 shows some pyrolysis studies at laboratory scale, such as thermogravimetric analysis (TGA), for different plastics.

Table 1.2. Summary of plastic thermal degradation studies.

Input	Conditions	Ref.
PE	Batch reactor, 823 K	[42]
PE	FBR, 773–973 K	[43]
PS	TGA and FBR (723–823 K)	[44]
PS	FBR, 923–1123 K	[45]
PB	TGA	[46]
PB	TGA	[47]
HIPS	TGA	[48]
HIPS	TGA and FBR (695–733 K)	[49]
ABS	STR 573–673 K	[50]
ABS	FBR (710–755 K)	[51]
PE/PP/PS	TGA and stainless steel reactor	[52]
Plastic mixture	FXR (703 K)	[53]
Plastic mixture	TGA and pyrolyzer reactor studies	[54]

Table 1.3 shows different pyrolysis facilities for plastic wastes degradation. These plants are based on different technologies like fluidized bed reactor (FBR), fixed bed reactor (FXR), moving bed reactor (MBR), rotary kiln (RK), stirred tank reactor (STR) and far-infrared inner heating system (FIR) and some of them are already shutdown due to economical reasons.

Table 1.3. Industrial facilities for plastic thermal degradation processes.

Technology	Input, %	Conditions	Output, %	Ref.
PYROPLEQ®	PW/MSW	RK 723–773 K	E	[55, 56]
AKZO Nobel	PVC rich PW	FBR 973–1173 K	HCl/CO/H_2/ CH_4	[57]
PKA–Kiener	PW/MSW	RK 723–773 K	G/E	[57, 58]
BP polymer cracking (not applied)	PW/PET (3)/ PVC (2)	FBR 773 K	O (85)/ G (15)	[59]
BASF (shutdown)	PW/PVC (2.5)	Multiple stages 673 K	HCl/O/G	[59]
Noell (shutdown)	PW/PVC (15)	RK 873–1023 K	C/O/G	[57]
Toshiba (shutdown)	PW/PVC (20)	RK	O	[60, 61]
Siemens–KWU	PW	RK 723–773 K	G (65)/ S (35)	[57]
DBA process	PW	RK 723–773 K	E	[57]
Kobe Steel	PW	RK 723–773 K	O/G	[57]
Ebara	PW	FBR	E	[56]
Mogami–Kiko	PP (67)/ PE (33)	STR	O (79)/ G (12)	[62]
Hitachi–Zosen	PE (55)/PP (28)/PS (17)	STR	O (84)/G (10)/S (6)	[62, 63]
Royco Beijing	PE/PP/ PS/HIPS/ waste oils	FIR system	O (87)/G (10)/S (3)	[62, 63]
Chiyoda process	PW	STR	O (50)/G (16)/S (34)	[62, 63]

O: oil; G: gas; S: solid; C: coke; E:energy; M: metals

- **Catalytic cracking**

Catalysts have been widely used to improve pyrolysis processes by reducing the temperature and increasing the degradation rate and improving the product selectivity of the fuel and valuable chemicals produced [64, 65]. There are many studies of catalytic cracking of polymer wastes and most of them are focused on acid catalysts due to their properties to break C–C bonds of polymer chains [66].

The most important studies related to plastic catalytic degradation are summarized in Table 1.4.

Table 1.4. Summary of plastic catalytic degradation studies.

Input	Conditions	Ref.
HDPE/PP	Batch reactor, 773 K, HZSM5, SiO_2	[67, 68]
PP/LDPE/PS/PVC	Batch reactor, 633–693 K, Al/Zn composite	[69]
LDPE/PP/PS/PVC	Batch reactor, 633–693 K, Al/Mg composite	[70]
PE/PP/PS/PVC	Extruder and STR, 633–713 K, SiO_2/Al_2O_3	[71]
PE/PP/PS/PVC/PET	Stainless steel unstirred reactor, 663–973 K, red mud	[72]
HDPE/LDPE/PP/PVC	FBR, 793 K, FCCR1, HUSY, SAHA, ZSM5	[73]
HDPE	TGA, HZSM5, MCM41	[74, 75]
HDPE/LDPE	HZSM5, MCM41, HY, AC, SiO_2/Al_2O_3, charcoal poder	[75]
HDPE	FBR, 633 K, HZSM5, SiO_2/Al_2O_3 and MCM41	[76]
PS/naphthalene	Pyrex tube, 623–653 K	[77]
PS/solvents	Autoclave, 523–723 K, 20 bar	[78]
PS/mineral oil	Flask with reflux, 548–623 K, MgO	[79]
PS/solvents	Autoclave, 623–723 K	[80]
PB/diphenyl ether	STR, 533–573 K, cobalt catalyst	[81]

These processes work under mass transfer limitations due to the big size of polymer molecules, which present high viscosity when melt down and form a liquid phase and have difficulties to access the inner surface of solid catalysts [82]. Using solvents to reduce viscosity is a common way to reduce mass transfer limitations and favors polymer degradation. A list of the industrial or pilot plants for catalytic degradation processes of plastic wastes is summarized in Table 1.5.

Table 1.5. Industrial facilities for plastic catalytic degradation processes.

Technology	Input, %	Conditions	Output, %	Ref.
Fuji process	PE/PP/PS/PET/PC (15)	673 K, HZSM5	O (85)	[57, 62]
Amoco	PE/PP/PS	763–853 K	O/G	[56]
Mazda	ASR/PE/PP/PS/PU/ABS	FBR/Al_2O_3, $ZrCl_4$ 473–723 K	O (60)	[83]
Nikko	PW	FBR/metal catalyst 473–523 K	O (80)	[56]
Reentech	PE/PP/PS/PVC	MBR/Aluminium-silicate/623–673 K	O (75)/G (15)/S (10)	[62, 63]
T–Technology Polymer Energy	PE/PP/PS	RK	O (78)	[62, 63]
NanoFuel	PP/PE/ biomass	HY, 543–643 K, <0.1 bar	O (94)	[62, 63]
Thermofuel/ Cynar	PE/PP/PS	623–698 K Metal catalyst	O/G/C	[62, 63]
Zadgaonkar	PW	623 K	O (75)/G (20)/C (5)	[62, 84]
Fuji	PE/PP/PS	FXR, HZSM5, 663 K	O (75)	[62, 83]
Smuda	PW/PET	STR/623 K/<0.1 bar/ Nickel silicate Ferrous silicate	O (95)	[62, 63]

O: oil; G: gas; S: solid; C: coke; E:energy; M: metals

However, the oil obtained from these processes at inert atmospheres and high temperatures contains mainly aromatic compounds, such as benzofurans and phenols. These structures are present in PS chains and they are also produced due to H_2-abstraction from light hydrocarbons and crosslinking and cyclization reactions of polyene chains.

These chemicals have been found to be carcinogenic substances and they are limited in liquid fuels. Thus, there must be a transformation of the aromatic compounds before the pyrolysis oil product can be used as fuel. In order to crack polyaromatic hydrocarbons, very high temperatures (>1473 K) are needed, and increasing reaction temperatures also yields to typical cracking gases such as H_2, C_2H_4 and C_2H_2 [1].

Halogenated and phosphate compounds from the decomposition of flame retardants are also produced in pyrolysis processes. Halogenated products should be removed because combustion of oil containing these chemicals can produce highly toxic compounds [85]. Thus, it is necessary to control the chloride content in the feedstock [86]. Fillers present in plastic wastes, like $CaCO_3$, can act as halogen trap, helping to remove halogenated compounds from the liquid fuel [87, 88]. But this is not enough and further hydrotreatment steps are still needed to upgrade pyrolysis oil to be used as fuel [89-95].

- **Hydrotreatment**

The next step after pyrolysis of waste plastics should be a hydrotreatment process to upgrade the pyrolysis oil product. However, just a few hydrotreatment studies or industrial plants for pyrolysis oil upgrading have been developed and they are shown in Table 1.6. These technologies are either shutdown at industrial scale, due to economical reasons, or still at the research stage.

Table 1.6. Industrial facilities for plastic hydrotreatment processes.

Technology	Input, %	Conditions	Output, %	Ref.
Veba VCC	PE (60)/PP (5)/ PVC (10)/ PS (15)/PA (5)/ PET (5)	Depolymerization/hydrogenation RK/623–723 K/ 100 bar	O/HCl/G	[59]
RWE	PW	Depolymerization/hydrogenation 673–773 K 300–400 bar	O (80)/G (10)/S	[57]
Hiedrierwerke	PW	Hydrocracking 673 K/250 bar	O/G	[57]
Freiberg	PW	Hydrocracking/ 673–708 K/ 280 bar	O/G/S	[57]
Böhlen	PW	Hydrocracking 723–743 K 270 bar	O (80)	[57]
ITC	PW	Hydrocracking 708 K 10–100 bar	O/G	[57]

O: oil; G: gas; S: solid; C: coke; E:energy; M: metals

Veba Oil was the most important hydrogenation industrial process for feedstock recycling of plastic materials. Veba Oil AG was a hydrogenation plant in Bottrop, Germany, using the Pier coal liquefaction technology to convert coal into fuel oil. The plant was modified to convert plastic wastes from packaging into fuel oil by adding a previous depolymerization unit and the Veba Combi Cracking (VCC) technology.

Lignite acts as both feedstock and catalyst of the process and Na_2CO_3 and CaO are added to neutralize the HCl generated in the reaction process. However, the commercial process of the plant was finally shutdown because hydrogenation was unable to compete economically with treatment in blast furnaces and with the SVZ process at Schwarze Pumpe. The flow diagram of the Veba Oil plant is described in Figure 1.6.

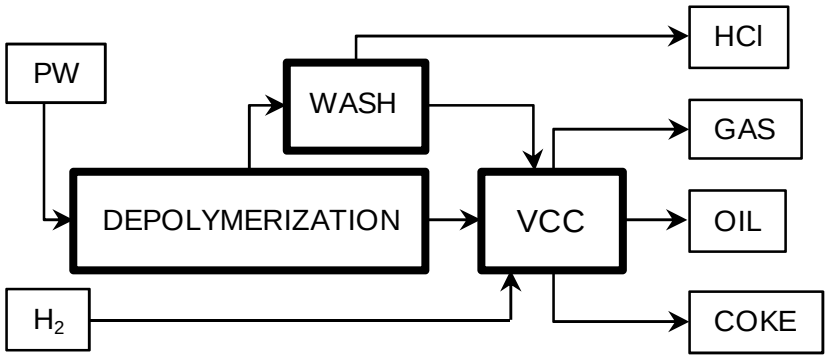

Figure 1.6. Veba Oil VCC plant diagram [59].

The plant includes a first depolymerization unit and then the VCC process. In the first stage, waste plastics are degraded and dechlorinated at 623–673 K. 80 wt.% of the total chlorine content is produced as HCl gas which is washed and finally sold. Condensable gases still contain chlorine and they need to be hydrogenated to remove the halogenated compounds. Then, the fuel oil is treated in VCC system at 100 bar and 673–723 K.

Comparing pyrolysis and hydrotreatment, gas and liquid yields obtained from pyrolysis is 50 and 40 wt.%, respectively. On the other hand, gas and liquid products obtained in hydrotreatment process are 10 and 85 wt.%, respectively.

Moreover, through this process, hetero-atoms contained in the plastics (Cl, O, N, S) are hydrogenated to produce secondary products.

Another interesting technology for plastic wastes decomposition including hydrotreatment stage after pyrolysis, is RWE process. Plastic waste is firstly mixed with vacuum oil fraction and then the mixture submitted to depolymerization. Halogenated compounds are then removed in a hydrotreatment unit at 673–773 K and 300–400 bar.

- **Hydrocracking**

Hydrocracking processes are different to hydrotreatments after pyrolysis. Hydrocracking is one of the most promising processes to convert plastic wastes into valuable chemicals and liquid fuels because it combines plastic degradation and reduction of aromatic and heteroatom concentration by hydrogenation and substitution reactions, in one main stage. The most relevant studies for hydrocracking of plastic wastes are presented in Table 1.7.

Hydrocracking is usually carried out in the presence of bifunctional catalysts (zeolites, SiO_2/Al_2O_3 or activated carbon (AC) catalysts) and in two different ways: direct hydrocracking of plastics [96-100], and hydrocracking of solved plastics in decalin (DC), tetralin (TT) or vacuum gas oil (VGO) and alkanes [101-111].

- **Gasification**

Gasification processes imply partial oxidation of plastic wastes at high temperatures, 1073–1673 K, under poor oxidation with steam, CO_2 or substoichiometric oxygen. Two step processes based on pyrolysis and gasification are also a method to produce valuable chemicals from plastic wastes [112]. The most common industrial facilities for gasification of plastic wastes have been summarized in Table 1.8.

Table 1.7. Summary of plastics hydrocracking studies.

Input	Process condition	Ref.
HDPE	Autoclave, 673–708 K, 35–140 bar $TiCl_3$, HZSM5	[96]
HDPE	Autoclave, 648 K, 17–70 bar NiMo/HSiAl, KC2600	[97]
PE	FXB, 673 K Pt/HZSM5, Pt/HY, Pt/HMCM41	[98]
LDPE	Autoclave, 693 K, 100 bar Ni–Mo/Al_2O_3	[99]
HDPE/LDPE/PP	Shaking autoclave, 648–723 K, 50 bar DHC8	[100]
PE/DC/TT	653–723 K, 55 bar SiO_2/Al_2O_3, HZSM5, HY	[101]
PVC/PET/ LDPE/TT	Microautoclave reactor, 693–713 K, 55 bar	[102]
HDPE/PP/PS/ alkanes	Microreactor, Pt and Ni over ZrO_2/SO_4 and ZrO_2/WO_3	[103]
LDPE/PP/ PVC/VGO	Shaking autoclave, 698–723 K, 65 bar DHC8, HZSM5, Co/AC	[104]
HDPE/VGO	Shaking autoclave, 698–723 K, 65 bar DHC8, Ni/AC, Co/AC, Mo/AC	[105]
PW/VGO	Shaking autoclave, 698–723 K, 65 bar DHC8	[106]
PS/DC	STR, 598–698 K, 180 bar Pt over h-HZSM5, HZSM5, Ferrierite, ITQ6	[110]
PS/DC	STR, 598–698 K, 180 bar Pt/Ferrierite, Pt/ITQ6	[111]

Table 1.8. Industrial facilities for plastic gasification processes.

Technology	Input, %	Conditions	Output, %	Ref.
Ebara TwinRec	PW/ARS	FBR/ 773–873 K	E/M	[56]
Texaco	PW (10)	FBR/ 1473–1773 K	G	[56]
Lurgi (SVZ)	PW/ASR/waste oil/lignite/WEEE	FXR/ 1873–2073 K	G/CH_3OH/E	[57]

O: oil; G: gas; S: solid; C: coke; E:energy; M: metals

1.3.3. INCINERATION AND ENERGY RECOVERY

Energy recovery by incineration implies burning plastic wastes to produce energy (heat, steam or electricity) due to the high calorific value of plastics. This method can achieve a volume reduction of 90–99 %; however, this process is the last option before landfilling because combustion of the toxic hazardous compounds present in plastic wastes produces pollutants in the flue gas, such as CO_2, NO_X and SO_X. Combustion of PW is also known to generate volatile organic compounds (VOCs), smoke (particulate matter), particulate-bound heavy metals, polycyclic aromatic hydrocarbons (PAHs), polychlorinated dibenzofurans (PCDFs) and dioxins. Thus, another option environmentally more favorable should be found first [1].

1.4. MANAGEMENT OF HAZARDOUS PLASTIC WASTES

The inherent toxicity problems of hazardous plastic wastes require consideration of a proper way for their management and recycling.

1.4.1. PVC MANAGEMENT

Due to the high chlorine content of PVC (60 wt.%) and its low thermal stability, some techniques for PVC recycling are not favorable. Chemical recycling may be disfavored because of the large amounts of hydrogen chloride and other toxic products that are present in the products.

If chemical recycling is used to obtain valuable chemicals, such as fuel, halogenated compounds should be firstly removed because combustion of chlorine-containing oils can produce highly hazardous compounds for environment and human health [85].

Moreover, it seems that there is no sense to obtain a liquid fuel when the hydrocarbon concentration of the raw material is only 40 wt.%. Chemical recycling only becomes a viable solution when feedstock products is above 40 wt.% yield and with a high commercial value [63].

Incineration is not favorable for PW, much less for highly halogenated plastics such as PVC, also because of the toxic compounds produced in combustion gases. Landfilling is no good idea either, because oxidative degradation of PVC can occur and toxic chemicals can be released to the environment [1].

Thus, if the origin of PVC wastes is known and they are clean enough to produce another saleable plastic product, mechanical recycling of PVC will be the best option. Even though only a very small part of PVC is nowadays recycled in the world, PVC wastes mechanical recycling has been practiced for many years and Germany is the most advanced country for PVC recycling [5].

PVC can be easily mechanically recycled due to its structure and composition, and good quality materials are produced. Rigid PVC recycled material is mainly used as an inner reinforcement layer in the production of pipes and profiles, garden furniture or the manufacture of rigid films. Flexible PVC waste is recycled into powder and used as filler in the production of floor coverings of various kinds. Other applications are traffic cones, fences, flexible hoses and tubes, footwear, bags, clothing, etc. [1].

The low thermal stability of PVC is widely known to make mechanical recycling difficult. Thus, low temperature thermo-mechanical recycling processes should be carried out to keep mechanical properties and to obtain new valuable plastic products. Thermal degradation of PVC is caused by dehydrochlorination (DHC) at the internal defects in its structure [113].

Hydrogen chloride produced in DHC step plays an important role as catalyst of the degradation process, by attacking monomer molecules to abstract hydrogen. This new product is a radical compound that reacts with another chlorine atom to generate a new structural defect on the polyene chain [114]. After DHC, thermal degradation of PVC at high temperatures implies chain scission, crosslinking and condensation reactions [115].

Some studies related to PVC thermal recycling have been developed by different authors. Thermogravimetric analyses were the first experiments to study the pyrolysis of PVC and determine the evolution of degradation products [116, 117]. Chattopadhyay and Madras also studied thermal and catalytic degradation of PVC (0.2 wt.%) in solution with diphenyl ether as solvent. The authors concluded that the use of HZSM5 catalyst favors PVC degradation due to the presence of acid

Brønsted sites, characteristic of the zeolite, where cracking reactions of polymer chains take place [118, 119].

Kamo et al. [120] studied thermal degradation of PVC, and the main products in the absence of solvent were HCl and a solid residue. HCl production approximately corresponds to chlorine concentration of the PVC sample. The authors also studied the chemical degradation of PVC in the presence of decalin and tetralin in an autoclave reactor vessel. Reaction temperatures were 573–733 K and nitrogen pressure 40–224 bar. Decalin was chosen due to its stability, and tetralin due to its hydrogen donor capacity [121].

The authors also concluded that yield to the solid product increases with pressure up to a maximum of 100 bar. At this pressure, the liquid products are partially polycondensed with the insoluble products forming the solid residue. Above this pressure, the yield to solids decreases because liquid products partially solve the solids at high pressures, and polycondensation reactions are inhibited. Regarding the liquid products, benzene and alkylbenzenes, obtained from cyclation reactions, are the main products at atmospheric pressure. Their yield decreases with pressure in detriment of paraffin products coming from hydrogenation of polyene chains [121].

Kamo et al. [121] suggested that the use of an adequate solvent plays an important role in the liquefaction of solid products, as it favors hydrogen transfer and dispersion to the polyene chains, helping solvolysis reactions and inhibiting polycondensation reactions which limit solid residue production. Kamo and Kodera [122] concluded that hydrotreatment of dehydrochlorinated PVC in tetralin at 77 bar of hydrogen in the presence of nickel–molybdenum catalysts improved the yield to liquid products in detriment of the production of a solid residue.

Tongamp et al. [123, 124] studied a one-step mechanochemical treatment of PVC and PE (673–823 K) to produce hydrogen gas, using powder $Ni(OH)_2$ as catalyst and CaO or $Ca(OH)_2$ for chlorine removal. Gasification processes to obtain valuable gaseous chemicals is another option for chemical recycling of PVC and dehydrochlorinated PVC [125-127]. There are some studies and industrial facilities or pilot plants where only PVC samples can be recycled as the main feedstock as shown in Table 1.9.

Table 1.9. Summary of PVC degradation studies.

Input	Studies or processes	Ref.
PVC	TG studies	[116, 117]
PVC	Thermal and catalytic degradation in solution	[118, 119]
PVC	Thermal degradation in solution	[120-122]
PVC	Mechanochemical treatment	[123, 124]
5%PVC	Metallurgy oven	[110]

1.4.2. WEEE MANAGEMENT

European Community established the WEEE Directive in 2003 in order to address the environmental problems associated with the management of WEEE [128]. According to the EU statistics, five countries from 28 EU members have achieved the 45 % target in 2010. On the other hand, Spain showed a collection ratio less than 20 % [129].

Nowadays, WEEE is stored in land fields [130] or uncontrolly exported to developing countries in Asia and Africa [131-133]. The Basel Convention prohibited the trans-boundary movements of toxic waste [134]. Although nowadays obsolete computers and cell phones are exported to developing countries for reuse, sometimes the word ‘waste’ is hidden behind the word ‘charity’. The percentage of WEEE collected in China from other countries increased by 70 % in 2010–2011 and 1.5−3.3 million tons of WEEE are estimated to be illegally exported to China every year [19]. 75 % of the estimated 8.7 million tons a year of WEEE in the European Union (EU) is the general ‘hidden flow’.

Greenpeace defined hidden flows as the amount of WEEE that escapes the control of responsible collection, reuse and recycle, causing environmental damage. In the United States (US), hidden flows are even larger: around 80 % is incinerated, sent to landfill, put into ‘storage or reuse’, or exported [12]. Huge amounts of these illegal movements of WEEE finish along the coast of southeastern China, which has become the biggest dumping ground of WEEE, accommodating more than 70 % WEEE all over the world annually [135].

Electronic wastes are occupying space and polluting our environment, and the rudimentary recycling methods used in developing countries are dangerous because workers are exposed to hazardous materials and processes are not very efficient to recover all valuable materials [136]. Only around 10 wt.% of WEEE generated in the world is being recycled in adequate recycling facilities [137], although some of these facilities are very efficient, recovering up to 80 wt.% of the materials in WEEE [138]. The use of recycled instead of virgin materials will also, as a whole, cause less pollution during extraction and further processing of the materials [139]. WEEE has become a global environmental issue and a proper solution for its management and recycling must be found.

Many routes have been established to reduce the impact of accumulating plastic wastes in landfills producing valuable products or energy [3, 140, 141]. Burning the electronic scrap has been demonstrated not to be a suitable process for WEEE treatment, due to the formation of hazardous compounds for environment and human health [142]. WEEE incineration may cause emission of toxic fly and bottom ash which contain hazardous metals such as lead and cadmium [143]. Recycling of WEEE is an important subject not only from the point of view of waste treatment but also of the recovery of valuable metals [144]. In Japan, there are already regulatory systems for WEEE and necessary technologies have been developed for metal recycling [145].

Some authors studied the recovery of materials from milled PCB residues and dismantled electronic wastes [146]; however, mechanical recycling of WEEE is neither economically nor environmentally profitable [147]. Few studies have been conducted on recovering useful materials from electronic packaging residues in order to improve the process economy [148]. In some processes, the recovery of precious metals from electronic waste is carried out by high temperature processes (~1473 K) such as pyrometallurgical processing, hydrometallurgical processing and biometallurgical processing [149]. Other authors studied solvothermal techniques to remove organohalogenated flame retardant compounds from the plastic fraction of WEEE [150].

Recently, many studies have been carried out about chemical recycling of WEEE [151] and some of them are presented in Table 1.10.

Table 1.10. Summary of WEEE degradation studies.

Input	Studies or processes	Ref.
WEEE plastics	Pyrolysis	[152]
PCBs	TG pyrolysis studies	[153]
PCBs	TG pyrolysis studies	[154]
Flame retarded plastics/PCBs	Pyrolysis studies, FXR	[155-157]
PCBs	Pyrolysis and combustion	[158]
PCBs	Pyrolysis	[159]
PCBs	Pyrolysis	[160-162]
PCBs	Gasification	[163]
Flame retarded plastics	Gasification	[164]

Thermogravimetric experiments for pyrolysis of integrated circuit boards have been carried out to study the kinetics of the degradation process [153, 154]. Hall and Williams [155, 156] widely studied the pyrolysis process of flame retarded plastics and PCBs in a fixed bed reactor at different temperatures and using zeolites for halogen removal [157]. Pyrolysis and combustion of PCBs were also studied by Moltó et al. [158]. Other authors studied the vacuum pyrolysis of PCBs at 823 K followed by mechanical processing to separate copper, glass fiber and carbon [165].

Blaszó et al. studied the pyrolysis and debromination of flame retarded polymers from electronic scrap, such as PCBs, in the range 723–863 K [159]. Vasile et al. studied a two-step degradation process for PCB wastes based on pyrolysis (573–723 K) and catalytic hydrotreatment to upgrade the pyrolysis oil (743 K) [160-162]. Some interesting advantages of pyrolysis processes are that metals present in WEEE are not oxidized and they can be separated after the recycling process and recovered for further use.

Gasification processes for hydrogen production is a feasible technology for chemical degradation of WEEE [166]. Yamawaki et al. [164] concluded that gasification of plastic WEEE at high temperature (1423 K) followed by a shock cooling step is an effective process to decompose the BFRs to comply with regulatory values. Zhang et al. [163] studied the gasification of phenol circuit boards at mild temperatures in the presence of molten carbonates to produce clean

hydrogen. Yang et al. [167-169] also studied a reactor with a mixture of molten carbonates for the abatement of halogenated compounds by oxidation of plastics at high temperatures (1173 K).

Therefore, conversion of plastics contained in WEEE to clean hydrogen by steam gasification at mild conditions contributes to use organic resources effectively and to recover useful metals easily after the process. Stelmachowski studied a process to obtain gas and gasoline products from waste polyolefins in a molten metal mixture of tin, lead and bismuth or their alloys [170]. Thermal treatment with steam at 455–530 K and 10–45 bar was carried out by Chen et al. [171] as an alternative process to separate valuable metals from printed circuit boards.

1.4.3. ASR MANAGEMENT

The 2000/53/CE European Directive establishes minimum levels of resources and energetic recovery that should be obtained from ELVs. Nowadays, there is a huge amount of this ASR still placed in land fields. However, there are some technologies for ASR treatment in order to obtain valuable products [172].

Mechanical treatments may not be a good way to recycle ELV because the average vehicle contains about 25–35 types of plastics and the identification of each material must be carried out before shredding, which can be difficult and expensive. There is no robust infrastructure for sorting and collection of end-of-life automotive plastics and post-shredder separation is not a viable recycling option [36].

Regarding chemical recycling of ASR, Zolezzi et al. [33] studied the fast pyrolysis at laboratory and pilot plant scale for temperature ranging from 773–1073 K. The authors concluded that, in both cases, carbon conversion was above 80 wt.% maximizing gas and liquid products at 35 and 20 wt.%, respectively. Vermeulen et al. [34, 35] studied the sustainability assessment of ASR and the authors concluded that, in order to solve ASR land filled storage in the short and long terms, recycling combined with energy valorization of the residual fractions is the most feasible way. Other possibility for chemical recycling is catalytic gasification process as studied by Lin et al. [173] to produce valuable fuel gas such as hydrogen.

Incineration of ASR is not a suitable process due to the characteristics of the feed. However, co-incineration of ASR with other residue streams, such as municipal solid waste, was studied by many authors and it can be concluded that there is no significant change in flue gas emissions compared to the incineration of MSW alone. Nissan modified the plant to obtain energy from the co-incineration of 4,800 tons of ASR per year in a fluidized bed combustor, and the gases produced are also used in the process [35]. More industrial facilities for ASR recycling are summarized in Table 1.11.

Table 1.11. Industrial facilities for thermal degradation processes of hazardous plastic wastes.

Technology	Input, %	Conditions	Output, %	Ref.
NKT	PVC rich PW	2–3 bar 648 K	HCl/C/M/O	[56]
AKZO Nobel	PVC rich PW	FBR 973–1173 K	HCl/CO/H_2/CH_4	[57]
KEU process	PVC	623–823 K	E/S	[57]
Toshiba	ASR	FBR	G/M	[56]
ConTherm®	ASR/PW	RK/773–823 K	E	[55, 58]
PKA	MSW/ASR/tires	RK/773–823 K	G/C	[174]
PyroMelt	MSW/ASR/PW	1473 K	O	[140, 175]

O: oil; G: gas; S: solid; C: coke; E:energy; M: metals

1.5. HYDROCRACKING BIFUNCTIONAL CATALYSTS

Supported noble metals are the most common bifunctional catalysts employed in this kind of processes. Zeolites are the most used supports due to their characteristic acidity (Brønsted and Lewis sites) which favor cracking reactions of long polymer chains by β-scission reactions [176]. On the other hand, hydrogenation reactions of aromatic compounds occur on the metallic surface of the catalyst and platinum is one of most widely used noble metals for hydrogenation-dehydrogenation reactions [177].

In order to reduce mass and heat transfer limitations, active sites of the catalyst should be accessible to the polymer molecules. Transport of polymer molecules in

the liquid phase to active sites of the catalyst involves two steps: a first transportation to the external surface area and, if possible, diffusion inside the catalyst pores [109, 178]. Therefore, the location of both acidic and metallic sites on the surface of the catalyst is an important issue to take into account for the accessibility to the polymer molecules [179, 180]. Product formation inside the pores of the support is also limited by structural characteristics of the catalyst [181, 182].

During the last decade, developing technology for synthesis of hierarchical structures has succeeded to reduce diffusional problems in processes with high mass transfer limitations [183, 184]. The concept of hierarchical zeolites is attributed to zeolitic materials which have a hierarchical porosity with, at least, two levels of pore size.

This fact means that those materials have not only the common and characteristic micropores of the zeolite but also a secondary porosity consisting of pores with different sizes (meso and macropores) substantially increasing the external surface area of the material. This entails an improvement in accessibility of the catalyst, especially in polymer degradation processes with high mass and heat transfer limitations. Apart from this, hierarchical catalysts improve also selectivity to the desired products, inhibit coke formation and extend the activity life of the catalyst [185].

Nowadays, there are two main strategies to produce hierarchical zeolites: template, or bottom-up, and non-template, or top-down, methods [186-189]. Bottom-up method requires the synthesis of a zeolite with the desired conditions and properties [190-192] and, from an economical point of view; it is not feasible due to the high cost and not always commercial availability of reactants such as mesopore-inducing agents [193].

Top-down method involves a modification step of a synthesized zeolite by a dealumination or a desilication treatment to create intracrystalline mesopores. This method requires the elimination of aluminum or silicon from the framework of the zeolite, and the characteristics of the new material depend on what type of atom (aluminum or silicon) is removed from the network [194]. Dealumination is normally performed by two methods: high temperature treatment with steam, or acid

treatment [195-199]. Desilication is mostly carried out by alkaline treatment to remove the framework silicon and produce an additional mesoporosity [200].

As polymer molecules cannot enter the inner pores of the catalyst and contact the metal phase in such pores, the active metal should be placed as close as possible to the external surface area of the catalyst particle. This kind of metal distribution is commonly known as egg-shell profile [201-207], and it can also favor selectivity for consecutive reactions, such as hydrogenation and isomerization [208, 209].

Thus, catalytic properties can be affected by the amount and distribution of the metallic material on the internal surface of the support [210]. Optimal metal content is essential to obtain the desired metal distribution in the catalyst [211], to improve the yield of the process and to benefit the global economy by reducing cost and pollution [212, 213].

Preparation of supported metal catalysts is basically based on three main steps: deposition of the active metal on the surface of the support, removal of the liquid solvent from the pores of the support by a drying stage, and activation step to obtain the final active metal [214, 215]. In this work, the activity effect of two of the most common preparation methods for low metal loading was studied: ion exchange and impregnation. These methods allow for the production of catalysts with different metal-support interaction and metal distribution [216].

The metal deposition and distribution over the support is controlled by metal addition step. Metal adsorption highly depends on metal-support interaction, ion concentration, adsorption equilibrium, permeability, and diffusion rates. These interactions may be physical (hydrogen bond) or chemical (ion or ligand exchange) [215]. Under strong interaction conditions, metal deposited on the support is greater than the metal amount in the solution; thus, the drying step has no relevant effect on the final catalyst distribution. However, for a weak metal-support interaction, metal distribution of the catalyst is directly related to metal loading and drying conditions (temperature, and mass and heat transfer) [217-219].

Therefore, in this work we studied the drying step for a weak metal-support interaction of the impregnation for low metal content catalysts. Using fast drying conditions combined with impregnation (e.g., high temperature), metal particles can migrate to the external surface of the catalyst to obtain an egg-shell profile. In case a more uniform metal distribution is desired, the drying step should be carried out

under moderate drying conditions [207, 215, 220-222]. Regarding metal loading, for low metal content, increasing the initial amount of active metal concentration can enhance the final egg-shell configuration [223-225].

1.6. OBJECTIVES

European regulations established environmental directives to reduce and control wastes streams for the next years. These directives have a global vision with specific statements for each waste stream, and they are focused on the origin of plastic wastes, such as packaging, construction, WEEE or ASR. Directives suggest an efficient use of natural resources, as well as proper solutions for plastic waste management, in order to minimize plastic wastes in landfills and reduce their impact to environment and human health.

Chemical or feedstock recycling of plastics consists of the transformation of plastic residues by chemical reactions in order to produce valuable hydrocarbons for feedstock to petrochemical industry or as fuels. Even though some plastic wastes can only be chemically recycled, chemical recycling is still placed on the third level of the hierarchical list for plastic waste management. Moreover, some chemical recycling processes require less pretreatment stages than other recycling methods best prioritized, which makes tertiary recycling favorable to other processes.

Nowadays, chemical recycling only considers obtaining raw material products for the petrochemical industry. Although it is the same chemical recycling method, if the product obtained is used as a fuel, the process is degraded to energy recovery in hierarchical plastic management. This issue is currently being discussed, because some chemical recycling processes have several environmental and economical advantages compared to energy recovery by incineration.

Previous work on hydrocracking of plastic wastes to obtain liquid fuels has been carried out in the research group, where the bases of the process were established. This thesis is specially related to valorization of plastic wastes such as WEEE and ASR, also considering the removal of high heteroatom content from the fuel product.

The first objective of the thesis is to advance on the design of bifunctional Pt/zeolite catalysts for hydrocracking of plastic wastes to liquid fuels for automotive

applications, focused on the modification of the acidic properties of the support on the one hand, and on the platinum content and distribution on the other. As the objective is related to catalyst design, the studies should be carried out under kinetic control, and with a simple polymer such as PS.

However, actual plastic wastes, such as WEEE and ASR, are composed of many different polymers. Thus, the effect of polymer composition on catalytic performance and distribution of products is the next objective to be studied, starting with polymers composed of just carbon and hydrogen, such as PB and HIPS, and continuing with plastics containing heteroatoms, such as ABS, and finishing with actual plastic wastes. At this stage, the objective is to determine the effect of process conditions on the quality of the liquid fuel, in order to minimize the presence of heteroatoms in a single step.

The heterogeneous nature of PCBs and some electronic capacitors (EC) obtained from WEEE, and also some actual plastic wastes, makes their chemical recycling by hydrocracking unfeasible. Thus, at the end of this thesis, valorization of these residues through steam gasification of these compounds PCBs and EC is the last objective, as an effective recycling solution to obtain clean hydrogen as gas fuel from complex WEEE and recover the valuable and useful metals after the gasification process for a next use.

Chapter 2

MATERIALS, METHODS AND EQUIPMENTS

Capítulo 2

MATERIALES, MÉTODOS Y EQUIPOS

RESUMEN.

En este capítulo se presentan los diferentes materiales utilizados a lo largo del trabajo, junto con sus especificaciones, de acuerdo con el fabricante. Se detallan, además, los procedimientos de fabricación y los métodos de caracterización de catalizadores, indicando para qué se han empleado, los equipos, el procedimiento experimental que se ha seguido en cada caso, y cómo se han hecho los cálculos.

Se describe, por otro lado, el equipo empleado para las reacciones de hidrocraqueo y de gasificación con vapor, los dos procesos de valorización de residuos plásticos que se han desarrollado en esta tesis doctoral, el procedimiento experimental, y la toma y análisis de muestras. Finalmente, se resumen los principales métodos de cálculo que se han aplicado.

2. MATERIALS, METHODS AND EQUIPMENTS

This chapter is devoted to the description of materials, protocols, equipments and methods used all over the thesis. Initially, the main chemicals and products used in the work are identified. Then, procedures for catalyst preparation and characterization are described. Finally, the reaction procedures are indicated, together with the way in which the results have been analyzed.

2.1. MATERIALS AND REACTANTS

The chemicals used in this work for synthesis, preparation, characterization, hydrocracking and steam gasification studies have been grouped as gases, liquids and solids, and are summarized in Table 2.1, Table 2.2 and Table 2.3, respectively, together with their composition, according to the suppliers.

Table 2.1. Gas reactants used in experimental work.

Gas	vol.%	Supplier
Helium (He)	99.999	Air Liquide
Hydrogen (H_2)	99.999	Air Liquide
Nitrogen (N_2)	99.999	Air Liquide
Synthetic air	99.999	Air Liquide
Ammonia/Helium (NH_3–He)	10/90	Praxair
Hydrogen/Nitrogen (H_2–N_2)	10/90	Praxair
Hydrogen/Argon (H_2–Ar)	5/95	Praxair
Oxygen/Helium (O_2–He)	5/95	Praxair

Additionally, Table 2.4 presents the commercial zeolitic supports used for the preparation of bifunctional catalysts, whereas plastic samples, polymers and plastic wastes used for characterization and reaction have been included in Table 2.5 together with their mass average molecular weight (M_W) and number average molecular weight (M_n), when available.

Table 2.2. Liquid reactants used in experimental work.

Liquid	wt.%	Supplier
Acetone (C_3H_6O)	>99.5	Sharlab
Ammonia (NH_3)	25	Panreac
Aniline (C_6H_7N)	99.5	Aldrich
Decahydronaphthalene (cis+trans) (Decaline, $C_{10}H_{18}$)	98	Aldrich
Deionized water milliQ (H_2O, <3 ppm)	–	Milipore
2,6-Di-*tert*-butylpyridine ($C_{13}H_{21}N$)	97	Aldrich
N,N-Dimethylformamide (C_3H_7NO)	≥99	Aldrich
Hydrofluoric acid (HF)	48	Aldrich
Isobutyronitrile (C_4H_7N)	99	Aldrich
Paraffins standard	mix.	Supelco
4-Phenylbutyronitrile ($C_{10}H_{11}N$)	99	Aldrich
PONA VI mix standard	mix.	Restek
Pyridine (C_5H_5N)	99	Aldrich
Sulfuric acid (H_2SO_4)	95–97	Sharlab
Tetrahydrofuran (C_4H_8O)	99.9	Aldrich
Tetrapropylammonium hydroxide (TPAOH, $C_{12}H_{29}NO$)	40	Aldrich

Table 2.3. Solid reactants used in experimental work.

Solid	wt.%	Supplier
Ammonium nitrate (NH_4NO_3)	98	Panreac
Lithium carbonate (Li_2CO_3)	99.50	Wako
Nickel powder (50–100 mesh) (Ni)	99.7	Alfa Aesar
Potasium carbonate (K_2CO_3)	99.00	Wako
Sodium carbonate (Na_2CO_3)	98.50	Wako
Sodium hydroxide (NaOH)	98	Scharlab
Tetraammineplatinum(II) nitrate ($Pt(NH_3)_4(NO_2)_2$)	99.99	Alfa Aesar

Table 2.4. Commercial supports for bifunctional catalysts.

Support	Ref.	SiO_2/Al_2O_3	Cation	Na_2O, wt.%	Supplier
Zeolite BEA	CP814E*	25	Ammonia	0.05	Zeolyst
Zeolite Y	CBV712	12	Ammonia	0.05	Zeolyst

Table 2.5. Samples used for characterization and degradation studies.

Sample	M_W, g·mol^{-1}	M_n, g·mol^{-1}	
Polystyrene (PS)	192,000	–	Sigma-Aldrich
Polystyrene (PS)	891	807	Tosoh
Polystyrene (PS)	2,980	2,790	Tosoh
Polystyrene (PS)	18,100	17,920	Tosoh
Polystyrene (PS)	96,400	95,455	Tosoh
Polystyrene (PS)	355,000	348,039	Tosoh
Polybutadiene (PB)	200,000	–	Sigma-Aldrich
High Impact Polystyrene (HIPS)	–	–	BP
ABS Magnum 3416 SC	–	–	Styron
Residual ABS (ABS-R)	–	–	Gaiker-IK4
Used cellular phones (CP)	–	–	Gaiker-IK4
Phenolic board (PhB)	–	–	Sumitomo Bakelite
Used tantalum capacitors (TC)	–	–	–

Polystyrene with 192,000 g·mol^{-1} was used as reactant in hydrocracking experiments, and the other PS samples were used as calibration standards for molecular weight in gel permeation chromatography.

Virgin polybutadiene used in this work is a low-cis PB (36 % cis-1,4-polybutadiene, 55 % trans-1,4-polybutadiene and 9 % vinyl-polybutadiene) which is commonly used as additive for plastics. Virgin high impact polystyrene (HIPS) is an impact-resistant plastic which presents a complex network where PS and PB can be found. It is prepared by polymerization of styrene in the presence of PB.

Acrylonitrile-butadiene-styrene (ABS) is a common amorphous thermoplastic terpolymer made by polymerizing styrene and acrylonitrile in the presence of PB

which has strong impact resistance and toughness. ABS-R is composed by used and shredder ABS pieces with a particle size between 0.5 and 0.1 mm.

Used cellular phones (CP) consisted of shredder pieces of a wide diversity of materials and colors, mostly of rubber or plastic characteristics, and a wide variety of particle sizes.

Phenolic boards (PhB) are used as virgin material for printed circuit boards manufacturing. PhB is made of phenol resin which is an important thermosetting material widely used due to excellent thermal, mechanical and electrical properties.

Tantalum capacitor (TC) is an electrolytic capacitor used as surface-mount devices in electronic industry. TC is made mainly of tantalum metal and it can be usually found in printed circuit boards (PCB). Used TC were recovered and selected from disassembled old printed circuit boards.

2.2. CATALYSTS PREPARATION

In this section, preparation of the bifunctional catalysts for hydrocracking is explained. Firstly, the procedures used to modify the zeolite supports by dealumination and desilication are described. Then, the methods used to incorporate platinum to the supports by ionic exchange (IE) or fast drying impregnation (FDI) are indicated. Finally, the activation procedure followed is indicated

2.2.1. PROTONATION AND DEALUMINATION OF BETA ZEOLITE

NH_4Beta zeolite in Table 2.4 was first calcined in air (1 $K \cdot min^{-1}$, 823 K) in order to obtain the desired HBeta material. HBeta is the base catalytic support used all over the work. HBeta zeolite has a three dimensional BEA-type structure with 12-membered ring cell and micropores of 0.7–0.8 nm. This material has been named as untreated HBeta, in order to indicate it was not dealuminated (Chapter 3), or just HBeta.

Dealumination was carried out in order to modify the acidic characteristics of the material and identify their impact in the performance of the subsequent catalysts.

However, dealumination can produce other modifications in the support properties which should also be considered.

Dealuminated zeolites can be prepared by partial dealumination of conventional zeolites with different reagents in solution or in vapor phase. Aluminum removal from the zeolite increases the SiO_2/Al_2O_3 ratio of its framework and strongly affects its acid properties: lower acid strength, lower unit cell size, lower ion exchange capacity, lower hydrophilic character, etc. [226].

In this work, dealumination of HBeta support was carried out under stirring with a solution of HCl (1 M) at 303 K [227]. The dealumination degree was regulated with varying contact time (20, 40 and 60 min) between HBeta and HCl solution. After treatment, the zeolite was recovered by filtration and washed with a large amount of warm ultrapure (MilliQ) water (343–353 K), until pH of the filtered water was around 7.

Then, the solid was overnight dried (393 K), calcined (1 K min^{-1} up to 823 K, 3 h at 823 K) and the supports coded as HBeta20, HBeta40 and HBeta60, where the number indicates dealumination contact time in minutes.

2.2.2. PROTONATION AND DESILICATION OF HY ZEOLITE

NH_4Y zeolite in Table 2.4 was first protonated by calcination in air (1 K·min^{-1}, 823 K) to obtain HY (untreated) support [228]. Desilication was carried out as an alternative strategy to modify the acid properties of the material, and to identify their impact on the performance of the bifunctional catalysts prepared from them. Other possible modifications of the support because of desilication should be also analyzed.

Desilicated supports were obtained by treating the original NH_4Y zeolite (10 g) with different concentrations (0.1, 0.2 and 0.3 M) of a solution of NaOH (1 L). 10 g of tetrapropilammonium hydroxide (TPAOH) were added as pore-directing agent (PDA) to each suspension. The presence of tetrapropilammonium ion (TPA^+) in alkaline solution can protect the zeolite structure during desilication [189, 193]. Each mixture of zeolite and NaOH was heated to 338 K and kept under magnetic stirring for 0.5 h.

After the treatment, the suspension was filtered and washed with abundant ultrapure water (MilliQ) at 343–353 K, until the pH of the filtered water was around 7. Then, the supports were overnight dried (393 K).

The three materials were calcined at 823 K for 8 h in order to remove possible nitrates and impurities remaining inside the structure, and to obtain the protonated materials, and the obtained desilicated supports were called as HY01, HY02 and HY03, where the number indicates the concentration of the NaOH solution (0.1, 0.2 and 0.3 M, respectively).

2.2.3. ION EXCHANGE PREPARATION PROCEDURE

Most bifunctional Pt/zeolite catalysts have been prepared in this work by incorporating platinum by ionic exchange (IE) to different nominal platinum contents (0.1–1.0 wt.%) and on several protonic zeolites (HBeta, dealuminated HBeta, HY and desilicated HY). The objective was to obtain catalysts with high platinum dispersion and narrow particle size distribution [229].

Tetraammineplatinum(II) nitrate has been used as the metallic precursor. Chlorine salts were avoided in order to prevent chloride from affecting the properties of the catalysts. The experimental procedure has been described in detail in a previous work [230].

The experimental procedure was as follows: 10 g of zeolite were slurred in 1 L of deionized water (MilliQ); the suspension was heated to 353 K and kept under constant stirring and reflux. Then, a 0.01 M solution of the metallic precursor was slowly added until the necessary volume for the nominal platinum content in the catalyst to be reached, and the suspension was kept at 353 K under stirring and reflux for 24 h. All over the process, the pH value should be kept in 7, with the addition of ammonium nitrate or ammonia solutions. Finally, the solid was filtered, intensively washed with ultrapure (MilliQ) water at 353 K, and dried (383 K, 12 h).

2.2.4. FAST DRYING IMPREGNATION PREPARATION PROCEDURE

In order to study the effect of platinum distribution in the catalyst on catalytic performance, two catalysts with nominal platinum contents of 0.3 and 0.5 wt.% were prepared by fast drying impregnation (FDI) on HBeta. The objective was to obtain catalysts with lower platinum dispersion and less uniform distribution. Also, some metal migration during fast drying to the outer surface was expected, towards an egg-shell distribution [222, 231]. Tetraammineplatinum(II) nitrate was used as metallic precursor, as well.

For the FDI method, 10 g of HBeta zeolite support powder were first pelletized, milled and sieved to a grain size of 0.16–0.3 mm and impregnation was carried out in a vacuum rotary evaporator, with the necessary amount of metallic precursor for the nominal platinum content to be reached in the catalyst solved in 20 mL ultrapure (MilliQ) water. The solution was added drop by drop to the zeolite. The solid was dried for 1 h, using a water bath at 373 K to accelerate drying.

2.2.5. ACTIVATION OF THE CATALYSTS

All prepared catalysts were activated in the same way, in three steps: drying, calcination and reduction. Drying was carried out in a stove at 383 K for 12 h. Then, the catalysts were calcined with a ramp of 0.5 $K \cdot min^{-1}$ from room temperature up to 623 K, where the temperature was kept for 2 h. Finally, the metal was reduced in a flow of 5 % hydrogen in argon (160 $cm^3 \cdot min^{-1}$) in a tubular reactor with a heating ramp of 0.5 $K \cdot min^{-1}$ from room temperature up to 723 K and keeping this temperature for 3 additional hours.

After activation, catalysts prepared by ionic exchange were pelletized, milled and sieved to a particle size of 0.16–0.3 mm. Thus, all catalysts presented finally the same range of particle sizes for reaction.

2.3. CATALYSTS CHARACTERIZATION

The prepared catalysts were characterized with several techniques, in order to extract information for correlating catalytic properties with performance, and draw conclusions in relation to catalytic design for plastic hydrocracking processes. The techniques, equipment and protocols used are briefly described in this section.

2.3.1. X-RAY DIFFRACTION (XRD)

XRD technique is based on the diffraction effect when X rays impact on the planes of the crystal lattice. Zeolites are crystal solids with characteristic X-ray diffraction patterns. These patterns have been used to identify the zeolite type of the supports and their crystallinity [232]. According to Bragg's law:

$$\lambda = 2d_{(hkl)} \sin\theta \qquad (2.1)$$

where λ is the wavelength of incident radiation, $d_{(hkl)}$ is the distance between reflection planes with Miller indexes (hkl) and θ is the incident angle.

Scherrer equation relates the size of crystal particles to the broadening of a peak in a diffraction pattern. It is used in the determination of size of crystals in the form of powder

$$\tau = \frac{K\lambda}{\beta\cos\theta} \qquad (2.2)$$

where τ is the mean size of the ordered (crystalline) domains in Å, K is a dimensionless shape factor, with a 0.9 value, λ is the X-ray wavelength, β is the line broadening at half the maximum intensity (FWHM), in radians, and θ is the Bragg angle.

For the experimental procedure, the support samples have been placed as powder in a flat glass on the holder cavity of the diffractometer with a few drops of acetone. When acetone evaporates, the powder is adhered to the glass surface and randomly oriented.

Measurements have been carried out in a Phillips PW1710 model diffractometer with monochromatic radiation under Bragg-Brentano geometry, operating with Cu

Kα (1.541874 Å). Measurement conditions were: angular 2θ scanning in the range 5–40, step size of 0.02, and step time of 1 s. The equipment is controlled with the Xpert Data Collector software. Analysis and data processing were carried out at the General Research Services (SGIker) of the UPV/EHU.

2.3.2. WAVELENGTH DISPERSIVE X-RAY FLUORESCENCE (WDXRF)

WDXRF is the fluorescent intensity diffracted from a material that has been excited by bombarding with high-energy X-rays or gamma rays. Si and Al concentrations of the catalysts were quantitatively measured by WDXRF.

WDXRF experiments were prepared by melting a microfurnace induction mixing flux Spectromelt A12 from Merck (ref 11802 no.) and dried sample powder in approximate proportions of 20:1.Then, chemical analysis of the mixture was carried out in vacuum atmosphere, using a XRF sequential spectrometer by wavelength dispersion (WDXRF) PANalytical AXIOS, provided with a Rh tube and three detectors. The equipment analyzes the usual major elements in the sample. Experiments and data processing was carried out at the General Research Services (SGIker) of the UPV/EHU.

2.3.3. FOURIER TRANSFORM INFRARED SPECTROSCOPY (FTIR)

FTIR spectroscopy measures the absorbed infrared radiation corresponding to the vibration frequency of the functional groups present in the molecules of the sample. We have used this technique to determine aluminum and silicon species in the framework, total acidity (Brønsted and Lewis acid sites) and accessible acidity of zeolites and/or catalysts.

Aluminum and silicon species in the framework were measured on the catalysts compressed into self-supporting wafers, in the hydroxyl region. Prior to the measurements, the samples were overnight pretreated in vacuum at 723 K. Then, the measurements were carried out under vacuum at 298 K.

Bands at different wavelengths can be found depending on the framework atoms. 3782 cm^{-1} band is associated to monomeric extraframework aluminum and tricoordinated aluminum atoms linked to the framework by two oxygen atoms.

Perturbations related to Al–OH and Al–O(H)–Si extraframework groups can be found around 3613 and 3663 cm^{-1}.

Regarding silicon species, 3746 cm^{-1} band is associated to amorphous silica and silanol groups. A band in the 3700–3300 cm^{-1} range can be also related to hydrogen bonded OH groups. Weakly perturbed Si–OH sites predominantly located inside the zeolite structure are represented at 3692 and 3728 cm^{-1}.

Information concerning total acidity of zeolite and/or catalyst and its Brønsted or Lewis character can be obtained after adsorption of a base on the sample, in the 1300–2500 cm^{-1} region. The use of a specific organic base is limited to structures with a pore size large enough for the molecule to enter and access all acid sites [233].

Pyridine has been widely used as probe molecule for zeolites of medium and large pore, as it can easily penetrate the 10 and 12 ring member channels of these materials, and therefore interact with their acid centers [234]. Wavelengths at 1540 cm^{-1} and 1450 cm^{-1} are used to detect and quantify Brønsted and Lewis acid sites, respectively.

The sample was treated at 673 K and vacuum until complete removal of adsorbed water and organic compounds. Then, the spectrum was recorded at room temperature. Adsorption of pyridine was carried out at 423 K and 0.67 kPa, with pyridine injected by a microsyringe.

Once adsorption equilibrium is reached, the samples were treated in vacuum for one hour at different temperatures (423, 573, 723 and 823 K), and the respective spectra recorded at room temperature.

Extinction coefficients of Emeis [235] determine the amount of pyridine adsorbed on Brønsted and Lewis acid sites with the intensity of the corresponding bands,

$$C_{Py} = 1.88 \cdot IA_{1540} \frac{r_d^2}{w} \tag{2.3}$$

$$C_{Py} = 1.42 \cdot IA_{1450} \frac{r_d^2}{w} \tag{2.4}$$

where C_{Py} is the adsorbed pyridine, in $mmol \cdot g_{cat}^{-1}$, r_d is the radius of the wafer, in cm, and w is the weight of the wafer, in g. IA is the integrated absorbance of

Brønsted or Lewis bands, in cm^{-1}. 1.88 and 1.42 correspond to the integrated molar extinction coefficients (I_{MEC}) for pyridine on Brønsted and Lewis sites, respectively.

External Brønsted acid sites in zeolite and/or catalyst have been estimated using 2,6-di-*tert*-butylpyridine (DTBPy) as base probe molecule [236]. Brønsted acid sites interacting with DTBPy can be estimated. Then, the number of adsorbed DTBPy molecules is assumed to be equal to that of adsorbed pyridine molecules (similar basicity), and accessibility of the acid sites of Beta zeolite to both probe molecules is assumed to be complete [237].

Again, the sample was treated at 673 K and vacuum until complete removal of adsorbed water and organic compounds, and the spectrum recorded at room temperature. Adsorption of DTBPy was carried out at 423 K and 0.67 kPa, injecting DTBPy with a microsyringe. Once adsorption equilibrium reached, the sample was treated in vacuum for one hour at 423 K, and the spectrum recorded at room temperature.

Bands at 3370 cm^{-1} [237] or 1616 cm^{-1} [238] are used with DTBPy. Initially, the theoretical peak area, considering that all Brønsted centers were accessible by DTBPy, S^{the}_{DTBPy}, was calculated using [237]:

$$S^{the}_{DTBPy} = \frac{I_{MEC} \cdot S^{sample}_{Py} \cdot S^{Beta}_{DTBPy}}{I_{MEC} \cdot S^{Beta}_{Py}} \qquad (2.5)$$

where, S^{sample}_{Py} is the integrated area of the corresponding band of adsorbed pyridine over the sample, S^{Beta}_{Py} is the integrated area of the corresponding band of adsorbed pyridine over Beta zeolite, and S^{Beta}_{DTBPy} is the integrated area of the corresponding band of adsorbed DTBPy over Beta zeolite.

Then, the percentage of Brønsted acid sites actually interacting with DTBPy is determined with the experimental area of adsorbed DTBPy in the sample, S^{exp}_{DTBPy}, and the theoretical peak area above calculated, S^{the}_{DTBPy}. This determines the percentage of accessibility as

$$\text{Access.} = \frac{S^{exp}_{DTBPy} \cdot 100}{S^{the}_{DTBPy}} \qquad (2.6)$$

IR spectra were obtained in a Nicolet 710 equipment operating with Fourier transform, using a quartz cell with CaF_2 windows. The adsorption studies were performed over sample wafer of 10 $mg \cdot cm^{-2}$, scanning in the 400–4000 cm^{-1} range, with resolution of 2 cm^{-1} and 100 accumulated scans.

2.3.4. TEMPERATURE PROGRAMMED DESORPTION OF AMMONIA (NH_3-TPD)

TPD is based on the chemisorption of a gas on a solid and subsequent desorption of the gas by a progressive temperature increase [239]. The amount of desorbed species at each temperature can be determined with different types of detectors. NH_3-TPD technique is a method used to determine total acidity and acid strength distribution of a catalyst [240].

Ammonia is a thermally stable basic molecule (pK_a = 9.27) with a kinetic diameter of 0.26 nm, which makes it virtually accessible to all acid sites. It can be adsorbed on centers with different acid strength and, consequently, its desorption will occur at different temperature. Thus, measuring the amount of NH_3 adsorbed over the sample and the location of the desorption peaks versus temperature gives information on the total number of acid centers and its strength.

NH_3-TPD experiments have been performed in a Micromeritics AutoChem 2910 equipment with a thermal conductivity detector. Before adsorption, the solid surface sample was cleaned and conditioned. 0.2 g of sample were treated in a U-shaped quartz tube in 20 $cm^3 \cdot min^{-1}$ N_2 flow at 823 K. Then, the sample was cooled down to 373 K. Ammonia adsorption step was performed at 373 K, introducing small pulses (5 $cm^3 \cdot g^{-1}$, standard) of 10 vol.% NH_3 in He until saturation.

Physisorbed NH_3 was removed with a He flow of 50 $cm^3 \cdot min^{-1}$ for 2 hours at 373 K. Chemisorbed NH_3 desorption was performed by increasing temperature from 373 up to 823 K with a heating rate of 10 $K \cdot min^{-1}$ in 50 $cm^3 \cdot min^{-1}$ of He. The final temperature was maintained for 2 hours to complete desorption, and the desorbed NH_3 was recorded.

Total acidity was obtained by integrating the area under the TPD curve. Additionally, integrating between three temperature ranges based on the temperature range in which NH_3 is desorbed, a distribution of the acid strength can

be estimated: weak acidity has been quantified between 373 and 553 K, medium acidity between 553 and 693 K, and strong acidity between 693 and 823 K.

2.3.5. NITROGEN PHYSISORPTION STUDIES

The most widely used method to study the textural properties of catalysts is nitrogen physisorption. N_2 adsorption-desorption isotherms provide information on surface area and pore structure. Specific surface of the catalysts was estimated using the method proposed by Brunauer, Emmet and Teller (BET) [241], based on two main principles: adsorbent surface is uniform and non-porous, and gas molecules are adsorbed onto successive layers when relative pressure, P/P_0, tends to 1, regardless of the lateral interactions, which is applicable only at very low relative pressures.

The first principle is not achieved for zeolites. Nevertheless, the method is usually applied for comparative purposes with different types of porous materials. BET equation can be written as:

$$\frac{P}{V_{ads}(P_0 - P)} = \frac{1}{V_m \cdot C} + \frac{(C-1)}{V_m \cdot C} \cdot \frac{P}{P_0} \qquad (2.7)$$

where V_{ads} ($cm^3 \cdot g^{-1}$) is the volume of nitrogen adsorbed per unit mass of solid in equilibrium with a given pressure, P (kPa); V_m ($cm^3 \cdot g^{-1}$) is the volume of nitrogen required to form a monolayer; P_0 (kPa) is the saturation pressure of nitrogen in the analysis conditions, and C is a constant exponentially related with nitrogen adsorption and desorption heats.

Fitting adsorption isotherm data to Equation 2.7 between 0.05 and 0.2 relative pressures allows for calculation of V_m and C parameters from intercept and slope. V_m is used to estimate solid surface area (S_{BET}, $m^2 \cdot g^{-1}$) with:

$$S_{BET} = 10^{-18} \cdot \frac{V_m \cdot N_A}{m \cdot V_{mol}} \cdot A_m \qquad (2.8)$$

where N_A is the Avogadro number, V_{mol} is the molar volume of N_2 ($cm^3 \cdot mol^{-1}$), A_m is the cross-sectional area of nitrogen (nm^2), and m (g) is the mass of solid used in the analysis.

Pore volume, V_p ($cm^3 \cdot g^{-1}$), and pore size distribution of the catalysts in the mesoporous region were estimated by the method proposed by Barret, Joyner and Halenda (BJH) [242]. Their model is based on the Kelvin equation for capillary condensation, which is applied to the desorption branch of the nitrogen isotherm, resulting in the following expression:

$$r_p = 10^3 \cdot \frac{2 \cdot \psi \cdot V_{ads} \cdot \cos\upsilon}{R \cdot T \cdot \ln\left(\frac{P}{P_0}\right)} + e \qquad (2.9)$$

where r_p is the pore radius (nm), ψ is the surface tension of nitrogen ($N \cdot m^{-1}$), υ is the angle of contact between condensed phase and solid, T is the absolute temperature (K), R is the ideal gas constant ($J \cdot mol^{-1} \cdot K^{-1}$), and e is the thickness of the adsorbed layer (nm).

For materials combining micro-, meso- and macropores, i.e. different types of isotherms [243], such as zeolites, t-plot method developed by de Boer [244] is very advantageous to evaluate microporosity. The amount of adsorbed nitrogen is represented versus the statistical thickness of an adsorbed layer over a nonporous surface at a certain relative pressure (t_{plot}). The value of t_{plot}, Å, can be obtained from the relative pressure using the Harkins and Jura equation [245]:

$$t_{plot} = \left[\frac{13.99}{0.034 - \log\left(\frac{P}{P_0}\right)}\right]^{\frac{1}{2}} \qquad (2.10)$$

The introduction of mesopores in a microporous system implies an upwardly deviation of the t-plot line for high values of t_{plot} [243]. The intercept measures the micropore volume, whereas the slope in the linear region of the curve is proportional to the mesopore area plus the external surface area of the particle.

Finally, pore volume and pore size distribution of the catalysts in the micropore range was estimated from the N_2 adsorption isotherm using the Horvath-Kawazoe formalism [246]:

$$\ln\left(\frac{P}{P_0}\right) = \frac{N_A}{R \cdot T}\frac{N_A\left(N_S \cdot K_{AS} + N_A \cdot K_{A\alpha}\right)}{\sigma^4\left(1-d\right)} \cdot \left[\frac{\sigma^4}{3\left(l-\frac{d}{2}\right)^8} - \frac{\sigma^{10}}{3\left(l-\frac{d}{2}\right)^9} - \frac{\sigma^4}{3\left(\frac{d}{2}\right)^8} - \frac{\sigma^{10}}{3\left(\frac{d}{2}\right)^9}\right] \quad (2.11)$$

where N_A is the Avogadro number, R is the ideal gas constant ($J \cdot mol^{-1} \cdot K^{-1}$), T is the absolute temperature (K), N_S is the number of atoms per unit surface (m^{-2}), K_{AS} is the Kirkwood-Mueller constant for the solid ($J \cdot cm^6$), $K_{A\alpha}$ is the Kirkwood-Mueller constant for nitrogen ($J \cdot cm^6$), σ is the distance between two molecules with zero interaction energy (nm), d is the distance between the solid and nitrogen molecules (nm), and l is the pore diameter of the solid (nm).

N_2 adsorption-desorption isotherms of the prepared catalysts were measured at normal boiling point of N_2 (77 K) in a Micromeritics ASAP 2010 equipment, in order to determine their textural properties. The analysis is optimal for a sample surface area in the range 20–50 m^2. Thus, sample weights providing about 35 m^2 have been selected. Prior to analysis, samples were degassed under vacuum (<1 Pa) and 573 K for 12 hours, so that moisture, air and possible condensation that may interfere with the measurement are removed.

Adsorption branch was obtained by adding successive known amounts of N_2 to the sample and the equilibrium pressures were recorded from the lowest (<1 Pa) up to the saturation pressure (~101.3 kPa). Eight points of N_2 partial pressures in the 0.05–0.2 kPa range were selected for the calculation of S_{BET}. Desorption branch was obtained by removing successive known volumes of N_2 and recording the values of equilibrium pressure until the closing hysteresis is reached.

In order to calculate pore size distribution by the BJH method, the entire desorption branch from 0.99 to 0.14 relative pressure range was considered. In order to determine the pore size distribution of the catalysts by the Horvath-Kawazoe method adsorption branch isotherm points from inception up to relative pressures of 0.01 were selected. Finally, the 0.01–0.65 range was selected for calculating the t curve.

2.3.6. TRANSMISSION ELECTRON MICROSCOPY (TEM)

TEM is based on irradiating a sample layer with a beam of high energy electrons (100–400 keV). Electrons are emitted from a filament and accelerated by a potential difference, and focus through a condensing lens to form a parallel beam incident on the sample. The experiment results in a number of different phenomena such as: Auger electrons, secondary electrons, backscattered electrons, X-rays, and transmitted electrons.

Electron microscopes operate under high vacuum to prevent electron beam from being scattered by gas molecules. Electrons transmitted and scattered by the sample are focused with an objective lens and amplified with a lens to finally form the image. TEM was used to determine platinum dispersion of the prepared catalysts, since this technique is particularly suitable for those materials having very small crystal sizes (<0.1 nm) [247].

TEM micrographs were performed in a Philips Tecnai 2000 microscope operating at 200 kV. The samples were dispersed in acetone, stirred in an ultrasonic bath and finally placed on a carbon rack. After drying, samples were introduced directly to the microscope. Experiments and data processing was carried out at the General Research Services (SGIker) of the UPV/EHU.

2.3.7. SCANNING ELECTRON MICROSCOPY (SEM)

SEM and TEM methods share the same concept, but the former analyzes the signal from secondary and backscattered electrons to create images of the sample [248]. SEM was used to study morphology and crystal size of the solid materials, with sizes in the range of 1 nm.

The images were obtained using a field emission type scanning electron microscope Schottky (JEOL JSM-7000F) with resolution of 30 kV, in secondary electron mode, of 1.2 nm. Experiments and data processing was carried out at the General Research Services (SGIker) of the UPV/EHU.

2.3.8. HYDROGEN CHEMISORPTION

Selective gas chemisorption, the most widely used technique for characterizing metal sites in heterogeneous catalysts, involves the formation of an irreversibly-adsorbed monolayer. Hydrogen is a particularly suitable gas for characterizing platinum surfaces. Platinum surface can be estimated by measuring the amount of hydrogen selectively adsorbed on the platinum monolayer. Pt dispersion is calculated as the ratio of the number of surface Pt atoms, N_S, to the number of total Pt atoms, N_T [249].

The study consists of successive isothermal pressure increments of hydrogen applied to the catalyst, waiting for equilibrium, and analyzing the amount of hydrogen dissociated and chemisorbed due to formation of chemical bonds with Pt. This adsorption is continued until the adsorbed gas forms a monolayer.

In order to determine the number of surface platinum atoms per unit mass of catalyst, N_S, the number of surface platinum atoms covered per adsorbed hydrogen molecule, X_m, must be known. With this value, the molar volume of hydrogen, V_{mol} ($cm^3 \cdot mol^{-1}$), and the experiment results, N_S can be evaluated by:

$$N_S = \frac{V_m \cdot N_A \cdot X_m}{V_{mol}} \tag{2.12}$$

where N_A is the Avogadro's number and V_m is the volume of hydrogen adsorbed on the monolayer per unit mass of catalyst ($cm^3 \cdot g^{-1}$).

Knowing the actual platinum content of the catalyst, G ($g_{Pt} \cdot g^{-1}$), and the molar mass of platinum, M_m, the total number of platinum atoms per unit mass, N_T, and therefore the dispersion, D_i, can be calculated:

$$D_i = \frac{N_S}{N_T} = \frac{N_S}{\frac{G \cdot N_A}{M_m}} \tag{2.13}$$

With dispersion value, D_i, and knowing the density of the metal, ρ ($g \cdot cm^{-3}$), and the surface occupied by a platinum atomic, σ ($cm^2 \cdot atom^{-1}$), characteristic length of the particles, d_p, can be calculated [250]:

$$d_P = \frac{c}{\rho \cdot \sigma \cdot D_i} \quad (2.14)$$

where c is a parameter that depends on the shape of the metallic crystal. If spherical particles are considered c has a value of six.

Hydrogen is one of the gases most used for chemisorption and its use presents a number of advantages such as low adsorption and negligible physical adsorption on the metal, and the simplicity of the adsorption mechanism entails a well defined stoichiometric factor. On the other hand, the main disadvantages are the possibility to present spillover effect or hydride formation, which entails an erroneous metal surface estimation [251].

Volumetric hydrogen chemisorption was used to determine the dispersion of Pt particles supported on the catalyst. The tests were performed on a Micromeritics ASAP 2020C equipment, with Chemisorption Controller, where the conditions for sample pretreatment and experiments were established.

Conditioning of the sample was carried out prior to chemisorption tests by: 573 K degassing under vacuum (<1 Pa) for 2 h, reduction in H_2 flow at 723 K for 4 h , evacuation in vacuum (<1 Pa) at 673 K for 4 h, and finally cooling down to 303 K.

Chemisorption experiments consisted of two hydrogen isotherms at 303 K with intermediate evacuation. Thus, the difference between the volumes obtained in each isotherm has been taken as chemisorbed H_2.

2.3.9. INDUCTIVELY COUPLED PLASMA OPTICAL EMISSION SPECTROSCOPY (ICP-OES)

ICP-OES is a very sensitive technique for qualitative and quantitative analysis, which allows for determination of the elements in the periodic table with lower potential ionization than Argon at very low concentrations. The technique is based on quantum theory, where each atom or ion has defined energy states for electrons. In the standard state, electrons are at their lowest energy level. Electrical excitation by thermal or other means can move one or more electrons to a state of higher energy and further away from the nucleus. The excited electrons tend to

return to their normal state and, during the process, emit energy in the form of a photon of radiant energy.

The wavelength of the light emitted by these electrons depends on the energy difference between excited and standard states, which, in turn, depends on the chemical structure of the element. Thus, by measuring the emitted wavelengths, the elements in the sample can be identified. Since the intensity of the emission is proportional to the concentration of the element, quantification is also possible at very low concentration (even traces). This technique has been used to determine the percentage of platinum present in each catalyst.

Analyses were performed on a Varian 710-ES ICP Optical in radial position equipment. In order to perform the analysis, the solid sample was treated in aqueous medium with a mixture of aqua regia and hydrofluoric acid in a hot sand bath until solution. The concentration of dissolved platinum was measured at 214.424 nm in nitric medium.

2.4. CHARACTERIZATION OF THE REACTANT PLASTICS

This section presents analytical procedures used to characterize virgin and residual polymers, and plastic wastes used as feed to hydrocracking or steam gasification. Solid products obtained after degradation of polymeric materials have been also characterized with similar procedures (when specified).

2.4.1. THERMOGRAVIMETRY ANALYSIS (TGA)

TGA measures the weight change of a sample as a function of time and temperature in the presence of a gas flow. The experiments can be developed under isothermal conditions or constant heating rate. Records obtained are characteristic of each sample and the results can be expressed by deriving the TG curves with respect to time or temperature, as dTG curves. TGA has been used in the characterization of plastics with the main objective to determine the degradation temperatures of the polymers and to estimate compositions.

Measurements were carried out in a Setaram Setsys Evolution thermobalance equipped with cylindrical graphite furnace and PIDU integrated temperature

control. The sample amount was around 10 mg and the assays were performed with a constant heating rate of 10 $K \cdot min^{-1}$ from room temperature up to 773 K in nitrogen flow for plastic samples in Chapters 5 and 6, whereas 20 K min^{-1} from room temperature up to 1173 K in synthetic air flow was used for TC samples in Chapter 7, where the main objective was to quantify the organic matter in the cover part of TC.

2.4.2. DIFFERENTIAL SCANNING CALORIMETRY (DSC)

DSC is a usual physical-chemical method of thermal analysis to determine energy changes in a substance. It is one of the most used techniques for the determination of melting temperatures, glass transition temperatures, and degree of crystallization of polymers. This technique measures the heat flow compensation required to maintain the temperature of a sample equal to the reference. The tests can be dynamic or isothermal.

DSC has been used to characterize different types of polymers. The measurements were performed in a DSC822e Mettler Toledo calorimeter. 10 mg of sample were heated with a 5 $K \cdot min^{-1}$ ramp between 273 and 523 K. In order to avoid interference of the thermal history of polymers, two complete heating-cooling cycles were performed, using the second cycle for the characterization data. Alumina was used as reference material.

2.4.3. ELEMENTAL ANALYSIS (EA)

EA allows for the determination of percent carbon, hydrogen, oxygen, nitrogen and sulfur present in each sample. In this work, this technique has been used for virgin polymers, recycled polymeric materials and solid products obtained from hydrocracking and gasification processes.

Specifically, EA was used to determine the weight of nitrogen present in ABS and ABS-R samples, used as the feed to hydrocracking process in Chapter 6. This has been named as N_{feed}.

Then, EA has been also used to determine the weight of nitrogen present in the solid products, $N_{solid\ product}$, obtained after hydrocracking studies of ABS-R. The solid

product is overnight dried at 353 K and then weighted. The weight of catalyst is subtracted from this value, in order to estimate the actual solid product. Thus, the percentage of nitrogen fed to the reaction system that is present in the solid products, N_{Solid}, has been estimated as:

$$N_{Solid} = \frac{N_{solid\ product}}{N_{feed}} \cdot 100 \qquad (2.15)$$

Samples were studied using an Euro EA Eurovector (CHNS) elemental analyzer, with the combustion chamber operating around 1293 K. The signals from each element were analyzed in a TCD, and converted to wt.%. Experiments and data processing were performed at the General Research Services (SGIker) of the UPV/EHU.

EA of solid products obtained from steam gasification processes in Chapter 7 was carried out with a Carlo Erba 1108 equipment, at the National Institute of Advanced Industrial Science and Technology (AIST) in Tsukuba, Ibaraki, Japan.

2.4.4. FOURIER TRANSFORM INFRARED SPECTROSCOPY (FTIR)

As described above, FTIR absorption peaks and bands at different wavenumbers represent the frequencies of the normal modes of vibration of molecules and are characteristic of specific functional groups, which facilitate the identification of the sample. It was applied for identification of specific groups in polymers.

Analyses were performed in the Nicolet 710 equipment described above, at room temperature, after vacuum cleaning the sample chamber. Samples were prepared as wafers in a hydraulic press or (preferably) by dissolving the plastic in decalin, THF or N,N-dimethylformamide, and evaporating the solvent so that a polymer film is supported on a KBr pellet.

2.4.5. X-RAY FLUORESCENCE (XRF)

A semiquantitative XRF analysis was useful to identify the metallic elements present in core and terminal samples obtained from thermal capacitors. The equipment used in this case was a Fischerscope X-ray System XDAL. For the core

thermal capacitor sample, the measurement was carried out on the bulk of the powder sample, whereas, for the terminal sample, the measurement was performed on different points of the surface.

Both measurements were carried out without any filter, at a distance of 0.05 mm, with a collimator of 0.6 mm. The high voltage used was 50 kV and the anode current was 128 μA. Experiments and data processing were performed at the General Research Services (SGIker) of the UPV/EHU.

2.4.6. INDUCTIVELY COUPLED PLASMA OPTICAL EMISSION SPECTROSCOPY (ICP-OAS)

ICP-OES was also used for the characterization and quantification of total metal content of tantalum capacitor terminal and core samples (Chapter 7). Samples were first treated with hydrofluoric acid and water in a hot sand bath until solution. After hydrofluoric acid was evaporated, analyses were performed in the Varian 710-ES ICP Optical in radial position equipment above described.

2.4.7. X-RAY DIFFRACTION (XRD)

XRD was used to determine the oxidation state of the metals present in the solid products obtained from steam gasification experiments of phenolic boards plus nickel powder and tantalum capacitors studied in Chapter 7. The samples were measured in the Phillips PW1710 diffractometer above described, at the General Research Services (SGIker) of the UPV/EHU.

2.5. HYDROCRACKING STUDIES

All hydrocracking studies have been performed at the laboratories of the research group “Chemical Technologies for Environmental Sustainability” (TQSA), at the Dept. of Chemical Engineering, Faculty of Science and Technology, UPV/EHU, located in Leioa, Basque Country, Spain.

2.5.1. EXPERIMENTAL EQUIPMENT

Degradation of plastics by catalytic hydrocracking was carried out in a reaction system which can be operated in discontinuous or semicontinuous regime. The diagram of the experimental equipment is shown in Figure 2.1, and comprises an Autoclave Engineers reactor with a capacity of 300 mL, made of Hastelloy C-276, which can operate at temperatures up to 873 K, and pressures up to 200 bar, and is resistant to HCl attack. The system model is fixed-head, so reactor and heating jacket are removed from the bottom while the top remains with all the connections.

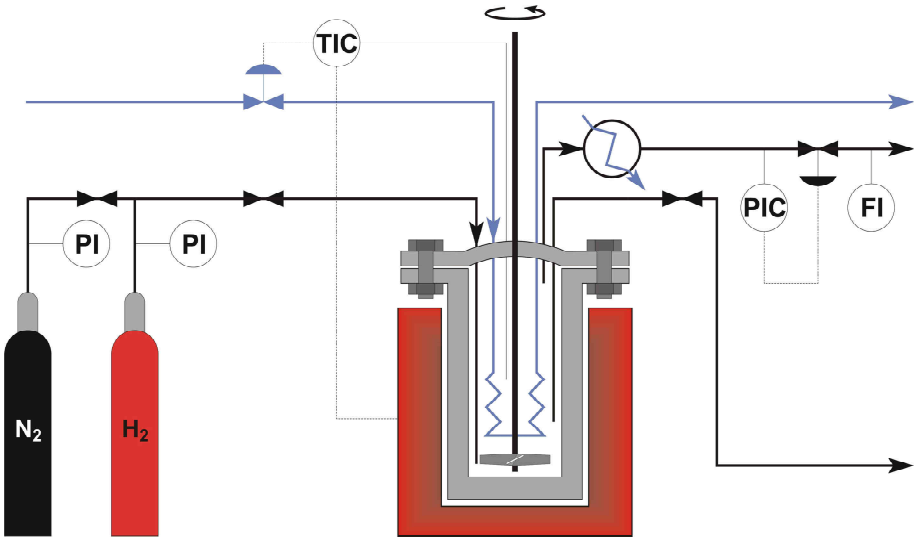

Figure 2.1. Scheme of plastic hydrocracking process.

A magnetic stirrer MagneDrive II is attached to the reactor head. The stirrer is connected to a motor, with a rotational speed inside the reactor regulated by a speed control system. Additionally, the reactor head has several connections:

- Gas inlet line: through which gas, mainly hydrogen, is supplied for pressurizing the reactor, with a pneumatically-actuated valve, a filter for impurities retention, a flow meter and a check valve to prevent reverse flow.
- Cooling water input and output line: through which circulates cooling water supplied to a coil located inside the reactor.

- Thermowell: where two thermocouples measure the temperature inside the reactor.
- Gas output line: with a gas condenser so that condensable products return to the reactor. Uncondensed gases pass through a manual valve, a coalescing filter and a mass VARY-P controller, which controls the outflow of gas. Additionally, just after the manual valve, another exhaust line is connected to a pneumatically actuated valve.
- Pressure transducer: measuring the pressure inside the reactor.
- Liquid outlet: with a manual valve and a filter, in order to take liquid samples during reaction.

The reaction system is equipped with a control unit, consisting of the following control loops:

- Temperature control. Reactor temperature is measured with two thermocouples inside the reactor (T1 and T2) and another one located in the outer wall of the reactor (T3), and read by a TOHO controller. One of the controllers inside the reactor (ICTs1) has two control outputs which are used to regulate the power supplied by heating jacket, and to actuate a solenoid valve which causes the flow of water through the cooling coil located inside the reactor. The two remaining controllers are alarms for temperature inside the reactor and on the reactor wall. The controller responsible for the alarm wall actuates the power of the heating jacket, whereas the alarm inside the reactor actuates the cooling system.
- Pressure control. Pressure transducer measures the pressure inside the reactor vessel up to 200 bar. The output signal (4–20 mA) is read by a PID controller, which compares the measured pressure with the set point and, if exceeded, the controller actuates the mechanism regulating power to the heating jacket, closes the gas inlet valve, opens the exhaust valve and causes the 100 % opening of the VARY-P.
- Gas flow control. A mass flow controller (VARY-P) controls gas flow. The output signal (analog 4–20 mA, proportional to flow) is read by a PID controller. Additionally, a mass flow meter controlled by a PID system measures the flow for input gases.

- Stirring speed control. This control is performed by an inverter that regulates engine speed, proportional to the rotational speed of the stirrer. Revolutions per minute are displayed on a screen.

2.5.2. EXPERIMENTAL PROCEDURE

Plastic reactants are ground to a size of 1 mm on a Retsh ZM 200 equipment with rotary blades, unless otherwise specified. The process is manually cooled with liquid nitrogen in order to prevent polymer melting.

A solution of, typically, 5 wt.% polymer in decalin at room temperature is prepared. The reactor is fed with 100 g of the solution and 0.25 g of bifunctional catalyst (for catalytic processes) is added. Then, the reactor is closed.

With the outlet valves closed, H_2 (or N_2, when specified) is fed until 50 bar are reached. At this point, the system is checked for leaks. Then, the heating jacket is installed and set point values of temperature and pressure are set. Initially, pressure is set to a value below the intended reaction set point in order to keep the system in the liquid phase. Then, cooling water valves for stirring, reactor coil and condenser are open. Once the temperature set point reached, pressure is adjusted to the reaction set point and stirrer is turned on (1800 rpm). This point is set to zero reaction time.

Most hydrocracking experiments were carried out with the system working as a dead-end. In dead-end reactions, the output valve is kept closed all over the experiment, and the gas products remain inside the reactor during reaction.

On the other hand, some experiments were carried out in an open-end system (when specified, in relation to Chapter 6). In this situation, the output valve is open to maintain a 6 $cm^3 \cdot min^{-1}$ flow, in order to evacuate the incondensable products during reaction.

Reactions proceed for, typically, 40 min (unless otherwise specified), with constant temperature (598–698 K, unless otherwise specified) and pressure (typically, 180 bar of hydrogen, unless otherwise specified). Samples for analysis are taken at specific intervals (usually, 10 min) through the liquid outlet. When final reaction time is reached, the set point temperature is lowered, for the system to cool down,

and the heating jacket is removed. Then, inlet gas valve is cut off and stirring is switched off.

When the system reaches room temperature, reactor pressure is decreased by programming an outflow in the VARY-P. The exhaust gases are analyzed by chromatography. With ABS and ABS-R, gas products pass through a scrubber for collection of water-soluble products for analysis, before chromatography. Finally, when atmospheric pressure is reached, the reactor is opened, the liquid products are weighed and a sample for gel permeation chromatography and gas chromatography is taken.

The above conditions have been selected to work under kinetic control, for catalyst design. Under these reaction conditions, differences in activity can be attributed only to the characteristics of the catalysts, such as the nature, concentration and accessibility of acid and metal sites [109].

2.5.3. CHARACTERIZATION OF HYDROCRACKING PRODUCTS

This section describes the techniques used to analyze gaseous and liquid products of hydrocracking. Analysis of the solid product is described in Section 2.4, as the characterization procedures were the same than those used for reactant polymers.

2.5.3.1. Gel permeation chromatography (GPC)

GPC is a separation technique based on the difference of effective molecular size of the molecules in solution. Separation is accomplished by injecting the sample into a continuous flow stream passing through a highly porous rigid gel, formed by particles packed in a column. Larger molecules elute earlier, while smaller molecules stay longer, retained in the pores.

GPC is used for characterization and quality control, especially for determining the size of medium and low molecular-weight molecules. To obtain molecular weight results requires a calibration with standard monodisperse polymers. This calibration curve is valid for a given polymer, solvent, temperature, flow and column.

Once the calibration curve of the studied polymer is defined, the relationship between elution volume (V_i) and molecular weight (M_i) is established, which enables the determination of different average molecular weight of the injected sample and also the distribution function of molecular weight [252].

Based on these considerations, two types of average molecular weight according to the following expressions can be calculated [253]:

$$M_n = \frac{\sum_{i=1}^{\infty} M_i \cdot N_i}{\sum_{i=1}^{\infty} N_i} \tag{2.16}$$

$$M_W = \frac{\sum_{i=1}^{\infty} M_n^2 \cdot N_i}{\sum_{i=1}^{\infty} M_i \cdot N_i} \tag{2.17}$$

Number average molecular weight (M_n) represents the total weight of all molecules contained in a sample, divided by the total number of molecules of the sample (N_i). M_W represents the specific weight of each molecule according to its size.

The concentration of plastic in solution requires an additional calibration with polymer solutions of known concentrations, where the integrated area of the peak corresponding to the polymer in GPC is represented versus the concentration of dissolved polymer.

Polymer exited from the GPC column before 18.75 min. Oligomers (less than 312 $g \cdot mol^{-1}$), located between 18.75 and 19.75 min, were considered as liquid products and their concentration was calculated the same way. Decalin and lighter products exited after 19.75 min.

Analyses were carried out in a Waters 616 GPC equipped with a furnace, a Waters 515 HPLC pump, a 717 injector and a Waters 2410 refraction index detector. The columns were Styragel HR1 and HR6, in order to cover molecular weights from 100 to 500000 $g \cdot mol^{-1}$. The mobile phase used was THF with a 1 $mL \cdot min^{-1}$ flow. The temperature inside the columns is 308 K and the analysis time is 30 min.

2.5.3.2. Gas chromatography with flame ionization detector (GC-FID)

GC is a technique to separate different components of a mixture according to the different speeds moving by a mobile phase through a stationary column. Flame ionization detector (FID) was used to distinguish among the different compounds of a mixture.

For analysis of the reaction products by GC-FID detector, a method called detailed hydrocarbon analysis (DHA) has been used, which is widely used to separate and identify components and further discriminate the components according to the type of hydrocarbon (paraffins, isoparaffins, olefins, naphthenes and aromatics, PIONA) of gasoline and other fuels. The identification is restricted to components eluting before *n*-C_{14}, i.e. hydrocarbons having a boiling point below 498 K [170].

DHA method is an open platform for temperature programmed gas chromatography, where the chromatograph is equipped with: autosampler, split/splitless injector, capillary polydimethylsiloxane column and FID. The methodology used in this work is a modification of ASTM D 6730 and D 6733 methods [254, 255] with a reduction in the time required for analysis while maintaining the quality criteria. The differences of this method compared to the standard are: carrier gas, column dimensions and temperature ramps, whereby analysis time is reduced from about 146 minutes to about 70 minutes with the 100 meter column, or 35 minutes with the 50 meter column [256, 257].

The GC-FID equipment used in this work was a 6890N from Agilent Technologies equipped with a RTX-5 DHA pre-column (5 m×0.25 mm×0.5 μm; 5 % polydiphenylsiloxane–95 % polydimethylsiloxane). The columns used were HP PONA (50 m×0.2 mm×0.5 μm) and RTX-DHA 100 (100 m×0.25 mm×0.5 μm), with a constant flow of He of 1.5 $cm^3 \cdot min^{-1}$ as carrier gas.

The injection was carried out by a programmable split/splitless, 1:100 split, injection at 523 K with a 0.5 μL syringe and the injected volume is 0.2 μL at low speed. The FID detector temperature was 523 K, with 450 $cm^3 \cdot min^{-1}$ of air and 45 $cm^3 \cdot min^{-1}$ of hydrogen. The oven conditions were programmed as follows: 278 K for 3.25 min; then, temperature was increased to 318 K with a 40 $K \cdot min^{-1}$ ramp and kept at that temperature for 13 min (retention time for ethylbenzene); and finally, temperature

was increased to 493 K with a 4 $K \cdot min^{-1}$ ramp and kept at that temperature for 5 min, in order to evacuate all the compounds.

Dragon-DHA software is the tool to process the chromatograms using the Kovats reference index to identify components of a mixture of hydrocarbons. The logarithmic form of Kovats index is the retention time (t_r) of a component associated with the *n*-paraffins eluting before and after that component:

$$RI_t = n \cdot 100 + 100 \cdot \frac{\log(t_r) - \log(t_{r,n})}{\log(t_{r,n+1}) - \log(t_{r,n})} \quad (2.18)$$

where RI_t is the reference index of the component at time t, t_r is the retention time of that component, $t_{r,n}$ is the retention time of the previous *n*-paraffin and $t_{r,n+1}$ is the retention time of the next *n*-paraffin.

Initially, the software looks for the presence of primary hydrocarbon references (*n*-paraffins) to set the resulting chromatogram. Additionally, the system uses other compounds as secondary references [230]. These references, presented in Table 2.6, allow the identification of hydrocarbons in a sample, by comparison with a database established as a reference file under the same operating conditions as the test samples.

In order to quantify, the software applies the theoretical response factors, to correct the detector response for each of the hydrocarbons. This procedure is necessary because the response of an FID to hydrocarbons is determined by the ratio of the molecular weight of the hydrocarbon to the total molecular weight of the analyte. Response factors, relative to heptanes, are presented in Table 2.7. The calculations are based on the following equation:

$$FR_i = \left[\frac{M_C \cdot n_C - M_H \cdot n_H}{n_C} \right] \cdot \frac{0.83905}{M_C} \quad (2.19)$$

where FR_i is the relative factor per hydrocarbon with a specific number of carbons, M_C is the atomic mass of carbon, n_C is the number of carbons in the group, M_H is the atomic mass of hydrogen, and n_H is the number of hydrogens in the group. 0.83905 is the correction factor considering that of *n*-heptane as unity (1.0000).

Table 2.6. Primary and secondary references of DHA method.

Primary references		Secondary references	
Compound	**T_r, min**	**Compound**	**T_r, min**
C_1	2.0435		
C_2	2.0765		
C_3	2.1724		
n-C_4	2.4774		
n-C_5	3.2422		
n-C_6	4.8643		
n-C_7	8.3268		
n-C_8	13.4557		
n-C_9	19.7638	1,2-dimethylbenzene	18.6746
n-C_{10}	23.7811	1,2,4-trimethylbenzene	23.1394
n-C_{11}	26.8489	1,2,3,5-tetramethylbenzene	27.1533
n-C_{12}	29.4347	Naphthalene	28.7102
n-C_{13}	31.7363	2-methylnaphthalene	31.4223
n-C_{14}	33.8455		

Table 2.7. Theoretical response factors FID related to heptane.

C	Saturated paraffins	Insaturated paraffins	Saturated naphthenes	Insaturated naphthenes	Aromatics
1	1.1207	–	–	–	–
2	1.0503	–	–	–	–
3	1.0268	0.9799	–	–	–
4	1.0151	0.9799	–	–	–
5	1.0080	0.9799	0.9799	0.9517	–
6	1.0034	0.9799	0.9799	0.9564	0.9095
7	1.0000	0.9799	0.9799	0.9598	0.9195
8	0.9975	0.9799	0.9799	0.9623	0.9271
9	0.9955	0.9799	0.9799	0.9642	0.9329
10	0.9940	0.9799	0.9799	0.9658	0.9376

Once the peaks are identified and their areas corrected, the mass percentage of each component is calculated with:

$$wt.\% = \left[\frac{\text{corrected area}}{\sum \text{corrected areas}} \right] \cdot 100 \qquad (2.20)$$

2.5.3.3. Gas chromatography with mass spectrometer detector (GC-MS)

Liquid products of hydrocracking of plastic wastes with ABS contain nitrogen. Thus, GC-MS equipment, with mass spectrometer detector (MS), was used to identify and quantify nitrogen-containing compounds in the liquid fuel. First, some liquid samples obtained from hydrocracking of real plastic wastes were used to determine the main nitrogen-containing compounds in SCAN mode. Propanenitrile, aniline, isobutyronitrile and 4-phenylbutyronitrile were the only nitrogen-containing compounds identified.

Then, quantification of these nitrogen-containing compounds was carried out in SIM mode selecting the most repetitive ions obtained from the rupture of the molecule. A chromatogram was obtained where the intensity of the compounds is represented versus retention time. The area of each intensity peak is proportional to the concentration of that compound. Thus, propanenitrile, aniline, isobutyronitrile and 4-phenylbutyronitrile were used as standards, to different concentrations in order to draw the calibration curves of intensity area versus concentration.

Quantification of the concentration of nitrogen-containing compounds in all liquid fractions was performed by integrating the area of the nitrogen-containing compound in SIM mode and introducing it in the calibration equation.

Liquid products were weighted after reaction in order to close the mass balance. The density of each liquid product obtained for all the reactions, especially for different ABS-R concentrations, was also calculated. Then, with the concentration of each nitrogen-containing compound and the volume of liquid product, the weight of nitrogen-containing compounds was calculated, and the weight of nitrogen.

Total weight of nitrogen in the gasoline fraction was calculated as the sum of nitrogen in all compounds, N_{sum}. With the nitrogen composition of plastic samples obtained from elemental analysis, the weight of nitrogen in the initial sample, N_{feed},

was also calculated. Thus, the percentage of fed nitrogen present in the gasoline product was calculated as:

$$N_{Gasoline} = \frac{N_{sum}}{N_{feed}} \cdot 100 \quad (2.21)$$

and the concentration of nitrogen in the gasoline fraction, in ppm, was calculated with total nitrogen in the gasoline fraction and total amount of gasoline.

GC-MS was carried out in an Agilent 6890 series GC equipped with a 5973 Mass detector. The column was a HP5-MS and the oven conditions were the same as those above explained for GC-FID. Experiments and data processing has been made at the General Research Services (SGIker) of the UPV/EHU.

2.5.3.4. Ammonia and hydrogen cyanide

Ammonia and hydrogen cyanide were recovered from gas products by solution in water. Ammonia concentration was measured with the indophenol blue method. Hydrogen cyanide was determined with the following method. Cyanide ions, with a coloring agent, form cyanogen chloride, which reacts with 1,3-dimethyl-barbituric acid in the presence of pyridine to produce a violet colour (König reaction). Cyanide concentration is semiquantitatively measured by visual comparison of the color of the measurement solution with the color fields in a card. Ammonia and hydrogen cyanide products were measured at the Normative Laboratory in the Health Department of the Basque Government.

With the concentration of ammonia and hydrogen cyanide (mg L^{-1}) obtained from the scrubber and the volume of the solution collected, the weight of nitrogen present in ammonia and in hydrogen cyanide, N_{NH3} and N_{HCN}, respectively, were calculated. Thus, the percentage of fed nitrogen present in the gas products as NH_3 and HCN, N_{Gas}, was calculated as:

$$N_{Gas} = \frac{N_{NH3} + N_{HCN}}{N_{feed}} \cdot 100 \quad (2.22)$$

2.5.4. HYDROCRACKING DATA TREATMENT

Plastic degradation processes generally involve the classic mechanisms of initiation, propagation and termination. In this work, a continuous distribution kinetics model [79, 258-265], widely reported in the literature for describing the degradation of plastics in solution, has been used. For applying the model, the evolution of conversion, X, and number-average molecular weight distribution of the polymer chains, M_n, has been used.

Polymer conversion in hydrocracking reactions is defined as the transformation of the polymer chains into oligomers, monomers, low molecular weight and volatile products. Conversion, X, for plastic hydrocracking reactions has been calculated from the polymer concentration in the liquid samples taken at different reaction times, $C_{P,t}$, determined by GPC as described above, and the initial concentration, $C_{P,0}$, as shown in the following equation:

$$X = \frac{C_{P,0} - C_{P,t}}{C_{P,0}} \tag{2.23}$$

Polymer conversion in hydrocracking is related to end-chain scission of the polymer chain, and has been used to determine kinetic constants for end-chain scission reactions with:

$$-\ln(1-X) = k_s \cdot t \tag{2.24}$$

where k_s is the kinetic constant for end-chain scission.

Unconverted polymer number-average molecular weight is related to random chain scission of the polymer and has been used to calculate kinetic constants of random scission reactions according to:

$$\frac{1}{M_n} - \frac{1}{M_{n0}} = k_r \cdot t \tag{2.25}$$

where M_{n0} is the initial number-average molecular weight of the polymer, M_n is the number-average molecular weight of unconverted polymer, determined by GPC as described above, k_r is the kinetic constant for random scission, and t is the reaction time.

The values of k_s and k_r obtained at different temperatures have been fitted to Arrhenius, from which pre-exponential factors, A_s and A_r, and apparent activation energies, E_{as} and E_{ar}, have been derived for each process, both thermal and catalytic, for all polymers where conversion values could be measured (Chapters 3–5). $\ln(k_s)$ has been represented versus E_{as}, and $\ln(k_r)$ versus E_{ar} for each series of catalysts and the thermal process, in order to analyze the presence of compensation effect in catalysts of the same series.

All straight lines obtained for different catalyst series and polymers have been found to be represented by lines with the same slope. Thus, although the thermal process for each polymer presents a single point, the corresponding straight line has been also drawn to facilitate comparison. The vertical distance between the point for the thermal process and the line corresponding to the catalyst series has been used to compare the activity of the catalyst series with the thermal process.

In order to analyze catalytic characteristics with activity, and to overcome the effect of compensation effect, a single parameter describing activity in end-chain scission has been derived for each series of catalysts by fitting all $\ln(k_s)$ vs. 1/T data to a common slope (common activation energy) by multiple linear regression. Thus, a single parameter, in the form of pre-exponential factor, A'_s, has been derived for each catalyst in the series.

The same way, all $\ln(k_r)$ vs. 1/T data for all the catalysts in the series have been fitted to a common slope (common activation energy) by multiple linear regression, to obtain a single parameter for describing catalytic activity in random scission, in the form of pre-exponential factor, A'_r.

Both A'_s and A'_r have been correlated with different catalytic properties to seek for correlations. Correlation has been analyzed with correlation coefficients, r, and Fisher-test values for the fitting, F.

The values of k_s and k_r have been used to estimate initial molar and mass reaction rates for the process as:

$$-r^{(0)} = -k_s \cdot C_{P,0} + k_r \cdot c_{P,0} \tag{2.26}$$

$$-r^{(1)} = -k_s \cdot c_{P,0} \tag{2.27}$$

where $r^{(0)}$ and $r^{(1)}$ are the initial molar and mass hydrocracking rates, respectively, $C_{P,0}$ is the initial molar concentration of polymer and $c_{P,0}$ is the initial mass concentration of polymer.

With the values of $r^{(0)}$ and $-r^{(1)}$, actual platinum content and dispersion of the catalysts, initial turn-over frequencies $TOF^{(0)}$ and $TOF^{(1)}$, have been estimated, respectively, for the catalysts.

Mass balance and selectivity to different reaction products has been calculated and based on carbon. Identification and quantification of products is performed by Dragon-DHA software, as described above, applied to the GC data. The analysis is performed for both liquid and gas samples. Chromatography results plus initial and final weight in the reactor have been used to close the mass balance.

2.6. STEAM GASIFICATION STUDIES

Steam gasification studies were carried out at the laboratories of the research group “Adsorption and Decomposition Technology”, Environmental Management Research Institute (EMRI), National Institute of Advanced Industrial Science and Technology (AIST) in Tsukuba, Ibaraki, Japan, under the supervision of Prof. Tohru Kamo and the support of Prof. Thallada Bhaskar.

Steam gasification was studied as a feasible valorization way for heterogeneous residues containing metals and plastics, in order to produce hydrogen and recover valuable metals. Phenolic boards (PhB) and tantalum capacitors (TC) were used as samples for steam gasification studies. PhB and TC samples were prepared and characterized prior to steam gasification studies to know the composition of the feed.

Steam gasification of PhB and TC was carried out in two different experimental systems: a thermobalance and a reactor vessel. As reported in previous studies [163], hydrogen formation by steam gasification of char proceeds by means of the following two endothermic reactions:

$$C + H_2O \rightarrow CO + H_2 \quad (2.28)$$

$$CO + H_2O \rightarrow CO_2 + H_2 \quad (2.29)$$

where the former corresponds to steam gasification (ΔH_0 = 131 kJ·mol^{-1}), and the latter to water-gas shift (ΔH_0 = 41.2 kJ·mol^{-1}).

2.6.1. STEAM GASIFICATION IN THERMOBALANCE

Steam gasification of PhB was carried out in a Rigaku Thermoplus TG8120 thermobalance connected to a mass spectrometer in order to measure the evolution of m/z = 2 and 44, corresponding to H_2 and CO_2, respectively. Samples grinded to below 0.15 mm were heated at 10 K·min^{-1} from 293 up to 1273 K under nitrogen. Nitrogen flowed into the TG from two routes: the regular line and a side pipe, both at 50 cm^3·min^{-1}.

Different experiments were performed, where the effect of the presence of steam, of the presence of nickel, of steam partial pressure, or heating rate is analyzed. The presence of steam was analyzed by comparison of experiments with just N_2 and with N_2 and steam. Steam was fed to the system through the side pipe, where N_2 fed to the system was first humidified by bubbling in hot water.

The effect of nickel was analyzed by comparing experiments in the presence and in the absence of nickel powder, with similar weight of PhB and atmosphere. With nickel, a weight ratio PhB/Ni of 1/3 was used. The effect of water partial pressure was analyzed in the presence of nickel by changing the temperature of hot water where side-pipe nitrogen is bubbled for humidification (323, 333 or 348 K).

In order to measure kinetic data, TG experiments were carried out at four different heating rates (5, 10, 20 and 30 K·min^{-1}) both in the absence and in the presence of H_2O. The conversion (relative weight loss) rate is represented by the following equation:

$$\frac{dx}{dt} = a\frac{dx}{dT} = K(T)\cdot f(x) \qquad (2.30)$$

where a represents the heating rate (dT/dt), f(x) is a function of conversion and K(T) is the kinetic constant of weight loss, which depends of temperature and is often successfully modeled by the Arrhenius equation. Then, the following expression can be derived:

$$\frac{dx}{f(x)} = \frac{A}{a} \cdot \exp\left(\frac{-E_a}{RT}\right) dT \tag{2.31}$$

where E_a is the apparent activation energy, A the pre-exponential factor and R the ideal-gas constant. Integration of Equation 2.31 with the initial condition that $x = 0$ at $T = T_0$, gives the following expression:

$$g(x) = \int_0^x \frac{dx}{f(x)} = \frac{A}{a} \cdot \int_{T_0}^{T} \exp\left(\frac{-E_a}{R \cdot T}\right) dT = \frac{A \cdot E_a}{a \cdot R} p(T) \tag{2.32}$$

where p(T)) is the temperature integral, which has no analytical solution.

To overcome this difficulty, the Kissinger-Akahira-Sunose method [266], an iso-conversional integral method, uses the Coats-Redfern approximation of the temperature integral that leads to:

$$\ln\left(\frac{a}{T^2}\right) = \ln\left(\frac{A \cdot R}{E_a \cdot g(x)}\right) - \frac{E_a}{R \cdot T} \tag{2.33}$$

where T is the absolute temperature for the maximum slope (K) and g(x) is a function depending on reaction order and conversion. Thus, if $\ln(a/T^2)$ is represented versus 1/T for experiments carried out at different heating rates, a straight line is obtained from whose slope the activation energy is derived.

2.6.2. STEAM GASIFICATION IN A REACTOR VESSEL

Steam gasification studies in a reactor vessel were carried out for PhB and TC in the presence of a ternary eutectic carbonates mixture (Li_2CO_3, Na_2CO_3 and K_2CO_3), LNK, in order to reduce the melting point of the liquid phase and to catalyze the steam gasification reactions of PhB [163]. The effect of nickel addition, for PhB, and the effect of the metals present in the sample, for TC, was also studied.

A schematic diagram of the experimental equipment is shown in Figure 2.2. Vessel dimensions were 32 mm of internal diameter and 125 mm of height. For steam gasification, LNK (30 g) and Ni (1.5 g, when used) were preloaded in the reactor vessel at the start of an experiment. The reactor vessel was closed with the head

of the reactor and weighted for the mass balance. Then, sample feeder, steam input and gas product output lines were connected to the head of the reactor vessel. The output line had an ice condenser for condensable products, a gas-liquid separator, a halogen trap and a moisture trap. The gas flow rate was measured by an integrating flow meter and, finally, a gas sample was analyzed every five minutes by a gas chromatograph (Varian CP-4900).

The thermocouple was introduced inside the reactor vessel through the thermowell, located on the head of the reactor. Then, the heating jacket surrounding the reactor was closed. The heating control was set to fix the operational temperature inside the reactor vessel (823, 873 or 948 K) and the oven started to heat.

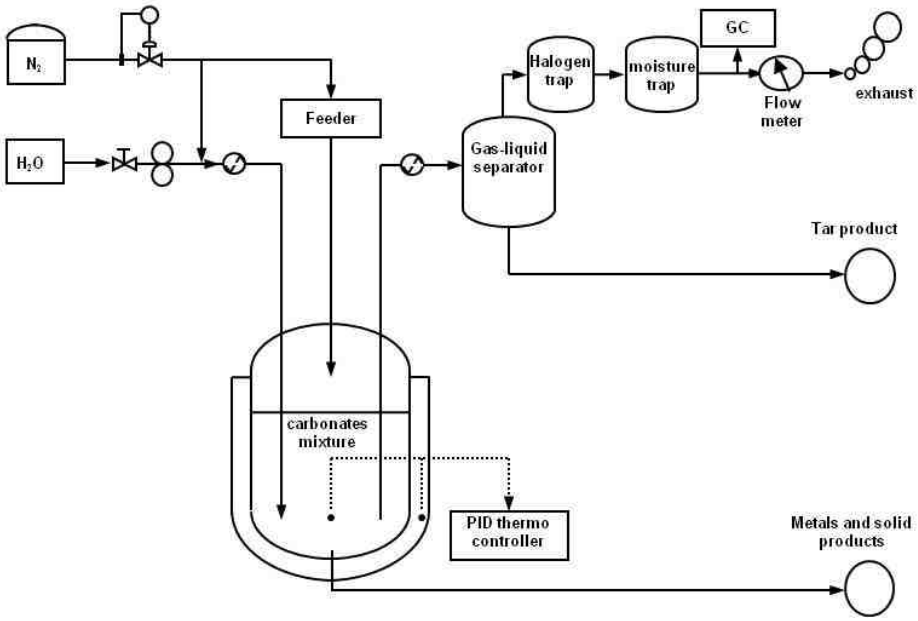

Figure 2.2. Diagram of plastic steam gasification process.

After the temperature reached 773 K, N_2 gas (40 $cm^3 \cdot min^{-1}$) and ultra pure water (0.26 $ml \cdot min^{-1}$) were introduced through a pipe and bubbled at the bottom of the reactor vessel. At this temperature, steam reacts with molten carbonates to produce CO_2 by hydrolysis. The mixture of N_2 gas and steam was preheated and injected into LNK to improve the efficiency of physical contact between the sample and molten LNK.

When equilibrium of carbonates hydrolysis is reached and the composition of the molten carbonates is stabilized, the CO_2 production is reduced to initial values. At this point, 0.5 g of sample (PhB or TC) was fed to the reactor and steam gasification reaction started. This was established as zero reaction time and gasification was stopped when no significant production of H_2 and CO_2 was measured, with a maximum reaction time of 240 min.

Finally, input valves were closed, heater switched off and the reactor vessel was cooled down and weighted. Tar products were collected from the condensation pipe with THF and weighted after evaporation of the solvent. LNK and solid product was washed with hot ultra pure water. Then, suspension was filtered, the solid was overnight dried in a stove and, finally, char was obtained [145, 267].

Chapter 8

SUMMARY AND CONCLUSIONS

Capítulo 8

RESUMEN Y CONCLUSIONES

RESUMEN.

Este trabajo se ha centrado, inicialmente, en la mejora del catalizador bifuncional de Pt/zeolita para procesos de hidrocraqueo de plásticos para obtener combustibles líquidos de buena calidad para automoción. Se ha comenzado estudiando plásticos simples, y se ha ido avanzando hacia mezclas cada vez más complejas, estudiando el efecto de las condiciones de operación en las características del combustible líquido.

Finalmente, cuando el proceso de hidrocraqueo no es viable, porque se genera una cantidad considerable de productos sólidos, principalmente, se ha buscado otra alternativa de valorización viable, mediante gasificación con vapor para producir hidrógeno. La combinación de ambos procesos puede ser una estrategia a nivel industrial para la valorización de residuos plásticos complejos.

8. SUMMARY AND CONCLUSIONS

In this chapter, a summary of the work in the thesis and the most relevant conclusions is presented. Finally, some ideas on possible alternatives for future works derived from this thesis have been proposed.

8.1. SUMMARY

The first chapter analyses the state of the art on plastic production and main sectors of application, and on generation of plastic wastes, focused on the environmental problem generated by uncontrolled dumping and the different alternatives and processes, at the research or industrial stage, proposed for the management and valorization of plastic wastes.

Pyrolysis has been found to be one of the most common strategies to produce liquid hydrocarbons from plastic wastes. However, the oil product obtained requires upgrading through hydrotreatment to be used as a fuel. Catalytic hydrocracking is proposed as an alternative treatment to pyrolysis and hydrotreatment, in a single stage. In a previous work, the conditions of catalytic hydrocracking of PS for working under kinetic control were established, and the kinetic model was proposed.

Hydrocracking of plastics has been carried out in a three-phase stirred reactor under kinetic control with bifunctional catalysts in slurry and hydrogen pressure. Bifunctional Pt/zeolite catalysts have been prepared and characterized, in order to establish a relationship between properties and performance. Several virgin plastics and plastic wastes have been characterized and tested, so that their behavior in reaction can be related to their composition. The required experimental equipments and procedures used all over the work for reaction, preparation and characterization are described in detail in Chapter 2.

Chapters 3 and 4 have been devoted to optimization of the bifunctional catalyst for hydrocracking of plastics, using virgin PS as the base polymer for comparison. In Chapter 3, the effect of the acid properties of the zeolitic supports on activity and

selectivity has been studied; the acid properties of the supports have been modified by either dealumination or desilication.

On the other hand, optimization of the metallic function has been studied in Chapter 4, where the effect of platinum content and preparation procedure on activity and selectivity has been analyzed. Platinum contents in the range 0.1–1.0 wt.% and prepared by either ionic exchange or impregnation on HBeta zeolite have been studied.

Plastic wastes are composed by a mixture of different polymeric materials. Hence, once catalyst was optimized for PS, its performance in hydrocracking with other polymeric materials was studied. In Chapter 5, common polymers with only carbon and hydrogen atoms in their composition, such as PB and HIPS, were chosen. HIPS, besides, is composed by a mixture of PS and PB. Thus, the effect of mixture has been also analyzed. Thermal hydrocracking experiments were also carried out for comparison.

Hydrocracking of more complex polymers has been studied in Chapter 6. Polymers in plastic wastes are not only composed of carbon and hydrogen. Thus, ABS, with also nitrogen, has been first studied. ABS, besides, is composed of PS, PB and PAN, and the effect of mixture can be also analyzed. Additionally, halogens are commonly found in plastic wastes, either in the polymer molecules or in additives such as flame retardants. Thus, a residual ABS, with additives and fillers, has been also studied in Chapter 6. The effect of pressure, temperature and concentration of polymer has been analyzed, mainly focused on the yield to gasoline and its composition.

Actual, more complex, plastic wastes have been also studied in Chapter 6. Plastic wastes from cellular phones (CP) have been chosen because of their content of ABS and complexity, focused also in the yield to gasoline and its composition.

Plastic wastes with a high content of inorganic components, such as many of the wastes from electrical and electronic equipment, are not suitable for catalytic hydrocracking. Thus, steam gasification to produce hydrogen has been proposed and studied as an alternative valorization process in Chapter 7, applied to phenolic boards, the main plastic component in printed circuits.

Electronic wastes usually include a significant amount of metals in their composition. These metals could act as catalysts in steam reforming of the plastics. This catalytic effect has been also studied, with nickel or tantalum capacitors (TC). The catalytic effect of the presence of molten carbonates in a vessel together with the wastes was the object of a previous study. In this work, the combined effect of nickel and molten carbonates has been also analyzed.

Finally, Chapters 9 and 10 summarize the nomenclature and the literature used all over the work, respectively.

8.2. CONCLUSIONS

The most relevant conclusions of this thesis work are summarized in this section. The conclusions have been classified for a more ordered presentation.

- **On bifunctional Pt/zeolite catalysts for polymer hydrocracking**

The mesopore distribution of the zeolite used as catalytic support has been shown to be a fundamental parameter in its catalytic activity in the hydrocracking of polymers. An adequate support should present an open pore structure with a significant amount of big pores accessible to polymer macromolecules. In this sense, HBeta has proven to be the best support for bifunctional catalysts among those studied.

Two main reaction pathways were identified on bifunctional Pt/zeolite catalysts for polymer chain scission: end-chain and random scission. Both end-chain and random scission reactions have been found to be improved by surface area of the support, provided that this surface area is accessible to the reactants, that is, above the hydraulic diameter of the polymer.

However, we have shown in this work that other characteristics associated to the catalytic support affect differently end-chain and random scission. Thus, the higher the acid strength of the catalyst, the higher the rate of end-chain scission reactions has been found to be. Random scission reactions, on the other hand, are improved by increasing the concentration of accessible Brønsted acid sites and the total pyridine acidity of the support.

Concerning the metallic function, platinum surface area in the catalysts has been found to improve both end-chain and random scission reaction rates. However, again, different factors related to the metal seem to affect end-chain and random scission. Thus, end-chain scission reaction rate has been found to increase with platinum particle size, which has been associated to majority big platinum particles being located in the outer surface of the catalyst.

On the other hand, random scission reaction rate increases with the combined effect of accessible Brønsted acid sites and platinum surface area. This effect has been interpreted in terms of the necessary proximity of both types of active sites (Brønsted acids and platinum) for catalytic random scission to occur. This result is in good agreement with the proposed reaction mechanism, and is supported by the calculated TOF values.

In the studied conditions, small differences have been found among catalysts on distribution of products. The main differences are associated to the lumps distribution in the gasoline fraction, which are associated to platinum. In short, naphthenic compounds in the gasoline fraction are favored, in detriment of aromatics, by higher platinum content in the catalysts.

FDI catalysts present lower platinum dispersion than IE catalysts. Also, FDI catalysts produce higher naphthenic and lower aromatic contents in the gasoline fraction than IE catalysts. This result supports the above conclusion that the majority big platinum particles are located on the outer surface of the catalyst.

- **On polymer hydrocracking feed**

The nature and composition of the polymers fed to the hydrocracking process has been found to be a critical factor affecting catalytic performance and distribution of products, and to which extent the thermal process contributes to the overall rate.

When the polymers are composed by just carbon and hydrogen, thermal end-chain scission seems to occur through the same pathway for the different studied polymers. The catalyst produces a significant increase in end-chain scission rate, particularly when phenyl groups are present in the polymer chain.

Thermal random scission, on the other hand, is clearly slower in the presence of phenyl groups in the polymer chain, which clearly stabilize the polymer. Thus, in the absence of phenyl groups in the polymer, catalytic random scission is barely

favored versus the thermal process. However, when phenyl groups are present in the polymer, the presence of catalyst clearly increases random scission reaction rate.

Concerning selectivity, the distribution of products obtained in the thermal process, in a wide range of carbons, is highly dependent of the polymer nature, and the results obtained with polymer mixtures is in reasonable agreement with the mixture of the reaction products of the individual polymers. However, when a bifunctional catalyst is used, the yields to gasoline and the distribution of products are relatively independent of the nature of the polymer reactants, the temperature and the degree of conversion, with yields to gasoline around 80 wt.% and a majority of naphthenic compounds with six and nine carbons.

Thus, catalytic hydrocracking with bifunctional Pt/HBeta catalysts assures a significant homogeneity in the reaction products when polymers composed only by carbon and hydrogen are used as reactants. This conclusion is relevant from the practical point of view, as the variation in the composition of the plastic mixture, which is to be expected in actual plastic wastes, will produce no significant effect in the product quality.

When polymers or plastic mixtures containing heteroatoms are considered for hydrocracking, a first analysis of thermal stability and product distribution must be performed before they are added to the feed mixture. Thermal stability will help fixing the most adequate temperature for hydrocracking. Product distribution should be focused on the yield to gasoline, to which extent heteroatoms remain in this fraction, and the yield to solids, which may deactivate the catalyst.

In particular, ABS terpolymer, a common nitrogen-containing polymer, has been studied. No particular problems have been found with this polymer, but higher catalytic hydrocracking temperatures, above 673 K, and an open-end reaction system, are required. ABS produces a high yield to gasoline with low concentration of nitrogen and a majority of isoparaffins and naphthenics, particularly at high concentration of ABS and intermediate hydrogen pressure.

When a residual ABS mixture with additives and fillers is used for hydrocracking, a significant amount of solid product is formed. This solid has been related to the presence of additives and fillers in the mixture, and it can substantially affect the process, in relation to the catalyst.

Plastic wastes from cellular phones, a complex mixture composed by a wide variety of components including ABS, HDPE, PC and silicone, have been also studied. The presence of silicone has been shown to produce solid silicon/silica in the products. Thus, silicone should be removed from the plastic wastes for this kind of treatments.

Once silicone is removed, the possibility to treat these plastic wastes in hydrocracking should be checked. The limiting factor would be formation of solids. If a significant amount of solids is formed, these plastic wastes should be considered for other valorization processes, such as steam gasification to hydrogen.

- **On steam gasification of plastic wastes**

Plastic wastes with a high content of inorganic components would be good candidates for steam gasification. The solid products, in this case, represent no problem, as the main product, hydrogen, is obtained in the gas phase.

Phenolic boards, representing one of the main components in electronic waste, have been shown to successfully produce hydrogen from steam gasification at high temperature with no solid residue. Solid residues would be related to inorganic components in electronic waste, where they are usually present to a high percentage.

Nickel, added to phenolic boards, significantly reduces the required operation temperature for steam reforming, which confirms its catalytic effect. This catalytic effect is observed both in the absence and in the presence of molten carbonates, which had been shown in a previous study to present some catalytic effect as well. In any case, good performance requires that the components are well mixed.

Steam reforming has been shown to occur in two steps: a first pyrolysis of the plastic wastes followed by steam gasification of the pyrolysis products, which occurs at higher temperature and only in the presence of steam.

Among the inorganic components in electronic wastes, metals represent a significant percentage. Tantalum capacitors, for example, have been shown to be composed by about 60 wt.% metals. When submitted to steam reforming, in any case, these metals presented also a catalytic effect.

Thus, this conclusion opens an interesting perspective for the valorization of hazardous heterogeneous materials such as wastes from electric and electronic equipment through steam reforming, without the requirement of a previous separation of the different components. Plastic components in the wastes would undergo steam reforming to produce hydrogen, and the metals in the wastes would act as catalysts for the process.

After steam reforming, the valuable metals, including nickel and tantalum, would be present in the reaction products, from where they could be easily recovered to be sold for reuse in the electronic industry. This way, the efficiency and the economy of the valorization process can be highly improved.

Chapter 9

NOMENCLATURE

Capítulo 9

NOMENCLATURA

9. NOMENCLATURE

Abbreviations and Acronyms

A	Aromatics
ABS	Acrylonitrile-Butadiene-Styrene
ABS-R	Residual Acrylonitrile-Butadiene-Styrene
AIST	National Institute of Advanced Industrial Science and Technology, Japan
ASR	Automotive Shedder Residue
B	Brønsted acid sites
BFRs	Brominated Flame Retardants
CP	Cellular Phones
dTG	Differential Thermogravimetry
DHC	Dehydrochlorination
DHA	Detailed Hydrocarbons Analysis
DTBPy	2,6-Di-*tert*-butylpyridine
EA	Elemental Analysis
EG	Ethylenglycol
ELV	End Life Vehicles
EMRI	Environmental Management Research Institute, Japan
F	Fisher test
FBR	Fluidized Bed Reactor
FDI	Fast Drying Impregnation
FID	Flame Ionizaion Detector
FIR	Far-Infrared Inner Heating System
FTIR	Fourier Transform Infrared Spectroscopy
FXR	Fixed Bed Reactor
GC	Gas Chromatography
GPC	Gel Permeation Chromatography
HC	Hydrocarbons
HDPE	High Density Polyethylene
HPW	Hazardous Plastic Wastes
HRTEM	High Resolution Transmission Electron Microscopy
I	Isoparaffins
ICP-OES	Inductively Coupled Plasma-Optical Emission Spectroscopy
IE	Ionic Exchange
IPW	Industrial Plastic Wastes

IUPAC	International Union of Pure and Applied Chemistry
L	Lewis acid sites
LDPE	Low Density Polyethylene
MBR	Moving Bed Reactor
MS	Mass Spectroscospy
MSW	Municipal Solid Waste
m/z	Mass-to-charge ratio in mass spectroscopy
N	Naphthenes
O	Olefins
P	Paraffins
PA	Polyamide
PAHs	Polycyclic Aromatic Hydrocarbons
PC	Polycarbonate
PCB	Printed Circuit Board
PCDFs	Polychlorinated dibenzofurans
PDA	Pore Directing Agent
PDMS	polydimethylsiloxane
PDPS	polydiphenylsiloxane
PE	Polyethylene
PET	Polyethylene terephthalate
PhB	Phenolic Board
PP	Polypropylene
PS	Polystyrene
PUR	Polyurethane
PVC	Polyvinyl chloride
PW	Plastic Wastes
Py	Pyridine
RK	Rotary Kiln
SAN	Styrene-Acrylonitrile
SEM	Scanning Electron Microscopy
SGIker	General Research Services, UPV/EHU
STR	Stirred Tank Reactor
TEM	Transmission Electron Microscopy
TC	Tantalum Capacitor
TC_{cover}	Cover part of the tantalum capacitor
TC_{core}	Inner part of the tantalum capacitor
$TC_{terminal}$	Terminal part of the tantalum capacitor
THF	Tetrahydrofuran

TGA	Thermogravimetric Analysis
TPAOH	Tetrapropylammonium hydroxide
TPA^+	Tetrapropylammonium ion
TPD	Temperature Programmed Desorption
TQSA	Chemical Technologies for Environmental Sustainability
EU	European Union
UPV/EHU	The University of the Basque Country
VOC	Volatile Organic Compound
XPS	X-Ray Photoelectron Spectroscopy
XRD	X-Ray Diffraction
US	United States
WDXRF	Wavelength Dispersive X-Ray Fluorescence
WEEE	Wastes from electrical and electronic equipment

Variables and Parameters

a	Heating rate in TG (Equations 2.30-2.33), $K \cdot min^{-1}$
A	Pre-exponential factor (Equations 2.31-2.33), units of K(T)
Access.	Accessibility of DTBPy to the Brønsted acid sites of the catalyst (Equation 2.6), %
A_m	Cross-sectional area of the adsorbate (Equation 2.8), nm^2
A_r	Pre-exponential factor of polymer random scission reactions, $mol \cdot g^{-1} \cdot min^{-1}$
A'_r	Pre-exponential factor of polymer random scission reactions assuming constant E_a, $mol \cdot g^{-1} \cdot min^{-1}$
A_s	Pre-exponential factor of polymer end-chain scission reactions, min^{-1}
A'_s	Pre-exponential factor of polymer end-chain scission reactions assuming constant E_a, min^{-1}
c	Shape parameter (Equation 2.14), dimensionless
C	Constant (Equation 2.7), dimensionless
$C_{P,0}$	Initial molar polymer concentration in the reactor (Equation 2.23, Equation 2.26), $\mu mol \cdot cm^{-3}$
$C_{P,t}$	Polymer concentration at t reaction time (Equation 2.23), $\mu mol\ cm^{-3}$
C_{Py}	Adsorbed pyridine (Equations 2.3-2.4), $mmol \cdot g_{cat}^{-1}$
d	Distance between adsorbent and adsorptive molecules (Equation 2.11), nm
$d_{(hkl)}$	Distance between reflection planes of Miller indexes (hkl) (Equation 2.1), Å
d_{meso}	Average diameter of mesopores, nm
d_{micro}	Average diameter of micropores, nm

d_{Pt}	Platinum particle diameter, nm
D_i	Metal dispersion (Equation 2.13), dimensionless
D_{Pt}	Platinum dispersion, %
e	Thickness of the adsorbed layer (Equation 2.9), nm
E_{ar}	Apparent activation energy of polymer random scission reactions, $kJ \cdot mol^{-1}$
E_{as}	Apparent activation energy of polymer end-chain scission reactions, $kJ \cdot mol^{-1}$
E_a^{LNK}	Apparent activation energy for steam gasification reaction in the presence of carbonates, $kJ \cdot mol^{-1}$
E_a^{LNK+Ni}	Apparent activation energy for steam gasification reaction in the presence of both nickel and carbonates, $kJ \cdot mol^{-1}$
E_a^{Ni}	Apparent activation energy for steam gasification reaction in the presence of nickel, $kJ \cdot mol^{-1}$
f(x)	Function of conversion in the TG (Equations 2.30-2.32)
FR_i	Relative factor per hydrocarbon with a specific number of carbons (Equation 2.19), dimensionless
g(x)	Integrated function of conversion in the TG (Equations 2.32-2.33)
G	Metal content of the catalyst (Equation 2.13), $g_{Pt} \cdot g_{cat}^{-1}$
I_{MEC}	Integrated molar extinction coefficient (Equation 2.5), $cm \cdot \mu mol^{-1}$
IA_{1450}	Absorbance peak area at 1450 cm^{-1} (Lewis, Equation 2.4), $cm^2 \cdot mg^{-1}$
IA_{1540}	Absorbance peak area at 1540 cm^{-1} (Brønsted, Equation 2.3), $cm^2 \cdot mg^{-1}$
k_r	Kinetic constant of polymer random scission reactions, $mol \cdot g^{-1} \cdot min^{-1}$
k_s	Kinetic constant of polymer end-chain scission reactions, min^{-1}
K_{AS}	Kirkwood-Mueller constant of the adsorbent (Equation 2.11), $J \cdot cm^6$
$K_{A\alpha}$	Kirkwood-Mueller constant of the adsorptive (Equation 2.11), $J \cdot cm^6$
k(LNK)	Steam gasification kinetic constant in the presence of carbonates, min^{-1}
k(LNK+Ni)	Steam gasification kinetic constant in the presence of both nickel and carbonates, min^{-1}
k(Ni)	Steam gasification kinetic constant in the presence of nickel powder, min^{-1}
l	Pore diameter of the solid (Equation 2.11), nm,
m	Mass of the solid used in the analysis (Equation 2.8), g
M_i	Molecular weight, $g \cdot mol^{-1}$
M_m	Molecular weight of the metal (Equation 2.13), $g \cdot mol^{-1}$
M_n	Polymer number-average molecular weight, $g \cdot mol^{-1}$
M_{n0}	Polymer initial number-average molecular weight (Equation 2.25), $g \cdot mol^{-1}$

M_W	Polymer weight-average molecular weight, $g \cdot mol^{-1}$
n_C	Number of carbons in the group (Equation 2.19), dimensionless
n_H	Number of hydrogens in the group (Equation 2.19), dimensionless
N_A	Avogadro's number, $6.022 \cdot 10^{23}$ mol^{-1}
N_{feed}	Weight of nitrogen in the reactor feed (Equations 2.15, 2.21-2.22), mg
N_{Gas}	Nitrogen fed to the reactor exiting in the gas products as ammonia and hydrogen cyanide (Equation 2.22), %
$N_{Gasoline}$	Nitrogen fed to the reactor exiting in the gasoline fraction (Equation 2.21), %
N_{HCN}	Amount of nitrogen as hydrogen cyanide in the gases (Equation 2.22), mg
N_i	Total number of molecules in the sample (Equation 2.16 and 2.17), dimensionless
N_{NH3}	Amount of nitrogen as ammonia in the gases (Equation 2.22), mg
N_S	Number of surface metal atoms in the catalyst (Equations 2.12-2.13), g_{cat}^{-1}
N_{Solid}	Nitrogen fed to the reactor exiting in the solids (Equation 2.15), %
N_{sum}	Total amount of nitrogen in the gasoline fraction (Equation 2.21), mg
N_T	Total number of metal atoms in the catalyst (Equation 2.13), g_{cat}^{-1}
P	Pressure, bar
P_0	Saturation pressure of the adsorbate (Equations 2.9-2.11), bar
r	Correlation coefficient of a fitting, dimensionless
R	Ideal gas constant, 8.314 $J \cdot mol^{-1} \cdot K^{-1}$
$r^{(0)}$	Hydrocracking initial molar reaction rate (Equation 2.26), $mol \cdot g_{cat}^{-1} \cdot min^{-1}$
$r^{(1)}$	Hydrocracking initial mass reaction rate (Equation 2.27), $g \cdot g_{cat}^{-1} \cdot min^{-1}$
r^2	Determination coefficient of a fitting, dimensionless
r_d	Radius of the catalyst wafer disk (Equations 2.3-2.4), cm
r_p	Pore radius of the catalyst (Equation 2.9), nm
RI_t	Reference index of a component at time t (Equation 2.18), dimensionless
S_{BET}	Specific solid surface calculated according to Brunauer, Emmett and Teller (Equation 2.8), $m^2 \cdot g_{cat}^{-1}$
S^{exp}_{DTBPy}	Experimental DTBPy adsorbed in the solid (Equation 2.6), $m^2 \cdot g_{cat}^{-1}$
S^{the}_{DTBPy}	Theoretical adsorbance area of DTBPy in the solid (Equations 2.5-2.6), $m^2 \cdot g_{cat}^{-1}$
S_{ext}	External specific surface area of the catalyst, $m^2 \cdot g_{cat}^{-1}$
S_{micro}	Micropore specific surface area of the catalyst, $m^2 \cdot g_{cat}^{-1}$
S_{Pt}	Platinum surface area of the catalyst, $m^2 \cdot g_{cat}^{-1}$

S_{Py}	Integrated area of the corresponding adsorbance band of Py on the sample (Equation 2.5), $m^2 \cdot g^{-1}$
t	Time, min
T	Temperature, K
$TOF^{(0)}$	Turn-over frequency (number of polymer molecules reacting per surface metal atom in the catalyst per second) corresponding to $r^{(0)}$, s^{-1}
$TOF^{(1)}$	Turn-over frequency (number of polymer molecules reacting per surface metal atom in the catalyst per second) corresponding to $-r^{(1)}$, s^{-1}
t_{plot}	Statistical thickness of a layer adsorbed over a nonporous surface (Equation 2.10), Å
t_r	Retention time, min
V_{ads}	Volume of adsorbate per unit mass of solid in equilibrium (Equation 2.7), $cm^3 \cdot g^{-1}$
V_m	Volume of adsorbate required to form a monolayer on the solid surface (Equation 2.7), $cm^3 \cdot g^{-1}$
V_{meso}	Mesopore volume of the catalyst, $cm^3 \cdot g_{cat}^{-1}$
V_{mol}	Molar volume of the adsorbate (Equation 2.8), $cm^3 \cdot mol^{-1}$
V_p	Pore volume of the catalyst, $cm^3 \cdot g_{cat}^{-1}$
x	Conversion in TG (relative weight loss, Equations 2.30-2.33), dimensionless
X	Conversion in hydrocracking (Equation 2.23), dimensionless
X_m	Surface metal atoms covered per chemisorbed molecule (Equation 2.12), dimensionless

Greek Symbols

β	X-ray line broadening at half the maximum intensity (Equation 2.2), rad
λ	Wavelength of incident radiation (Equation 2.1), nm
θ	Incident angle of X radiation (Equation 2.1), dimensionless
ρ	Density of the metal (Equation 2.14), $g \cdot cm^{-3}$
σ	Surface occupied per metal atom (Equation 2.14), cm^2
σ	Distance between two adsorbate molecules with zero interaction energy (Equation 2.11), nm
τ	Mean size of the crystalline domains (Equation 2.2), Å
υ	Contact angle between condensed phase and solid walls (Equation 2.9), rad
ψ	Surface tension of the adsorbate (Equation 2.9), $N \cdot m^{-1}$

Chapter 10

LITERATURE

Capítulo 10

BIBLIOGRAFÍA

10. LITERATURE

[1] S.M. Al-Salem, P. Lettieri, J. Baeyens, Recycling and recovery routes of plastic solid waste (PSW): A review, Waste Manage. 29 (2009) 2625. http://dx.doi.org/10.1016/j.wasman.2009.06.004.

[2] Association of Plastics Manufacturers in Europe (APME), Plastics: the Facts 2014/2015: An analysis of European plastics production, demand and waste data, http://www.plasticseurope.org/, 2015. (last consulted: 05/09/2016).

[3] T. Bhaskar, J.A. Salbidegoitia, T. Kamo, Effective and environment friendly processes for waste plastics utilization, in: L. Shu, V. Jegatheesan, A. Pandey, J. Virkutyte and H.D. Utomo (Eds.), Solutions to Environmental Challenges through Innovations in Research, Asiatech Publishers Inc., New Delhi, 2013, p. 424.

[4] A.K. Panda, R.K. Singh, D.K. Mishra, Thermolysis of waste plastics to liquid fuel: A suitable method for plastic waste management and manufacture of value added products. A world prospective, Renew. Sust. Energ. Rev. 14 (2010) 233. http://dx.doi.org/10.1016/j.rser.2009.07.005.

[5] M. Sadat-Shojai, G. Bakhshandeh, Recycling of PVC wastes, Polym. Degrad. Stabil. 96 (2011) 404. http://dx.doi.org/10.1016/j.polymdegradstab.2010.12.001.

[6] S.M. Alston, J.C. Arnold, Environmental impact of pyrolysis of mixed WEEE plastics part 2: Life cycle assessment, Environ. Sci. Technol. 45 (2011) 9386. http://dx.doi.org/10.1021/es2016654.

[7] Y. Feng, Y. Yang, C. Zhang, E. Song, D. Shen, Y. Long, Characterization of residues from dismantled imported wastes, Waste Manage. 33 (2013) 1073. http://dx.doi.org/10.1016/j.wasman.2013.01.007.

[8] F.O. Ongondo, I.D. Williams, Greening academia: Use and disposal of mobile phones among university students, Waste Manage. 31 (2011) 1617. http://dx.doi.org/10.1016/j.wasman.2011.01.031.

[9] F.O. Ongondo, I.D. Williams, Mobile phone collection, reuse and recycling in the UK, Waste Manage. 31 (2011) 1307. http://dx.doi.org/10.1016/j.wasman.2011.01.032.

[10] Y. Jang, M. Kim, Management of used & end-of-life mobile phones in Korea: A review, Resour. Conserv. Recycl. 55 (2010) 11. http://dx.doi.org/10.1016/j.resconrec.2010.07.003.

[11] L.H. Yamane, V.T. de Moraes, D.C.R. Espinosa, J.A.S. Tenório, Recycling of WEEE: Characterization of spent printed circuit boards from mobile phones and computers, Waste Manage. 31 (2011) 2553. http://dx.doi.org/10.1016/j.wasman.2011.07.006.

[12] M. Cobbing, Toxic Tech: Not in Our Backyard. Uncovering the Hidden Flows of e-Waste, Greenpeace International, Amsterdam, 2008. http://www.greenpeace.org/. (last consulted: 05/09/2016).

[13] Basel Action Network (BAN), Mobile Toxic Waste: Recent Findings on the Toxicity of End-of-Life Cell Phones, 2004. http://archive.ban.org/. (last consulted: 05/09/2016).

[14] T. Uryu, J. Yoshinaga, Y. Yanagisawa, Environmental Fate of Gallium Arsenide Semiconductor Disposal, J. Ind. Ecol. 7 (2003) 103. http://dx.doi.org/10.1162/108819803322564370.

[15] N. Menad, S. Guignot, J.A. van Houwelingen, New characterisation method of electrical and electronic equipment wastes (WEEE), Waste Manage. 33 (2013) 706. http://dx.doi.org/10.1016/j.wasman.2012.04.007.

[16] European Union, Directive 2012/19/EU on waste electrical and electronic equipment (WEEE), Official Journal, 197 (2012) 38. http://data.europa.eu/eli/dir/2012/19/oj. (last consulted: 05/09/2016).

[17] J. Cui, E. Forssberg, Mechanical recycling of waste electric and electronic equipment: A review, J. Hazard. Mater. 99 (2003) 243. http://dx.doi.org/10.1016/S0304-3894(03)00061-X.

[18] P. Gramatyka, R. Nowosielski, P. Sakiewicz, Recycling of waste electrical and electronic equipment, JAMME 20 (2007) 535. http://www.journalamme.org/papers_vol20/1530s.pdf. (last consulted: 05/09/2016).

[19] L. Zhou, Z. Xu, Response to waste electrical and electronic equipments in China: Legislation, recycling system, and advanced integrated process, Environ. Sci. Technol. 46 (2012) 4713. http://dx.doi.org/10.1021/es203771m.

[20] I. de Marco, B.M. Caballero, M.J. Chomón, M.F. Laresgoiti, A. Torres, G. Fernández, S. Arnaiz, Pyrolysis of electrical and electronic wastes, J. Anal. Appl. Pyrolysis 82 (2008) 179. http://dx.doi.org/10.1016/j.jaap.2008.03.011.

[21] G. Martinho, A. Pires, L. Saraiva, R. Ribeiro, Composition of plastics from waste electrical and electronic equipment (WEEE) by direct sampling, Waste Manage. 32 (2012) 1213. http://dx.doi.org/10.1016/j.wasman.2012.02.010.

[22] E. Stenvall, S. Tostar, A. Boldizar, M.R.S. Foreman, K. Möller, An analysis of the composition and metal contamination of plastics from waste electrical and electronic equipment (WEEE), Waste Manage. 33 (2013) 915. http://dx.doi.org/10.1016/j.wasman.2012.12.022.

[23] M.C. Santos, J.A. Nóbrega, S. Cadore, Determination of Cd, Cr, Hg and Pb in plastics from waste electrical and electronic equipment by inductively coupled plasma mass spectrometry with collision-reaction interface technology, J. Hazard. Mater. 190 (2011) 833. http://dx.doi.org/10.1016/j.jhazmat.2011.04.004.

[24] L. Tange, D. Drohmann, Waste electrical and electronic equipment plastics with brominated flame retardants – from legislation to separate treatment – thermal processes, Polym. Degrad. Stabil. 88 (2005) 35. http://dx.doi.org/10.1016/j.polymdegradstab.2004.03.025.

[25] S. Kemmlein, D. Herzke, R.J. Law, Brominated flame retardants in the European chemicals policy of REACH—Regulation and determination in materials, J. Chromatogr. A 1216 (2009) 320. http://dx.doi.org/10.1016/j.chroma.2008.05.085.

[26] Y. Zhong, P. Peng, Z. Yu, H. Deng, Effects of metals on the transformation of hexabromocyclododecane (HBCD) in solvents: Implications for solvent-based recycling of brominated flame retardants, Chemosphere 81 (2010) 72. http://dx.doi.org/10.1016/j.chemosphere.2010.06.061.

[27] N. Kajiwara, Y. Noma, H. Takigami, Brominated and organophosphate flame retardants in selected consumer products on the Japanese market in 2008, J. Hazard. Mater. 192 (2011) 1250. http://dx.doi.org/10.1016/j.jhazmat.2011.06.043.

[28] A. Covaci, S. Voorspoels, M.A. Abdallah, T. Geens, S. Harrad, R.J. Law, Analytical and environmental aspects of the flame retardant tetrabromobisphenol-A and its derivatives, J. Chromatogr. A 1216 (2009) 346. http://dx.doi.org/10.1016/j.chroma.2008.08.035.

[29] Y. Zhong, P. Peng, W. Huang, Transformation of tetrabromobisphenol A in the presence of different solvents and metals, Chemosphere 87 (2012) 1141. http://dx.doi.org/10.1016/j.chemosphere.2012.02.019.

[30] I. van der Veen, J. de Boer, Phosphorus flame retardants: Properties, production, environmental occurrence, toxicity and analysis, Chemosphere 88 (2012) 1119. http://dx.doi.org/10.1016/j.chemosphere.2012.03.067.

[31] H. Wang, M. Hirahara, M. Goto, T. Hirose, Extraction of flame retardants from electronic printed circuit board by supercritical carbon dioxide, J. Supercrit. Fluids 29 (2004) 251. http://dx.doi.org/10.1016/S0896-8446(03)00073-1.

[32] Y. Wang, F. Zhang, Degradation of brominated flame retardant in computer housing plastic by supercritical fluids, J. Hazard. Mater. 205-206 (2012) 156. http://dx.doi.org/10.1016/j.jhazmat.2011.12.055.

[33] M. Zolezzi, C. Nicolella, S. Ferrara, C. Iacobucci, M. Rovatti, Conventional and fast pyrolysis of automobile shredder residues (ASR), Waste Manage. 24 (2004) 691. http://dx.doi.org/10.1016/j.wasman.2003.12.005.

[34] I. Vermeulen, J. Van Caneghem, C. Block, J. Baeyens, C. Vandecasteele, Automotive shredder residue (ASR): Reviewing its production from end-of-life vehicles (ELVs) and its recycling, energy or chemicals' valorisation, J. Hazard. Mater. 190 (2011) 8. http://dx.doi.org/10.1016/j.jhazmat.2011.02.088.

[35] I. Vermeulen, C. Block, J. Van Caneghem, W. Dewulf, S.K. Sikdar, C. Vandecasteele, Sustainability assessment of industrial waste treatment processes: The case of automotive shredder residue, Resour. Conserv. Recycl. 69 (2012) 17. http://dx.doi.org/10.1016/j.resconrec.2012.08.010.

[36] D. Duval, H.L. MacLean, The role of product information in automotive plastics recycling: A financial and life cycle assessment, J. Clean. Prod. 15 (2007) 1158. http://dx.doi.org/10.1016/j.jclepro.2006.05.030.

[37] K. Bocz, A. Toldy, Á Kmetty, T. Bárány, T. Igricz, G. Marosi, Development of flame retarded self-reinforced composites from automotive shredder plastic waste, Polym. Degrad. Stabil. 97 (2012) 221. http://dx.doi.org/10.1016/j.polymdegradstab.2011.12.029.

[38] European Union, Directive 2008/98/EC of the European Parliament and of the Council on waste and repealing certain Directives, Official Journal, 312 (2008) 3. http:/data.europa.eu/eli/dir/2008/98/oj. (last consulted: 05/09/2016).

[39] A. Villanueva, P. Eder, End-of-waste criteria for waste plastic for conversion, JRC Technical Reports, European Union, Luxembourg, 2014. http://dx.doi.org/10.2791/13033.

[40] R.E.N. de Castro, G.J. Vidotti, A.F. Rubira, E.C. Muniz, Depolymerization of poly(ethylene terephthalate) wastes using ethanol and ethanol/water in supercritical conditions, J. Appl. Polym. Sci. 101 (2006) 2009. http://dx.doi.org/10.1002/app.23748.

[41] R. López-Fonseca, I. Duque-Ingunza, B. de Rivas, S. Arnaiz, J.I. Gutiérrez-Ortiz, Chemical recycling of post-consumer PET wastes by glycolysis in the presence of metal salts, Polym. Degrad. Stabil. 95 (2010) 1022. http://dx.doi.org/10.1016/j.polymdegradstab.2010.03.007.

[42] A. Marcilla, M.I. Beltrán, R. Navarro, Evolution of products during the degradation of polyethylene in a batch reactor, J. Anal. Appl. Pyrolysis 86 (2009) 14. http://dx.doi.org/10.1016/j.jaap.2009.03.004.

[43] G. Elordi, M. Olazar, G. López, M. Artetxe, J. Bilbao, Product yields and compositions in the continuous pyrolysis of high-density polyethylene in a conical spouted bed reactor, Ind. Eng. Chem. Res. 50 (2011) 6650. http://dx.doi.org/10.1021/ie200186m.

[44] R. Aguado, M. Olazar, B. Gaisán, R. Prieto, J. Bilbao, Kinetics of polystyrene pyrolysis in a conical spouted bed reactor, Chem. Eng. J. 92 (2003) 91. http://dx.doi.org/10.1016/S1385-8947(02)00119-5.

[45] W. Kaminsky, M. Predel, A. Sadiki, Feedstock recycling of polymers by pyrolysis in a fluidised bed, Polym. Degrad. Stabil. 85 (2004) 1045. http://dx.doi.org/10.1016/j.polymdegradstab.2003.05.002.

[46] J. Lin, C. Chang, C. Wu, S. Shih, Thermal degradation kinetics of polybutadiene rubber, Polym. Degrad. Stabil. 53 (1996) 295. http://dx.doi.org/10.1016/0141-3910(96)00098-5.

[47] F. Chen, J. Qian, Studies on the thermal degradation of polybutadiene, Fuel Process. Technol. 67 (2000) 53. http://dx.doi.org/10.1016/S0378-3820(00)00073-4.

[48] A. Marcilla, A. Gómez-Siurana, J.C.G. Quesada, D. Berenguer, Characterization of styrene-butadiene copolymers by catalytic pyrolysis over Al-MCM-41, J. Anal. Appl. Pyrolysis 85 (2009) 327. http://dx.doi.org/10.1016/j.jaap.2008.08.010.

[49] S. Jung, S. Kim, J. Kim, Fast pyrolysis of a waste fraction of high impact polystyrene (HIPS) containing brominated flame retardants in a fluidized bed reactor: The effects of various Ca-based additives (CaO, $Ca(OH)_2$ and oyster shells) on the removal of bromine, Fuel 95 (2012) 514. http://dx.doi.org/10.1016/j.fuel.2011.11.048.

[50] K. Lee, D. Shin, Y. Seo, Thermal degradation of nitrogen-containing polymers, acrylonitrile-butadiene-styrene and styrene-acrylonitrile, Korean J. Chem. Eng. 23 (2006) 224. http://dx.doi.org/10.1007/BF02705720.

[51] S. Jung, S. Kim, J. Kim, Thermal degradation of acrylonitrile-butadiene-styrene (ABS) containing flame retardants using a fluidized bed reactor: The effects of Ca-based additives on halogen removal, Fuel Process. Technol. 96 (2012) 265. http://dx.doi.org/10.1016/j.fuproc.2011.12.039.

[52] A. Demirbas, Pyrolysis of municipal plastic wastes for recovery of gasoline-range hydrocarbons, J. Anal. Appl. Pyrolysis 72 (2004) 97. http://dx.doi.org/10.1016/j.jaap.2004.03.001.

[53] W.J. Hall, N.M.M. Mitan, T. Bhaskar, A. Muto, Y. Sakata, P.T. Williams, The co-pyrolysis of flame retarded high impact polystyrene and polyolefins, J. Anal. Appl. Pyrolysis 80 (2007) 406. http://dx.doi.org/10.1016/j.jaap.2007.05.002.

[54] Z. Czégény, E. Jakab, M. Blazsó, T. Bhaskar, Y. Sakata, Thermal decomposition of polymer mixtures of PVC, PET and ABS containing brominated flame retardant: Formation of chlorinated and brominated organic compounds, J. Anal. Appl. Pyrolysis 96 (2012) 69. http://dx.doi.org/10.1016/j.jaap.2012.03.006.

[55] T. Malkow, Novel and innovative pyrolysis and gasification technologies for energy efficient and environmentally sound MSW disposal, Waste Manage. 24 (2004) 53. http://dx.doi.org/10.1016/S0956-053X(03)00038-2.

[56] U. Arena, M.L. Mastellone, Fluidized bed pyrolysis of plastic wastes, in: J. Scheirs and W. Kaminsky (Eds.), Feedstock Recycling and Pyrolysis of Waste Plastics, John Wiley & Sons, Ltd., 2006, p. 435.

[57] A. Tukker, H. de Groot, L. Simons, S. Wiegersma, Chemical recycling of plastic waste (PVC and other resins), TNO Institute of Strategy, Technology and Policy. STB-99-55. Final report, European Commission, 1999. http://ec.europa.eu/environment/waste/studies/pvc/chem_recycle.pdf. (last consulted: 05/09/2016).

[58] A. Hornung, H. Seifert, Rotary kiln pyrolysis of polymers containing heteroatoms, in: J. Scheirs and W. Kaminsky (Eds.), Feedstock Recycling and Pyrolysis of Waste Plastics, John Wiley & Sons, Ltd., 2006, p. 549.

[59] A. Buekens, Introduction to feedstock recycling of plastics, in: J. Scheirs and W. Kaminsky (Eds.), Feedstock Recycling and Pyrolysis of Waste Plastics, John Wiley & Sons, Ltd., 2006, p. 1.

[60] A. Okuwaki, T. Yoshioka, M. Asai, H. Tachibana, K. Wakai, K. Tada, The liquefaction of plastic containers and packaging in Japan, in: J. Scheirs and W. Kaminsky (Eds.), Feedstock Recycling and Pyrolysis of Waste Plastics, John Wiley & Sons, Ltd., 2006, p. 663.

[61] United Nations Environmental Programme (UNEP), Converting Waste Plastics into a Resource. Compedium of Technologies, Technical Report, Division of Technology, Industry and Economics International Environmental Technology Centre, United Nations, Osaka, 2009. http://www.unep.or.jp/letc/Publications/spc/wasteplasticsest_compendium.pdf. (last consulted: 05/09/2016).

[62] E. Butler, G. Devlin, K. McDonnell, Waste polyolefins to liquid fuels via pyrolysis: Review of commercial state-of-the-art and recent laboratory research, Waste Biomass Valorization 2 (2011) 227. http://dx.doi.org/10.1007/s12649-011-9067-5.

[63] J. Scheirs, Overview of commercial pyrolysis processes for waste plastics, in: J. Scheirs and W. Kaminsky (Eds.), Feedstock Recycling and Pyrolysis of Waste Plastics, John Wiley & Sons, Ltd., 2006, p. 381.

[64] A.G. Buekens, H. Huang, Catalytic plastics cracking for recovery of gasoline-range hydrocarbons from municipal plastic wastes, Resour. Conserv. Recycl. 23 (1998) 163. http://dx.doi.org/10.1016/S0921-3449(98)00025-1.

[65] D.P. Serrano, J. Aguado, J.M. Escola, Developing advanced catalysts for the conversion of polyolefinic waste plastics into fuels and chemicals, ACS Catal. 2 (2012) 1924. http://dx.doi.org/10.1021/cs3003403.

[66] L.J. Broadbelt, Catalytic resource recovery from waste polymers, in: J.J. Spivey (Ed.), Catalysis, vol. 14, Royal Society of Chemistry, 1999, p. 110. http://dx.doi.org/ 10.1039/9781847553263-00110.

[67] Y. Sakata, M.A. Uddin, K. Koizumi, K. Murata, Thermal degradation of polyethylene mixed with poly(vinyl chloride) and poly(ethyleneterephthalate), Polym. Degrad. Stabil. 53 (1996) 111. http://dx.doi.org/10.1016/0141-3910(96)00077-8.

[68] M.A. Uddin, Y. Sakata, A. Muto, Y. Shiraga, K. Koizumi, Y. Kanada, K. Murata, Catalytic degradation of polyethylene and polypropylene into liquid hydrocarbons with mesoporous silica, Microporous Mesoporous Mat. 21 (1998) 557. http://dx.doi.org/10.1016/S1387-1811(98)00036-5.

[69] C. Tang, Y. Wang, Q. Zhou, L. Zheng, Catalytic effect of Al–Zn composite catalyst on the degradation of PVC-containing polymer mixtures into pyrolysis oil, Polym. Degrad. Stabil. 81 (2003) 89. http://dx.doi.org/10.1016/S0141-3910(03)00066-1.

[70] Q. Zhou, C. Tang, Y. Wang, L. Zheng, Catalytic degradation and dechlorination of PVC-containing mixed plastics via Al–Mg composite oxide catalysts, Fuel 83 (2004) 1727. http://dx.doi.org/10.1016/j.fuel.2004.02.015.

[71] K. Murata, M. Brebu, Y. Sakata, The effect of PVC on thermal and catalytic degradation of polyethylene, polypropylene and polystyrene by a continuous flow reactor, J. Anal. Appl. Pyrolysis 86 (2009) 33. http://dx.doi.org/10.1016/j.jaap.2009.04.003.

[72] A. Adrados, I. de Marco, B.M. Caballero, A. López, M.F. Laresgoiti, A. Torres, Pyrolysis of plastic packaging waste: A comparison of plastic residuals from material recovery facilities with simulated plastic waste, Waste Manage. 32 (2012) 826. http://dx.doi.org/10.1016/j.wasman.2011.06.016.

[73] Y.H. Lin, M.H. Yang, T.T. Wei, C.T. Hsu, K.J. Wu, S.L. Lee, Acid-catalyzed conversion of chlorinated plastic waste into valuable hydrocarbons over post-use commercial FCC catalysts, J. Anal. Appl. Pyrolysis 87 (2010) 154. http://dx.doi.org/10.1016/j.jaap.2009.11.006.

[74] A. Garforth, S. Fiddy, Y.H. Lin, A. Ghanbari-Siakhali, P.N. Sharratt, J. Dwyer, Catalytic degradation of high density polyethylene: An evaluation of

mesoporous and microporous catalysts using thermal analysis, Thermochim. Acta 294 (1997) 65. http://dx.doi.org/10.1016/S0040-6031(96)03145-0.

[75] R. van Grieken, D.P. Serrano, J. Aguado, R. García, C. Rojo, Thermal and catalytic cracking of polyethylene under mild conditions, J. Anal. Appl. Pyrolysis 58-59 (2001) 127. http://dx.doi.org/10.1016/S0165-2370(00)00145-5.

[76] Y.H. Lin, M.H. Yang, T.F. Yeh, M.D. Ger, Catalytic degradation of high density polyethylene over mesoporous and microporous catalysts in a fluidised-bed reactor, Polym. Degrad. Stabil. 86 (2004) 121. http://dx.doi.org/10.1016/j.polymdegradstab.2004.02.015.

[77] H.H.G. Jellinek, K.J. Turner, Thermal degradation of vinyl polymers in solution. I. Degradation of polystyrene in naphthalene solution, J. Polym. Sci. 11 (1953) 353. http://dx.doi.org/10.1002/pol.1953.120110405.

[78] T. Murakata, Y. Saito, T. Yosikawa, T. Suzuki, S. Sato, Solvent effect on thermal degradation of polystyrene and poly-α-methylstyrene, Polym. J. 34 (1993) 1436. http://dx.doi.org/10.1016/0032-3861(93)90857-7.

[79] W.J. Sterling, K.S. Walline, B.J. McCoy, Experimental study of polystyrene thermolysis to moderate conversion, Polym. Degrad. Stabil. 73 (2001) 75. http://dx.doi.org/10.1016/S0141-3910(01)00069-6.

[80] A. Karaduman, E.H. Şimşek, B. Çiçek, A.Y. Bilgesü, Thermal degradation of polystyrene wastes in various solvents, J. Anal. Appl. Pyrolysis 62 (2002) 273. http://dx.doi.org/10.1016/S0165-2370(01)00125-5.

[81] S.L. Gupte, G. Madras, Catalytic degradation of polybutadiene, Polym. Degrad. Stabil. 86 (2004) 529. http://dx.doi.org/10.1016/j.polymdegradstab.2004.06.006.

[82] T. Szekely, G. Varhegyi, F. Till, P. Szabo, E. Jakab, The effects of heat and mass transport on the results of thermal decomposition studies: Part 2. Polystyrene, polytetrafluoroethylene and polypropylene, J. Anal. Appl. Pyrolysis 11 (1987) 83. http://dx.doi.org/10.1016/0165-2370(87)85021-0.

[83] Y. Xingzhong, Converting waste plastics into liquid fuel by pyrolysis: Developments in China, in: J. Scheirs and W. Kaminsky (Eds.), Feedstock Recycling and Pyrolysis of Waste Plastics, John Wiley & Sons, Ltd., 2006, p. 729.

[84] A. Zadgaonkar, Process and equipment for conversions of waste plastics into fuels, in: J. Scheirs and W. Kaminsky (Eds.), Feedstock Recycling and Pyrolysis of Waste Plastics, John Wiley & Sons, Ltd., 2006, p. 709.

[85] M.A. Keane, Catalytic conversion of waste plastics: focus on waste PVC, J. Chem. Technol. Biotechnol. 82 (2007) 787.

http://dx.doi.org/10.1002/jctb.1757.

[86] W. Kaminsky, B. Schlesselmann, C. Simon, Olefins from polyolefins and mixed plastics by pyrolysis, J. Anal. Appl. Pyrolysis 32 (1995) 19. http://dx.doi.org/10.1016/0165-2370(94)00830-T.

[87] T. Karayildirim, J. Yanik, M. Yuksel, M. Saglam, C. Vasile, H. Bockhorn, The effect of some fillers on PVC degradation, J. Anal. Appl. Pyrolysis 75 (2006) 112. http://dx.doi.org/10.1016/j.jaap.2005.04.012.

[88] A. López, I. de Marco, B.M. Caballero, M.F. Laresgoiti, A. Adrados, Dechlorination of fuels in pyrolysis of PVC containing plastic wastes, Fuel Process. Technol. 92 (2011) 253. http://dx.doi.org/10.1016/j.fuproc.2010.05.008.

[89] H.S. Joo, J.A. Guin, Hydrocracking of a plastics pyrolysis gas oil to naphtha, Energy Fuels 11 (1997) 586. http://dx.doi.org/10.1021/ef960151g.

[90] H.S. Joo, J.A. Guin, Continuous upgrading of a plastics pyrolysis liquid to an environmentally favorable gasoline range product, Fuel Process. Technol. 57 (1998) 25. http://dx.doi.org/10.1016/S0378-3820(98)00067-8.

[91] A. Hornung, A.I. Balabanovich, S. Donner, H. Seifert, Detoxification of brominated pyrolysis oils, J. Anal. Appl. Pyrolysis 70 (2003) 723. http://dx.doi.org/10.1016/S0165-2370(03)00049-4.

[92] J.M. Escola, J. Aguado, D.P. Serrano, A. García, A. Peral, L. Briones, R. Calvo, E. Fernández, Catalytic hydroreforming of the polyethylene thermal cracking oil over Ni supported hierarchical zeolites and mesostructured aluminosilicates, Appl. Catal. B-Environ. 106 (2011) 405. http://dx.doi.org/10.1016/j.apcatb.2011.05.048.

[93] J.M. Escola, J. Aguado, D.P. Serrano, L. Briones, J.L. Díaz de Tuesta, R. Calvo, E. Fernández, Conversion of polyethylene into transportation fuels by the combination of thermal cracking and catalytic hydroreforming over Ni-supported hierarchical Beta zeolite, Energy Fuels 26 (2012) 3187. http://dx.doi.org/10.1021/ef300938r.

[94] J.M. Escola, J. Aguado, D.P. Serrano, L. Briones, Transportation fuel production by combination of LDPE thermal cracking and catalytic hydroreforming, Waste Manage. 34 (2014) 2176. http://dx.doi.org/10.1016/j.wasman.2014.06.010.

[95] D.P. Serrano, J.M. Escola, L. Briones, S. Medina, A. Martínez, Hydroreforming of the oils from LDPE thermal cracking over Ni–Ru and Ru supported over hierarchical Beta zeolite, Fuel 144 (2015) 287. http://dx.doi.org/10.1016/j.fuel.2014.12.040.

[96] W. Ding, J. Liang, L.L. Anderson, Thermal and catalytic degradation of high density polyethylene and commingled post-consumer plastic waste, Fuel

Process. Technol. 51 (1997) 47. http://dx.doi.org/10.1016/S0378-3820(96)01080-6.

[97] W. Ding, J. Liang, L.L. Anderson, Hydrocracking and hydroisomerization of high-density polyethylene and waste plastic over zeolite and silica-alumina-supported Ni and Ni-Mo sulfides, Energy Fuels 11 (1997) 1219. http://dx.doi.org/10.1021/ef970051q.

[98] N.D. Hesse, R.L. White, Polyethylene catalytic hydrocracking by PtHZSM-5, PtHY, and PtHMCM-41, J. Appl. Polym. Sci. 92 (2004) 1293. http://dx.doi.org/10.1002/app.20083.

[99] J. Mosio-Mosiewski, M. Warzala, I. Morawski, T. Dobrzanski, High-pressure catalytic and thermal cracking of polyethylene, Fuel Process. Technol. 88 (2007) 359. http://dx.doi.org/10.1016/j.fuproc.2006.10.009.

[100] I. Hakki Metecan, A.R. Ozkan, R. Isler, J. Yanik, M. Saglam, M. Yuksel, Naphtha derived from polyolefins, Fuel 84 (2005) 619. http://dx.doi.org/10.1016/j.fuel.2004.10.006.

[101] R. Ochoa, H. Van Woert, W.H. Lee, R. Subramanian, E. Kugler, P.C. Eklund, Catalytic degradation of medium density polyethylene over silica-alumina supports, Fuel Process. Technol. 49 (1996) 119. http://dx.doi.org/10.1016/S0378-3820(96)01055-7.

[102] M.V.S. Murty, P. Rangarajan, E.A. Grulke, D. Bhattacharyya, Thermal degradation/hydrogenation of commodity plastics and characterization of their liquefaction products, Fuel Process. Technol. 49 (1996) 75. http://dx.doi.org/10.1016/S0378-3820(96)01040-5.

[103] K.R. Venkatesh, J. Hu, W. Wang, G.D. Holder, J.W. Tierney, I. Wender, Hydrocracking and hydroisomerization of long-chain alkanes and polyolefins over metal-promoted anion-modified zirconium oxides, Energy Fuels 10 (1996) 1163. http://dx.doi.org/10.1021/ef960049j.

[104] S. Uçar, S. Karagöz, T. Karayildirim, J. Yanik, Conversion of polymers to fuels in a refinery stream, Polym. Degrad. Stabil. 75 (2002) 161. http://dx.doi.org/10.1016/S0141-3910(01)00215-4.

[105] S. Karagöz, J. Yanik, S. Uçar, M. Saglam, C. Song, Catalytic and thermal degradation of high-density polyethylene in vacuum gas oil over non-acidic and acidic catalysts, Appl. Catal. A-Gen. 242 (2003) 51. http://dx.doi.org/10.1016/S0926-860X(02)00505-7.

[106] S. Karagöz, T. Karayildirim, S. Uçar, M. Yuksel, J. Yanik, Liquefaction of municipal waste plastics in VGO over acidic and non-acidic catalysts, Fuel 82 (2003) 415. http://dx.doi.org/10.1016/S0016-2361(02)00250-8.

[107] M.F. Ali, M.N. Siddiqui, Thermal and catalytic decomposition behavior of PVC mixed plastic waste with petroleum residue, J. Anal. Appl. Pyrolysis 74 (2005) 282. http://dx.doi.org/10.1016/j.jaap.2004.12.010.

[108] R.K. Balakrishnan, C. Guria, Thermal degradation of polystyrene in the presence of hydrogen by catalyst in solution, Polym. Degrad. Stabil. 92 (2007) 1583. http://dx.doi.org/10.1016/j.polymdegradstab.2007.04.014.

[109] E.G. Fuentes-Ordóñez, J.A. Salbidegoitia, J.L. Ayastuy, M.A. Gutiérrez-Ortiz, M.P. González-Marcos, J.R. González-Velasco, High external surface Pt/zeolite catalysts for improving polystyrene hydrocracking, Catal. Today 227 (2014) 163. http://dx.doi.org/10.1016/j.cattod.2013.09.004.

[110] E.G. Fuentes-Ordóñez, J.A. Salbidegoitia, M.P. González-Marcos, J.L. Ayastuy, M.A. Gutiérrez-Ortiz, J.R. González-Velasco, Pt/ITQ-6 zeolite as a bifunctional catalyst for hydrocracking of waste plastics containing polystyrene, J. Mater. Cycles Waste Manag. 17 (2015) 465. http://dx.doi.org/10.1007/s10163-014-0322-2.

[111] E.G. Fuentes-Ordóñez, J.A. Salbidegoitia, M.P. González-Marcos, J.R. González-Velasco, Transport phenomena in catalytic hydrocracking of polystyrene in solution, Ind. Eng. Chem. Res. 52 (2013) 14798. http://dx.doi.org/10.1021/ie401968r.

[112] C. Wu, P.T. Williams, Investigation of Ni-Al, Ni-Mg-Al and Ni-Cu-Al catalyst for hydrogen production from pyrolysis-gasification of polypropylene, Appl. Catal. B-Environ. 90 (2009) 147. http://dx.doi.org/10.1016/j.apcatb.2009.03.004.

[113] W.H. Starnes Jr., Structural and mechanistic aspects of the thermal degradation of poly(vinyl chloride), Prog. Polym. Sci. 27 (2002) 2133. http://dx.doi.org/10.1016/S0079-6700(02)00063-1.

[114] W.H. Starnes, X. Ge, Mechanism of autocatalysis in the thermal dehydrochlorination of poly(vinyl chloride), Macromolecules 37 (2004) 352. http://dx.doi.org/10.1021/ma0352835.

[115] H. Zweifel, R. Maier, M. Schiller, Plastics Additives Handbook, Hanser, Munich, 2009.

[116] A. Marongiu, T. Faravelli, G. Bozzano, M. Dente, E. Ranzi, Thermal degradation of poly(vinyl chloride), J. Anal. Appl. Pyrolysis 70 (2003) 519. http://dx.doi.org/10.1016/S0165-2370(03)00024-X.

[117] A. Castro, D. Soares, C. Vilarinho, F. Castro, Kinetics of thermal de-chlorination of PVC under pyrolytic conditions, Waste Manage. 32 (2012) 847. http://dx.doi.org/10.1016/j.wasman.2012.01.004.

[118] S. Chattopadhyay, G. Madras, Thermal degradation kinetics of poly(vinyl chloride-co-vinyl acetate), Polym. Degrad. Stabil. 78 (2002) 519. http://dx.doi.org/10.1016/S0141-3910(02)00224-0.

[119] S. Chattopadhyay, G. Madras, Influence of HZSM-5 catalyst on the thermal degradation of poly(vinyl chloride) in solution, J. Appl. Polym. Sci. 84 (2002) 791. http://dx.doi.org/10.1002/app.10332.

[120] T. Kamo, Y. Kondo, Y. Kodera, Y. Sato, S. Kushiyama, Effects of solvent on degradation of poly(vinyl chloride), Polym. Degrad. Stabil. 81 (2003) 187. http://dx.doi.org/10.1016/S0141-3910(03)00088-0.

[121] T. Kamo, Y. Kodera, Y. Sato, S. Kushiyama, Effects of pressure on the degradation of poly(vinyl chloride), Polym. Degrad. Stabil. 84 (2004) 79. http://dx.doi.org/10.1016/j.polymdegradstab.2003.09.014.

[122] T. Kamo, Y. Kodera, Effect of hydrogen transferred from solvent and gaseous hydrogen on thermal decomposition of dehydrochlorinated poly(vinyl chloride), Polym. Degrad. Stabil. 87 (2005) 95. http://dx.doi.org/10.1016/j.polymdegradstab.2004.07.010.

[123] W. Tongamp, Q. Zhang, F. Saito, Hydrogen generation from polyethylene by milling and heating with $Ca(OH)_2$ and $Ni(OH)_2$, Int. J. Hydrog. Energy 33 (2008) 4097. http://dx.doi.org/10.1016/j.ijhydene.2008.05.027.

[124] W. Tongamp, Q. Zhang, M. Shoko, F. Saito, Generation of hydrogen from polyvinyl chloride by milling and heating with CaO and $Ni(OH)_2$, J. Hazard. Mater. 167 (2009) 1002. http://dx.doi.org/10.1016/j.jhazmat.2009.01.076.

[125] C. Borgianni, P. De Filippis, F. Pochetti, M. Paolucci, Gasification process of wastes containing PVC, Fuel 81 (2002) 1827. http://dx.doi.org/10.1016/S0016-2361(02)00097-2.

[126] T. Kamo, K. Takaoka, J. Otomo, H. Takahashi, Effect of steam and sodium hydroxide for the production of hydrogen on gasification of dehydrochlorinated poly(vinyl chloride), Fuel 85 (2006) 1052. http://dx.doi.org/10.1016/j.fuel.2005.10.002.

[127] T. Kamo, K. Takaoka, J. Otomo, H. Takahashi, Production of hydrogen by steam gasification of dehydrochlorinated poly(vinyl chloride) or activated carbon in the presence of various alkali compounds, J. Mater. Cycles Waste Manag. 8 (2006) 109. http://dx.doi.org/10.1007/s10163-006-0152-y.

[128] J. Ylä-Mella, K. Poikela, U. Lehtinen, R.L. Keiski, E. Pongrácz, Implementation of waste electrical and electronic equipment Directive in Finland: Evaluation of the collection network and challenges of the effective WEEE management, Resour. Conserv. Recycl. 86 (2014) 38. http://dx.doi.org/10.1016/j.resconrec.2014.02.001.

[129] J. Ylä-Mella, R.L. Keiski, E. Pongrácz, Electronic waste recovery in Finland: Consumers' perceptions towards recycling and re-use of mobile phones, Waste Manage. 45 (2015) 374. http://dx.doi.org/10.1016/j.wasman.2015.02.031.

[130] F.O. Ongondo, I.D. Williams, T.J. Cherrett, How are WEEE doing? A global review of the management of electrical and electronic wastes, Waste Manage. 31 (2011) 714. http://dx.doi.org/10.1016/j.wasman.2010.10.023.

[131] I.C. Nnorom, J. Ohakwe, O. Osibanjo, Survey of willingness of residents to participate in electronic waste recycling in Nigeria – A case study of mobile phone recycling, J. Clean. Prod. 17 (2009) 1629. http://dx.doi.org/10.1016/j.jclepro.2009.08.009.

[132] C.R. de Oliveira, A.M. Bernardes, A.E. Gerbase, Collection and recycling of electronic scrap: A worldwide overview and comparison with the Brazilian situation, Waste Manage. 32 (2012) 1592. http://dx.doi.org/10.1016/j.wasman.2012.04.003.

[133] P. Tanskanen, Management and recycling of electronic waste, Korean J. Chem. Eng. 61 (2013) 1001. http://dx.doi.org/10.1016/j.actamat.2012.11.005.

[134] H. Alter, Environmentally sound management of the recycling of hazardous wastes in the context of the Basel Convention, Resour. Conserv. Recycl. 29 (2000) 111. http://dx.doi.org/10.1016/S0921-3449(99)00061-0.

[135] K. Huang, J. Guo, Z. Xu, Recycling of waste printed circuit boards: A review of current technologies and treatment status in China, J. Hazard. Mater. 164 (2009) 399. http://dx.doi.org/10.1016/j.jhazmat.2008.08.051.

[136] P.A. Wäger, M. Schluep, E. Müller, R. Gloor, RoHS regulated substances in mixed plastics from waste electrical and electronic equipment, Environ. Sci. Technol. 46 (2012) 628. http://dx.doi.org/10.1021/es202518n.

[137] M. Polák, L. Drápalová, Estimation of end of life mobile phones generation: The case study of the Czech Republic, Waste Manage. 32 (2012) 1583. http://dx.doi.org/10.1016/j.wasman.2012.03.028.

[138] J. LaDou, Printed circuit board industry, Int. J. Hyg. Environ. Health 209 (2006) 211. http://dx.doi.org/10.1016/j.ijheh.2006.02.001.

[139] J. Cui, L. Zhang, Metallurgical recovery of metals from electronic waste: A review, J. Hazard. Mater. 158 (2008) 228. http://dx.doi.org/10.1016/j.jhazmat.2008.02.001.

[140] S.M. Al-Salem, P. Lettieri, J. Baeyens, The valorization of plastic solid waste (PSW) by primary to quaternary routes: From re-use to energy and chemicals, Prog. Energy Combust. Sci. 36 (2010) 103. http://dx.doi.org/10.1016/j.pecs.2009.09.001.

[141] J. Gong, J. Liu, Z. Jiang, X. Chen, X. Wen, E. Mijowska, T. Tang, Converting mixed plastics into mesoporous hollow carbon spheres with controllable diameter, Appl. Catal. B-Environ. 152-153 (2014) 289. http://dx.doi.org/10.1016/j.apcatb.2014.01.051.

[142] R. Wang, Z. Xu, Recycling of non-metallic fractions from waste electrical and electronic equipment (WEEE): A review, Waste Manage. 34 (2014) 1455. http://dx.doi.org/10.1016/j.wasman.2014.03.004.

[143] H. Shent, R.J. Pugh, E. Forssberg, A review of plastics waste recycling and the flotation of plastics, Resour. Conserv. Recycl. 25 (1999) 85. http://dx.doi.org/10.1016/S0921-3449(98)00017-2.

[144] E. Yamasue, K. Nakajima, I. Daigo, S. Hashimoto, H. Okumura, K.N. Ishihara, Evaluation of the potential amounts of dissipated rare metals from WEEE in Japan, Mater. T. JIM 48 (2007) 2353. http://dx.doi.org/10.2320/matertrans.MAW200781.

[145] T. Kamo, T. Bhaskar, J.A. Salbidegoitia, Technology and apparatus for recovering of valuable materials from e-waste by using steam gasification. Japanese Patent Application number 2014-35799 (2014).

[146] J. Hanafi, E. Jobiliong, A. Christiani, D.C. Soenarta, J. Kurniawan, J. Irawan, Material Recovery and Characterization of PCB from Electronic Waste, Procedia Soc. Behav. Sci. 57 (2012) 331. http://dx.doi.org/10.1016/j.sbspro.2012.09.1194.

[147] M.P. Luda, A.I. Balabanovich, M. Zanetti, Pyrolysis of fire retardant anhydride-cured epoxy resins, J. Anal. Appl. Pyrolysis 88 (2010) 39. http://dx.doi.org/10.1016/j.jaap.2010.02.008.

[148] T. Liou, Kinetics study of thermal decomposition of electronic packaging material, Chem. Eng. J. 98 (2004) 39. http://dx.doi.org/10.1016/S1385-8947(03)00181-5.

[149] L. Flandinet, F. Tedjar, V. Ghetta, J. Fouletier, Metals recovering from waste printed circuit boards (WPCBs) using molten salts, J. Hazard. Mater. 213-214 (2012) 485. http://dx.doi.org/10.1016/j.jhazmat.2012.02.037.

[150] C. Zhang, F. Zhang, Removal of brominated flame retardant from electrical and electronic waste plastic by solvothermal technique, J. Hazard. Mater. 221-222 (2012) 193. http://dx.doi.org/10.1016/j.jhazmat.2012.04.033.

[151] X. Yang, L. Sun, J. Xiang, S. Hu, S. Su, Pyrolysis and dehalogenation of plastics from waste electrical and electronic equipment (WEEE): A review, Waste Manage. 33 (2013) 462. http://dx.doi.org/10.1016/j.wasman.2012.07.025.

[152] S.M. Alston, A.D. Clark, J.C. Arnold, B.K. Stein, Environmental Impact of Pyrolysis of Mixed WEEE Plastics Part 1: Experimental Pyrolysis Data, Environ. Sci. Technol. 45 (2011) 9380. http://dx.doi.org/10.1021/es201664h.

[153] H. Chiang, K. Lin, M. Lai, T. Chen, S. Ma, Pyrolysis characteristics of integrated circuit boards at various particle sizes and temperatures, J. Hazard. Mater. 149 (2007) 151. http://dx.doi.org/10.1016/j.jhazmat.2007.03.064.

[154] J. Li, H. Duan, K. Yu, L. Liu, S. Wang, Characteristic of low-temperature pyrolysis of printed circuit boards subjected to various atmosphere, Resour. Conserv. Recycl. 54 (2010) 810. http://dx.doi.org/10.1016/j.resconrec.2009.12.011.

[155] W.J. Hall, P.T. Williams, Separation and recovery of materials from scrap printed circuit boards, Resour. Conserv. Recycl. 51 (2007) 691. http://dx.doi.org/10.1016/j.resconrec.2006.11.010.

[156] W.J. Hall, P.T. Williams, Processing waste printed circuit boards for material recovery, Circuit World 33 (2007) 43. http://dx.doi.org/10.1108/03056120710836936.

[157] W.J. Hall, P.T. Williams, Removal of organobromine compounds from the pyrolysis oils of flame retarded plastics using zeolite catalysts, J. Anal. Appl. Pyrolysis 81 (2008) 139. http://dx.doi.org/10.1016/j.jaap.2007.09.008.

[158] J. Moltó, R. Font, A. Gálvez, J.A. Conesa, Pyrolysis and combustion of electronic wastes, J. Anal. Appl. Pyrolysis 84 (2009) 68. http://dx.doi.org/10.1016/j.jaap.2008.10.023.

[159] M. Blazsó, Z. Czégény, C. Csoma, Pyrolysis and debromination of flame retarded polymers of electronic scrap studied by analytical pyrolysis, J. Anal. Appl. Pyrolysis 64 (2002) 249. http://dx.doi.org/10.1016/S0165-2370(02)00035-9.

[160] C. Vasile, M.A. Brebu, T. Karayildirim, J. Yanik, H. Darie, Feedstock recycling from plastic and thermoset fractions of used computers (I): pyrolysis, J. Mater. Cycles Waste Manag. 8 (2006) 99. http://dx.doi.org/10.1007/s10163-006-0151-z.

[161] C. Vasile, M.A. Brebu, T. Karayildirim, J. Yanik, H. Darie, Feedstock recycling from plastics and thermosets fractions of used computers. II. Pyrolysis oil upgrading, Fuel 86 (2007) 477. http://dx.doi.org/10.1016/j.fuel.2006.08.010.

[162] C. Vasile, M.A. Brebu, M. Totolin, J. Yanik, T. Karayildirim, H. Darie, Feedstock recycling from the printed circuit boards of used computers, Energy Fuels 22 (2008) 1658. http://dx.doi.org/10.1021/ef700659t.

[163] S. Zhang, K. Yoshikawa, H. Nakagome, T. Kamo, Kinetics of the steam gasification of a phenolic circuit board in the presence of carbonates, Appl. Energy 101 (2013) 815. http://dx.doi.org/10.1016/j.apenergy.2012.08.030.

[164] T. Yamawaki, The gasification recycling technology of plastics WEEE containing brominated flame retardants, Fire Mater. 27 (2003) 315. http://dx.doi.org/10.1002/fam.833.

[165] L. Long, S. Sun, S. Zhong, W. Dai, J. Liu, W. Song, Using vacuum pyrolysis and mechanical processing for recycling waste printed circuit boards, J. Hazard. Mater. 177 (2010) 626. http://dx.doi.org/10.1016/j.jhazmat.2009.12.078.

[166] J.C. Acomb, M.A. Nahil, P.T. Williams, Thermal processing of plastics from waste electrical and electronic equipment for hydrogen production, J. Anal. Appl. Pyrolysis 103 (2013) 320. http://dx.doi.org/10.1016/j.jaap.2012.09.014.

[167] H. Yang, Y. Cho, J. Yun, J. Kim, Destruction of halogenated plastics in a molten salt oxidation reactor, Can. J. Chem. Eng. 81 (2003) 713. http://dx.doi.org/10.1002/cjce.5450810350.

[168] H. Yang, Y. Cho, H. Eun, J. Kim, Y. Kang, Destruction of chlorinated organic solvents in a molten carbonate with transition metal oxides, Stud. Surf. Sci. Catal. 159 (2006) 577. http://dx.doi.org/10.1016/S0167-2991(06)81662-9.

[169] H. Yang, Y. Cho, H. Eun, E. Kim, Destruction of chlorinated organic solvents in a two-stage molten salt oxidation reactor system, Chem. Eng. Sci. 62 (2007) 5137. http://dx.doi.org/10.1016/j.ces.2007.01.055.

[170] M. Stelmachowski, Thermal conversion of waste polyolefins to the mixture of hydrocarbons in the reactor with molten metal bed, Energy Convers. Manage. 51 (2010) 2016. http://dx.doi.org/10.1016/j.enconman.2010.02.035.

[171] Y. Chen, J. Li, H. Duan, Z. Wang, Thermal cracking of waste printed wiring boards for mechanical recycling by using residual steam preprocessing, Front. Environ. Sci. En. 5 (2011) 167. http://dx.doi.org/10.1007/s11783-011-0308-4.

[172] European Union, Directive 2000/53/EC of the European Parliament and of the Council on end-of-life vehicles, Official Journal, 269 (2005) 34. http://eur-lex.europa.eu/legal-content/EN/TXT/PDF/?uri=CELEX:02000L0053-20130611&qid=1405610569066&from=EN. (last consulted: 05/09/2016).

[173] K. Lin, S. Chowdhury, Z. Wang, Catalytic gasification of automotive shredder residues with hydrogen generation, J. Power Sources 195 (2010) 6016. http://dx.doi.org/10.1016/j.jpowsour.2010.03.084.

[174] California Integrated Waste Management Board, Technology Evaluation and Economic Analysis of Waste Tire Pyrolysis, Gasification, and Liquefaction, California Environmental Protection Agency, 2006.

[175] X. Elías, E. Velo, La Pirólisis: Tratamiento y Valorización Energética de Residuos, Díaz de Santos, Madrid, 2005.

[176] A. Corma, State of the art and future challenges of zeolites as catalysts, J. Catal. 216 (2003) 298. http://dx.doi.org/10.1016/S0021-9517(02)00132-X.

[177] R. Henry, M. Tayakout-Fayolle, P. Afanasiev, C. Lorentz, G. Lapisardi, G. Pirngruber, Vacuum gas oil hydrocracking performance of bifunctional Mo/Y zeolite catalysts in a semi-batch reactor, Catal. Today 220-222 (2014) 159. http://dx.doi.org/10.1016/j.cattod.2013.06.024.

[178] D. Xu, R.G. Carbonell, D.J. Kiserow, G.W. Roberts, Kinetic and Transport Processes in the Heterogeneous Catalytic Hydrogenation of Polystyrene, Ind. Eng. Chem. Res. 42 (2003) 3509. http://dx.doi.org/10.1021/ie0301841.

[179] W. Ding, G.D. Meitzner, E. Iglesia, The Effects of Silanation of External Acid Sites on the Structure and Catalytic Behavior of Mo/H-ZSM5, J. Catal. 206 (2002) 14. http://dx.doi.org/10.1006/jcat.2001.3457.

[180] J. Kim, W. Kim, Y. Seo, J. Kim, R. Ryoo, *n*-Heptane hydroisomerization over Pt/MFI zeolite nanosheets: Effects of zeolite crystal thickness and platinum location, J. Catal. 301 (2013) 187. http://dx.doi.org/10.1016/j.jcat.2013.02.015.

[181] F. Pinto, P. Costa, I. Gulyurtlu, I. Cabrita, Pyrolysis of plastic wastes: 2. Effect of catalyst on product yield, J. Anal. Appl. Pyrolysis 51 (1999) 57. http://dx.doi.org/10.1016/S0165-2370(99)00008-X.

[182] S. Chatterjee, G.M. Schütz, Diffusion of a hydrocarbon mixture in a one-dimensional zeolite channel: An exclusion model approach, Microporous Mesoporous Mat. 125 (2009) 143. http://dx.doi.org/10.1016/j.micromeso.2009.01.017.

[183] S. van Donk, A.H. Janssen, J.H. Bitter, K.P. de Jong, Generation, Characterization, and Impact of Mesopores in Zeolite Catalysts, Catal. Rev. 45 (2003) 297. http://dx.doi.org/10.1081/CR-120023908.

[184] M. Choi, K. Na, J. Kim, Y. Sakamoto, O. Terasaki, R. Ryoo, Stable single-unit-cell nanosheets of zeolite MFI as active and long-lived catalysts, Nature 461 (2009) 246. http://dx.doi.org/10.1038/nature08288.

[185] J. Čejka, G. Centi, J. Perez-Pariente, W.J. Roth, Zeolite-based materials for novel catalytic applications: Opportunities, perspectives and open problems, Catal. Today 179 (2012) 2. http://dx.doi.org/10.1016/j.cattod.2011.10.006.

[186] J. Aguado, D.P. Serrano, J.M. Escola, Fuels from Waste Plastics by Thermal and Catalytic Processes: A Review, Ind. Eng. Chem. Res. 47 (2008) 7982. http://dx.doi.org/10.1021/ie800393w.

[187] Y. Huang, K. Wang, D. Dong, D. Li, M.R. Hill, A.J. Hill, H. Wang, Synthesis of hierarchical porous zeolite NaY particles with controllable particle sizes, Microporous Mesoporous Mat. 127 (2010) 167. http://dx.doi.org/10.1016/j.micromeso.2009.07.026.

[188] M. Silaghi, C. Chizallet, P. Raybaud, Challenges on molecular aspects of dealumination and desilication of zeolites, Microporous Mesoporous Mat. 191 (2014) 82. http://dx.doi.org/10.1016/j.micromeso.2014.02.040.

[189] D. Verboekend, J. Pérez-Ramírez, Towards a sustainable manufacture of hierarchical zeolites, ChemSusChem 7 (2014) 753. http://dx.doi.org/10.1002/cssc.201301313.

[190] R. Chal, T. Cacciaguerra, S. van Donk, C. Gerardin, Pseudomorphic synthesis of mesoporous zeolite Y crystals, Chem. Commun. 46 (2010) 7840. http://dx.doi.org/10.1039/C0CC02073G.

[191] F.N. Gu, F. Wei, J.Y. Yang, N. Lin, W.G. Lin, Y. Wang, J.H. Zhu, New strategy to synthesis of hierarchical mesoporous zeolites, Chem. Mater. 22 (2010) 2442. http://dx.doi.org/10.1021/cm903785r.

[192] H. Chen, J. Wydra, X. Zhang, P. Lee, Z. Wang, W. Fan, M. Tsapatsis, hydrothermal synthesis of zeolites with three-dimensionally ordered mesoporous-imprinted structure, J. Am. Chem. Soc. 133 (2011) 12390. http://dx.doi.org/10.1021/ja2046815.

[193] D. Verboekend, G. Vilé, J. Pérez-Ramírez, Hierarchical Y and USY zeolites designed by post-synthetic strategies, Adv. Funct. Mater. 22 (2012) 916. http://dx.doi.org/10.1002/adfm.201102411.

[194] D.P. Serrano, J.M. Escola, P. Pizarro, Synthesis strategies in the search for hierarchical zeolites, Chem. Soc. Rev. 42 (2013) 4004. http://dx.doi.org/10.1039/C2CS35330J.

[195] H. Beyer, Dealumination techniques for zeolites, in: H.G. Karge and J. Weitkamp (Eds.), Post-Synthesis Modification I, Springer Berlin Heidelberg, 2002, p. 203.

[196] I. Batonneau-gener, A. Yonli, S. Hazael-pascal, J. Pedro Marques, J. Madeira Lopes, M. Guisnet, F. Ramôa Ribeiro, S. Mignard, Influence of steaming and acid-leaching treatments on the hydrophobicity of HBEA zeolite determined under static conditions, Microporous Mesoporous Mat. 110 (2008) 480. http://dx.doi.org/10.1016/j.micromeso.2007.06.037.

[197] C.J. Van Oers, W.J.J. Stevens, E. Bruijn, M. Mertens, O.I. Lebedev, G. Van Tendeloo, V. Meynen, P. Cool, Formation of a combined micro- and mesoporous material using zeolite Beta nanoparticles, Microporous Mesoporous Mat. 120 (2009) 29. http://dx.doi.org/10.1016/j.micromeso.2008.08.056.

[198] A.N. Pinheiro, A. Valentini, J.M. Sasaki, A.C. Oliveira, Highly stable dealuminated zeolite support for the production of hydrogen by dry reforming of methane, Appl. Catal. A-Gen. 355 (2009) 156. http://dx.doi.org/10.1016/j.apcata.2008.12.007.

[199] W. Lutz, H. Toufar, D. Heidemann, N. Salman, C.H. Rüscher, T.M. Gesing, J.-. Buhl, R. Bertram, Siliceous extra-framework species in dealuminated Y zeolites generated by steaming, Microporous Mesoporous Mat. 104 (2007) 171. http://dx.doi.org/10.1016/j.micromeso.2007.01.028.

[200] J.C. Groen, S. Abelló, L.A. Villaescusa, J. Pérez-Ramírez, Mesoporous beta zeolite obtained by desilication, Microporous Mesoporous Mat. 114 (2008) 93. http://dx.doi.org/10.1016/j.micromeso.2007.12.025.

[201] R.C. Vincent, R.P. Merrill, Concentration profiles in impregnation of porous catalysts, J. Catal. 35 (1974) 206. http://dx.doi.org/10.1016/0021-9517(74)90199-7.

[202] F. Melo, J. Cervelló, E. Hermana, Impregnation of porous supports—I Theoretical study of the impregnation of one or two active species, Chem. Eng. Sci. 35 (1980) 2165. http://dx.doi.org/10.1016/0009-2509(80)85041-X.

[203] A.V. Neimark, L.I. Kheifets, V.B. Fenelonov, Theory of preparation of supported catalysts, Ind. Eng. Chem. Prod. Res. Dev. 20 (1981) 439. http://dx.doi.org/10.1021/i300003a006.

[204] S. Lee, R. Aris, The distribution of active ingredients in supported catalysts prepared by impregnation, Catal. Rev. 27 (1985) 207. http://dx.doi.org/10.1080/01614948508064737.

[205] E. Peluso, C. Galarraga, H. de Lasa, Eggshell catalyst in Fischer-Tropsch synthesis: Intrinsic reaction kinetics, Chem. Eng. Sci. 56 (2001) 1239. http://dx.doi.org/10.1016/S0009-2509(00)00345-6.

[206] C. Galarraga, E. Peluso, H. de Lasa, Eggshell catalysts for Fischer-Tropsch synthesis: Modeling catalyst impregnation, Chem. Eng. J. 82 (2001) 13. http://dx.doi.org/10.1016/S1385-8947(00)00352-1.

[207] A. Lekhal, B.J. Glasser, J.G. Khinast, Impact of drying on the catalyst profile in supported impregnation catalysts, Chem. Eng. Sci. 56 (2001) 4473. http://dx.doi.org/10.1016/S0009-2509(01)00120-8.

[208] W. Su, W. Chen, J. Chang, Impact of iron deposition on Pd/δ-Al_2O_3 in selective hydrogenation of pyrolysis gasoline, Ind. Eng. Chem. Res. 39 (2000) 4063. http://dx.doi.org/10.1021/ie000292c.

[209] X. Wen, R. Li, Y. Yang, J. Chen, F. Zhang, An egg-shell type Ni/Al2O3 catalyst derived from layered double hydroxides precursor for selective hydrogenation of pyrolysis gasoline, Appl. Catal. A-Gen. 468 (2013) 204. http://dx.doi.org/10.1016/j.apcata.2013.08.040.

[210] R.W. Maatman, C.D. Prater, Adsorption and exclusion in impregnation of porous catalytic supports, Ind. Eng. Chem. 49 (1957) 253. http://dx.doi.org/10.1021/ie50566a040.

[211] M. Komiyama, R.P. Merrill, H.F. Harnsberger, Concentration profiles in impregnation of porous catalysts: Nickel on alumina, J. Catal. 63 (1980) 35. http://dx.doi.org/10.1016/0021-9517(80)90058-5.

[212] S. Minhas, J.J. Carberry, On the merits of partially impregnated catalysts, J. Catal. 14 (1969) 270. http://dx.doi.org/10.1016/0021-9517(69)90436-9.

[213] T.G. Smith, J.J. Carberry, On the use of partially impregnated catalysts for yield enhancement in non-isothermal non-adiabatic fixed bed reactors, Can. J. Chem. Eng. 53 (1975) 347. http://dx.doi.org/10.1002/cjce.5450530318.

[214] W.D. Li, Y.W. Li, Z.F. Qin, S.Y. Chen, Theoretical prediction and experimental validation of the egg-shell distribution of Ni for supported ni/Al_2O_3 catalysts, Chem. Eng. Sci. 49 (1994) 4889. http://dx.doi.org/10.1016/S0009-2509(05)80067-3.

[215] X. Liu, J.G. Khinast, B.J. Glasser, A parametric investigation of impregnation and drying of supported catalysts, Chem. Eng. Sci. 63 (2008) 4517. http://dx.doi.org/10.1016/j.ces.2008.06.013.

[216] J.A. Schwarz, C. Contescu, A. Contescu, Methods for preparation of catalytic materials, Chem. Rev. 95 (1995) 477. http://dx.doi.org/10.1021/cr00035a002.

[217] M. Kotter, L. Riekert, The influence of impregnation, drying and activation on the activity and distribution of CuO on α-alumina, Stud. Surf. Sci. Catal. 3 (1979) 51. http://dx.doi.org/10.1016/S0167-2991(09)60204-4.

[218] M.P. Hollewand, L.F. Gladden, Probing the structure of porous pellets: An NMR study of drying, Magn. Reson. Imaging 12 (1994) 291. http://dx.doi.org/10.1016/0730-725X(94)91538-5.

[219] S.J. Kowalski, Toward a thermodynamics and mechanics of drying processes, Chem. Eng. Sci. 55 (2000) 1289. http://dx.doi.org/10.1016/S0009-2509(99)00400-5.

[220] A. Lekhal, J.G. Khinast, B.J. Glasser, Predicting the effect of drying on supported coimpregnation catalysts, Ind. Eng. Chem. Res. 40 (2001) 3989. http://dx.doi.org/10.1021/ie010126k.

[221] A. Lekhal, B.J. Glasser, J.G. Khinast, Influence of pH and ionic strength on the metal profile of impregnation catalysts, Chem. Eng. Sci. 59 (2004) 1063. http://dx.doi.org/10.1016/j.ces.2003.12.009.

[222] P. Munnik, P.E. de Jongh, K.P. de Jong, Control and impact of the nanoscale distribution of supported cobalt particles used in Fischer-Tropsch catalysis, J. Am. Chem. Soc. 136 (2014) 7333. http://dx.doi.org/10.1021/ja500436y.

[223] X. Liu, J.G. Khinast, B.J. Glasser, Drying of supported catalysts: A comparison of model predictions and experimental measurements of metal profiles, Ind. Eng. Chem. Res. 49 (2010) 2649. http://dx.doi.org/10.1021/ie9014606.

[224] X. Liu, J.G. Khinast, B.J. Glasser, Drying of supported catalysts for low melting point precursors: Impact of metal loading and drying methods on the metal distribution, Chem. Eng. Sci. 79 (2012) 187. http://dx.doi.org/10.1016/j.ces.2012.05.046.

[225] X. Liu, J.G. Khinast, B.J. Glasser, Drying of Ni/alumina catalysts: Control of the metal distribution using surfactants and the melt infiltration method, Ind. Eng. Chem. Res. 53 (2014) 5792. 10.1021/ie500099c.

[226] J. Scherzer, A. Gruia, Hydrocracking Science and Technology Chemical Industries, CRC Press, Illinois, 1996.

[227] J.P. Marques, I. Gener, P. Ayrault, J.C. Bordado, J.M. Lopes, F.R. Ribeiro, M. Guisnet, Dealumination of HBEA zeolite by steaming and acid leaching: Distribution of the various aluminic species and identification of the hydroxyl groups, C. R. Chimie 8 (2005) 399. http://dx.doi.org/10.1016/j.crci.2005.01.002.

[228] M. Ogura, S. Shinomiya, J. Tateno, Y. Nara, M. Nomura, E. Kikuchi, M. Matsukata, Alkali-treatment technique — new method for modification of structural and acid-catalytic properties of ZSM-5 zeolites, Appl. Catal. A-Gen. 219 (2001) 33. http://dx.doi.org/10.1016/S0926-860X(01)00645-7.

[229] J. de Graaf, A.J. van Dillen, K.P. de Jong, D.C. Koningsberger, Preparation of highly dispersed Pt particles in zeolite Y with a narrow particle size distribution: Characterization by hydrogen chemisorption, TEM, EXAFS spectroscopy, and particle modeling, J. Catal. 203 (2001) 307. http://dx.doi.org/10.1006/jcat.2001.3337.

[230] E.G. Fuentes-Ordóñez, Diseño de Catalizadores Bifuncionales para el Proceso de Hidrocraqueo de Poliestireno en Fase Líquida Aplicado a la

Valorización de Residuos Plásticos, PhD Thesis, Universidad del País Vasco, UPV/EHU, Leioa, 2015.

[231] J. Wang, J. Chen, Development of a simple method for the preparation of novel egg-shell type Pt catalysts using hollow silica nanostructures as supporting precursors, Mater. Res. Bull. 43 (2008) 889. http://dx.doi.org/10.1016/j.materresbull.2007.05.002.

[232] M.M.J. Treacy, J.B. Higgins, Collection of Simulated XRD Powder Patterns for Zeolites, Elsevier B.V., Amsterdam, 2007.

[233] J.A. Lercher, C. Gründling, G. Eder-Mirth, Infrared studies of the surface acidity of oxides and zeolites using adsorbed probe molecules, Catal. Today 27 (1996) 353. http://dx.doi.org/10.1016/0920-5861(95)00248-0.

[234] N. Topsøe, K. Pedersen, E.G. Derouane, Infrared and temperature-programmed desorption study of the acidic properties of ZSM-5-type zeolites, J. Catal. 70 (1981) 41. http://dx.doi.org/10.1016/0021-9517(81)90315-8.

[235] C.A. Emeis, Determination of integrated molar extinction coefficients for infrared absorption bands of pyridine adsorbed on solid acid catalysts, J. Catal. 141 (1993) 347. http://dx.doi.org/10.1006/jcat.1993.1145.

[236] K. Góra-Marek, K. Tarach, M. Choi, 2,6-Di-*tert*-butylpyridine sorption approach to quantify the external acidity in hierarchical zeolites, J. Phys. Chem. C 118 (2014) 12266. http://dx.doi.org/10.1021/jp501928k.

[237] A. Corma, V. Fornés, L. Forni, F. Márquez, J. Martínez-Triguero, D. Moscotti, 2,6-Di-*tert*-butyl-pyridine as a probe molecule to measure external acidity of zeolites, J. Catal. 179 (1998) 451. http://dx.doi.org/10.1006/jcat.1998.2233.

[238] J. Zhou, Z. Liu, L. Li, Y. Wang, H. Gao, W. Yang, Z. Xie, Y. Tang, Hierarchical mesoporous ZSM-5 zeolite with increased external surface acid sites and high catalytic performance in o-xylene isomerization, Chinese J. Catal. 34 (2013) 1429. http://dx.doi.org/10.1016/S1872-2067(12)60602-0.

[239] R.J. Gorte, Temperature-programmed desorption for the characterization of oxide catalysts, Catal. Today 28 (1996) 405. http://dx.doi.org/10.1016/S0920-5861(96)00249-0.

[240] B. Hunger, M. von Szombathely, J. Hoffmann, P. Bräuer, Characterization of the acidic properties of zeolites by means of temperature-programmed desorption (TPD) of ammonia, J. Therm. Anal. 44 (1995) 293. http://dx.doi.org/10.1007/BF02636120.

[241] S. Brunauer, P.H. Emmett, E. Teller, Adsorption of gases in multimolecular layers, J. Am. Chem. Soc. 60 (1938) 309.

http://dx.doi.org/10.1021/ja01269a023.

[242] E.P. Barrett, L.G. Joyner, P.P. Halenda, The determination of pore volume and area distributions in porous substances. I. Computations from nitrogen isotherms, J. Am. Chem. Soc. 73 (1951) 373. http://dx.doi.org/10.1021/ja01145a126.

[243] E. Falabella Sousa-Aguiar, A. Liebsch, B.C. Chaves, A.F. Costa, Influence of the external surface area of small crystallite zeolites on the micropore volume determination, Microporous Mesoporous Mat. 25 (1998) 185. http://dx.doi.org/10.1016/S1387-1811(98)00206-6.

[244] J.H. de Boer, B.C. Lippens, B.G. Linsen, J.C.P. Broekhoff, A. van den Heuvel, T.J. Osinga, The t-curve of multimolecular N2-adsorption, J. Colloid Interface Sci. 21 (1966) 405. http://dx.doi.org/10.1016/0095-8522(66)90006-7.

[245] W.D. Harkins, G. Jura, An absolute method for the determination of the area of a fine crystalline powder, J. Chem. Phys. 11 (1943) 430. http://dx.doi.org/10.1063/1.1723869.

[246] G. Horváth, K. Kawazoe, Method for the calculation of effective pore size distribution in molecular sieve carbon, J. Chem. Eng. Japan 16 (1983) 470. http://doi.org/10.1252/jcej.16.470.

[247] S. Kulprathipanja, Zeolites in Industrial Separation and Catalysis, Wiley, Weinheim, 2010.

[248] A.W. Chester, E.G. Derouane, Zeolite characterization and catalysis: A tutorial, Springer, New York, 2009.

[249] V. Ponec, G.C. Bond, Catalysis by Metals and Alloys, Elsevier, Amsterdam, 1995.

[250] G. Bergeret, P. Gallezot, Particle size and dispersion measurements, in: G. Ertl, H. Knozinger, F. Schuth and J. Weitkamp (Eds.), Handbook of Heterogeneous Catalysis, Wiley, 2008.

[251] J. Anderson, M. Fernández-García, Supported Metals in Catalysis, Imperial College Press, London, 2005.

[252] D. Braun, H. Cherdron, M. Rehahn, H. Ritter, B. Voit, Polymer Synthesis: Theory and practice, Springer, Berlin, 2012.

[253] C. Wu, Handbook of Size Exclusion Chromatography and Related Techniques, Marcel Dekker, New York, 1995.

[254] ASTM International, ASTM D 6730: Determination of individual components in spark ignition engine fuels by 100-metre capillary (with precolumn) high-resolution gas chromatography (2004). https://www.astm.org/Standards/D6730.htm. (last consulted: 05/09/2016).

[255] ASTM International, ASTM D 6733: Determination of individual components in spark ignition engine fuels by 50-meter capillary high resolution gas chromatography (2011). http://www.astm.org/Standards/D6733.htm. (last consulted: 05/09/2016).

[256] Analytical Controls, Application manual fast DHA combi, (2007). http://www.rofa.sk/downloads/00_00_002_AC_DHA_Solutions_Product_Brochure_February_2007.pdf. (last consulted: 05/09/2016).

[257] B. Burger, N. Johansen, V. Gamble, D. Rhoades, High speed PONA analysis for detailed hydrocarbon analysis extended (DHAX) using hydrogen carrier gas for the determination of Individual components in spark ignition fuels (2015). http://www.restek.com/pdfs/pres-2006-700-11P.pdf. (last consulted: 05/09/2016).

[258] V. Karmore, G. Madras, Continuous distribution kinetics for the degradation of polystyrene in supercritical benzene, Ind. Eng. Chem. Res. 39 (2000) 4020. http://dx.doi.org/10.1021/ie0005203.

[259] B.J. McCoy, G. Madras, Discrete and continuous models for polymerization and depolymerization, Chem. Eng. Sci. 56 (2001) 2831. http://dx.doi.org/10.1016/S0009-2509(00)00516-9.

[260] Y. Kodera, Y. Sato, T. Kamo, Continuous-distribution kinetic model for macromolecular conversion: Asphaltene and polymer, Fuels for the year 2000, Boston, 1998. https://web.anl.gov/PCS/acsfuel/preprint%20archive/Files/43_3_BOSTON_08-98_0658.pdf. (last consulted: 05/09/2016).

[261] Y. Kodera, T. Kondo, I. Saito, Y. Sato, K. Ukegawa, Continuous-distribution kinetic analysis for asphaltene hydrocracking, Energy Fuels 14 (2000) 291. http://dx.doi.org/10.1021/ef990089y.

[262] N.A. Sezgi, W.S. Cha, J.M. Smith, B.J. McCoy, Polyethylene Pyrolysis: Theory and Experiments for Molecular-Weight-Distribution Kinetics, Ind. Eng. Chem. Res. 37 (1998) 2582. http://dx.doi.org/10.1021/ie980106r.

[263] G. Madras, S. Kumar, S. Chattopadhyay, Continuous distribution kinetics for ultrasonic degradation of polymers, Polym. Degrad. Stabil. 69 (2000) 73. http://dx.doi.org/10.1016/S0141-3910(00)00042-2.

[264] G. Madras, V. Karmore, Continuous distribution kinetics for ultrasonic degradation of poly(methyl methacrylate), Polym. Int. 50 (2001) 683. http://dx.doi.org/10.1002/pi.677.

[265] K. Huang, L. Tang, Z. Zhu, W. Ying, Continuous distribution kinetics for degradation of polystyrene in sub- and supercritical toluene, J. Anal. Appl. Pyrolysis 76 (2006) 186. http://dx.doi.org/10.1016/j.jaap.2005.11.005.

[266] G. Grause, J. Ishibashi, T. Kameda, T. Bhaskar, T. Yoshioka, Kinetic studies of the decomposition of flame retardant containing high-impact polystyrene, Polym. Degrad. Stabil. 95 (2010) 1129. http://dx.doi.org/10.1016/j.polymdegradstab.2010.02.008.

[267] J.A. Salbidegoitia, E.G. Fuentes-Ordóñez, M.P. González-Marcos, J.R. González-Velasco, T. Bhaskar, T. Kamo, Steam gasification of printed circuit board from e-waste: Effect of coexisting nickel to hydrogen production, Fuel Process. Technol. 133 (2015) 69. http://dx.doi.org/10.1016/j.fuproc.2015.01.006.

[268] E.G. Fuentes-Ordóñez, J.A. Salbidegoitia, M.P. González-Marcos, J.R. González-Velasco, Mechanism and kinetics in catalytic hydrocracking of polystyrene in solution, Polym. Degrad. Stabil. 124 (2016) 51. http://dx.doi.org/10.1016/j.polymdegradstab.2015.12.009.

[269] M.A. Camblor, A. Corma, S. Valencia, Characterization of nanocrystalline zeolite Beta, Microporous Mesoporous Mat. 25 (1998) 59. http://dx.doi.org/10.1016/S1387-1811(98)00172-3.

[270] S. Mintova, V. Valtchev, T. Onfroy, C. Marichal, H. Knözinger, T. Bein, Variation of the Si/Al ratio in nanosized zeolite Beta crystals, Microporous Mesoporous Mat. 90 (2006) 237. http://dx.doi.org/10.1016/j.micromeso.2005.11.026.

[271] E.G. Derouane, I. Schmidt, H. Lachas, C.J.H. Christensen, Improved performance of nano-size H-BEA zeolite catalysts for the Friedel-Crafts acetylation of anisole by acetic anhydride, Catal. Lett. 95 (2004) 13. http://dx.doi.org/10.1023/B%3ACATL.0000023715.41857.56.

[272] J. Aguado, D.P. Serrano, J.M. Escola, E. Garagorri, J.A. Fernández, Catalytic conversion of polyolefins into fuels over zeolite beta, Polym. Degrad. Stabil. 69 (2000) 11. http://dx.doi.org/10.1016/S0141-3910(00)00023-9.

[273] J.R. Sohn, S.J. DeCanio, J.H. Lunsford, D.J. O'Donnell, Determination of framework aluminium content in dealuminated Y-type zeolites: A comparison based on unit cell size and wavenumber of I.R. bands, Zeolites 6 (1986) 225. http://dx.doi.org/10.1016/0144-2449(86)90054-0.

[274] M.M.J. Treacy, J.B. Higgins, BEA – Beta, polymorph A SiO_2 framework, in: M.M.J. Treacy and J.B. Higgins (Eds.), Collection of Simulated XRD Powder Patterns for Zeolites (fifth), Elsevier Science B.V., 2007, p. 82.

[275] S. Akbar, Characterization of Beta zeolites by X-Ray Diffraction, Scanning Electron Microscopy and Refracrtive Index Techniques, J. Chem. Soc. Pak. 32 (2010) 592. http://jcsp.org.pk/ArticleUpload/201-719-1-CE.pdf.

[276] G.C. Bond, The significance of the compensation effect and the definition of active centres in metal catalysts, Z. Phys. Chem. 144 (1985) 21. https://doi.org/10.1524/zpch.1985.144.144.021.

[277] B. Liu, F. Chen, L. Zheng, J. Ge, H. Xi, Y. Qian, Synthesis and structural properties of hierarchically structured aluminosilicates with zeolite Y (FAU) frameworks, RSC Adv. 3 (2013) 15075. http://dx.doi.org/10.1039/C3RA41862F.

[278] M.M.J. Treacy, J.B. Higgins, FAU – Faujasite, in: M.M.J. Treacy and J.B. Higgins (Eds.), Collection of Simulated XRD Powder Patterns for Zeolites (fifth), Elsevier Science B.V., 2007, p. 166.

[279] V.M. Le, S. Xiao, A. Ramsaran, J. Yao, Selective removal of silicon from zeolite frameworks using sodium carbonate, J. Mater. Chem. 4 (1994) 605. http://dx.doi.org/10.1039/JM9940400605.

[280] N.A.S. Ramli, N.A.S. Amin, Fe/HY zeolite as an effective catalyst for levulinic acid production from glucose: Characterization and catalytic performance, Appl. Catal. B-Environ. 163 (2015) 487. http://dx.doi.org/10.1016/j.apcatb.2014.08.031.

[281] M.S. Holm, S. Svelle, F. Joensen, P. Beato, C.H. Christensen, S. Bordiga, M. Bjørgen, Assessing the acid properties of desilicated ZSM-5 by FTIR using CO and 2,4,6-trimethylpyridine (collidine) as molecular probes, Appl. Catal. A-Gen. 356 (2009) 23. http://dx.doi.org/10.1016/j.apcata.2008.11.033.

[282] C. Martínez, D. Verboekend, J. Pérez-Ramírez, A. Corma, Stabilized hierarchical USY zeolite catalysts for simultaneous increase in diesel and LPG olefinicity during catalytic cracking, Catal. Sci. Technol. 3 (2013) 972. http://dx.doi.org/10.1039/C2CY20688A.

[283] D. Verboekend, R. Caicedo-Realpe, A. Bonilla, M. Santiago, J. Pérez-Ramírez, Properties and Functions of Hierarchical Ferrierite Zeolites Obtained by Sequential Post-Synthesis Treatments, Chem. Mater. 22 (2010) 4679. http://dx.doi.org/10.1021/cm100886y.

[284] J. Horáček, G. Šťávová, V. Kelbichová, D. Kubička, Zeolite-Beta-supported platinum catalysts for hydrogenation/hydrodeoxygenation of pyrolysis oil model compounds, 204 (2013) 38. http://dx.doi.org/10.1016/j.cattod.2012.08.015.

[285] M. Schlummer, L. Gruber, A. Mäurer, G. Wolz, R. van Eldik, Characterisation of polymer fractions from waste electrical and electronic equipment (WEEE) and implications for waste management, Chemosphere 67 (2007) 1866. http://dx.doi.org/10.1016/j.chemosphere.2006.05.077.

[286] I. Watanabe, S. Sakai, Environmental release and behavior of brominated flame retardants, Environ. Int. 29 (2003) 665.

http://dx.doi.org/10.1016/S0160-4120(03)00123-5.

[287] F. Vilaplana, P. Karlsson, A. Ribes-Greus, P. Ivarsson, S. Karlsson, Analysis of brominated flame retardants in styrenic polymers: Comparison of the extraction efficiency of ultrasonication, microwave-assisted extraction and pressurised liquid extraction, J. Chromatogr. A 1196-1197 (2008) 139. http://dx.doi.org/10.1016/j.chroma.2008.05.001.

[288] J.A. Salbidegoitia, E.G. Fuentes-Ordóñez, M.P. González-Marcos, J.R. González-Velasco, Recycle of plastic residues in cellular phones through catalytic hydrocracking to liquid fuels, J. Mater. Cycles Waste Manage. First online (2016) 1. http://dx.doi.org/10.1007/s10163-016-0478-z.

[289] D.W. Brazier, N.V. Schwartz, The effect of heating rate on the thermal degradation of polybutadiene, J. Appl. Polym. Sci. 22 (1978) 113. http://dx.doi.org/10.1002/app.1978.070220109.

[290] I.C. McNeill, W.T.K. Stevenson, Thermal degradation of styrene-butadiene diblock copolymer: Part 1—Characteristics of polystyrene and polybutadiene degradation, Polym. Degrad. Stabil. 10 (1985) 247. http://dx.doi.org/10.1016/0141-3910(85)90006-0.

[291] M.C. Gupta, S.G. Viswanath, Effect of metal oxides on the thermal degradation of high impact polystyrene, J. Therm. Anal. Calorim. 53 (1998) 931. http://dx.doi.org/10.1023/A%3A1010154804771.

[292] J. Rieger, The glass transition temperature of polystyrene, J. Therm. Anal. 46 (1996) 965. http://dx.doi.org/10.1007/BF01983614.

[293] M.A. Mansilla, A.L. Rodríguez Garraza, L. Silva, W. Salgueiro, C. Macchi, A.J. Marzocca, A. Somoza, Evolution of the free volume and glass transition temperature with the degree of cure of polybutadiene rubbers, Polym. Test. 32 (2013) 686. http://dx.doi.org/10.1016/j.polymertesting.2013.03.001.

[294] G. Socrates, Infrared and Raman Characteristic Group Frequencies: Tables and Charts, Wiley, New York, 2001.

[295] P. Larkin, Infrared and Raman Spectroscopy. Principles and Spectral Interpretation, Elsevier, Oxford, 2011, p. 230.

[296] M. Blazsó, Composition of liquid fuels derived from the pyrolysis of plastics, in: J. Scheirs and W. Kaminsky (Eds.), Feedstock Recycling and Pyrolysis of Waste Plastics, John Wiley & Sons, Ltd., 2006, p. 315.

[297] J.C. Arnold, S. Alston, A. Holder, Void formation due to gas evolution during the recycling of Acrylonitrile-Butadiene-Styrene copolymer (ABS) from waste electrical and electronic equipment (WEEE), Polym. Degrad. Stabil. 94 (2009) 693. http://dx.doi.org/10.1016/j.polymdegradstab.2008.12.019.

[298] G. Wypych, ABS poly(acrylonitrile-co-butadiene-co-styrene), in: G. Wypych (Ed.), Handbook of Polymers, Elsevier, 2012, p. 3.

[299] M. Brebu, M.A. Uddin, A. Muto, Y. Sakata, C. Vasile, The role of temperature program and catalytic system on the quality of acrylonitrile-butadiene-styrene degradation oil, J. Anal. Appl. Pyrolysis 63 (2002) 43. http://dx.doi.org/10.1016/S0165-2370(01)00140-1.

[300] B.M. Caballero, I. de Marco, A. Adrados, A. López-Urionabarrenechea, J. Solar, N. Gastelu, Possibilities and limits of pyrolysis for recycling plastic rich waste streams rejected from phones recycling plants, Waste Manage. In press (2016). http://dx.doi.org/10.1016/j.wasman.2016.01.002.

[301] G. Wypych, PC polycarbonate, in: G. Wypych (Ed.), Handbook of Polymers, Elsevier, 2012, p. 308.

[302] G. Wypych, PET poly(ethylene terephthalate), in: G. Wypych (Ed.), Handbook of Polymers, Elsevier, 2012, p. 385.

[303] M. Barthes, O. Mantaux, M. Pedros, E. Lacoste, M. Dumon, Recycling of aged ABS from real WEEE through ABS/PC blends in the ABS-rich compositions, Adv. Polym. Technol. 31 (2012) 343. http://dx.doi.org/10.1002/adv.20257.

[304] J.W.S. H-G. Franck, Industrial Aromatic Chemistry. Raw Materials. Processes. Products, Springer, Frankfurt, 1988.

[305] J.J. McKetta, Encyclopedia of Chemical Processing and Design: Volume 56 - Supercritical Fluid Technology: Theory and Application to Technology Forecasting, CRC Press, New York, 1996.

[306] M. Buchert, A. Manhart, D. Bleher, D. Pingel, Recycling Critical Raw Materials from Waste Electronic Equipment, Technical Report, Institute for Applied Ecology, Öko-Institut, e.V., Freiburg (2012). http://www.oeko.de/oekodoc/1375/2012-010-en.pdf. (last consulted: 05/09/2016)

[307] K. Mineta, T.H. Okabe, Development of a recycling process for tantalum from capacitor scraps, J. Phys. Chem. Solids 66 (2005) 318. http://dx.doi.org/10.1016/j.jpcs.2004.06.060.

[308] N. Ortuño, J. Moltó, S. Egea, R. Font, J.A. Conesa, Thermogravimetric study of the decomposition of printed circuit boards from mobile phones, J. Anal. Appl. Pyrolysis 103 (2013) 189. http://dx.doi.org/10.1016/j.jaap.2012.12.020.

[309] W. Liu, K. Tian, H. Jiang, X. Zhang, G. Yang, Preparation of liquid chemical feedstocks by co-pyrolysis of electronic waste and biomass without formation of polybrominated dibenzo-p-dioxins, Bioresour. Technol. 128 (2013) 1. http://dx.doi.org/10.1016/j.biortech.2012.10.160.

[310] X. Yang, S. Xu, H. Xu, X. Liu, C. Liu, Nickel supported on modified olivine catalysts for steam reforming of biomass gasification tar, Catal. Commun. 11 (2010) 383. http://dx.doi.org/10.1016/j.catcom.2009.11.006.

[311] P. Azadi, J. Otomo, H. Hatano, Y. Oshima, R. Farnood, Interactions of supported nickel and nickel oxide catalysts with methane and steam at high temperatures, Chem. Eng. Sci. 66 (2011) 4196. http://dx.doi.org/10.1016/j.ces.2011.06.002.

[312] P.R. Buchireddy, R.M. Bricka, J. Rodríguez, W. Holmes, Biomass gasification: Catalytic removal of tars over zeolites and nickel supported zeolites, Energy Fuels 24 (2010) 2707. http://dx.doi.org/10.1021/ef901529d.

[313] G. Guan, G. Chen, Y. Kasai, E.W.C. Lim, X. Hao, M. Kaewpanha, A. Abuliti, C. Fushimi, A. Tsutsumi, Catalytic steam reforming of biomass tar over iron- or nickel-based catalyst supported on calcined scallop shell, Appl. Catal. B-Environ. 115-116 (2012) 159. http://dx.doi.org/10.1016/j.apcatb.2011.12.009.

[314] C. Wu, P.T. Williams, Pyrolysis-gasification of post-consumer municipal solid plastic waste for hydrogen production, Int. J. Hydrogen Energy 35 (2010) 949. http://dx.doi.org/10.1016/j.ijhydene.2009.11.045.

[315] S. Kumagai, J. Alvarez, P.H. Blanco, C. Wu, T. Yoshioka, M. Olazar, P.T. Williams, Novel Ni–Mg–Al–Ca catalyst for enhanced hydrogen production for the pyrolysis-gasification of a biomass/plastic mixture, J. Anal. Appl. Pyrolysis. http://dx.doi.org/10.1016/j.jaap.2014.09.012.